Publisher Version: https://doi.org/10.1016/j.surfcoat.2017.05.027

Atmospheric pressure non-equilibrium plasma jet technology: general features, specificities and applications in surface processing of materials

Dr. Fiorenza Fanelli[a,*], Prof. Francesco Fracassi[a,b]

[a] *Institute of Nanotechnology (NANOTEC), National Research Council (CNR), c/o Department of Chemistry, University of Bari "Aldo Moro", via Orabona 4, 70126 Bari, Italy*

[b] *Department of Chemistry, University of Bari "Aldo Moro", via Orabona 4, 70126 Bari, Italy*

* Corresponding author at: Institute of Nanotechnology (NANOTEC), National Research Council, c/o Department of Chemistry, University of Bari "Aldo Moro", via Orabona 4, 70126 Bari, Italy

E-mail address: fiorenza.fanelli@cnr.it (F. Fanelli).

Abstract

Atmospheric pressure non-equilibrium (cold) plasma jet technology received enormous attention in surface processing of materials in the last two decades, and still continues nowadays to attract growing interest. In addition to the advantages of the atmospheric pressure operation such as the potential cost reduction of apparatuses as well as their easier handling and maintenance, due to the distinctive remote operation, plasma jets give the unique possibility of placing the substrate outside the source boundaries. Consequently, the processing of complex three-dimensional objects and the integration into existing production lines are expected to be much easier. However, while appealing, plasma jet technology has the drawback that great efforts are required for process optimization, since many factors can affect, for instance, the physical and chemical proprieties of the so-called "plasma plume" emanating from the devices and propagating in open space towards the substrate to be treated. The aim of this paper is to provide a critical literature review on the utilization of atmospheric pressure non-equilibrium plasma jets in surface processing of materials. Starting from the description and classification of the multitude of devices used in this applicative field so far, the attention will be drawn on some very important aspects to be taken into account in process optimization. The discussion will be focused on basic concepts and peculiarities closely related to the remote operation of the plasma sources, which include the characteristics and dynamics of the plasma plume interacting with the substrate and the surrounding atmosphere. Since the plasma jet approach allows the surface modification of small localized regions of the sample, the strategies implemented to enlarge the treated area will be also addressed. Finally, a brief overview will be given of the available applications and recent developments in the field of etching, thin film deposition and treatment.

Keywords

plasma jet

atmospheric pressure non-equilibrium plasma

surface processing

plasma treatment

plasma-assisted deposition

plasma etching

Contents

1. Introduction

Atmospheric pressure non-equilibrium plasma jet devices (also referred to as non-thermal or low-temperature or cold plasma jets or torches) can be defined as remote plasma sources operating at atmospheric pressure (AP) and moderate gas temperatures under non-equilibrium plasma conditions [1–6]. Several different approaches are currently available in plasma jet technology to obtain non-equilibrium plasma conditions at atmospheric pressure [6–11]. These approaches can exploit for instance highly asymmetric electrode geometries and sharply curved electrodes (such as in corona discharges), dielectric barriers, sub-millimeter plasma confinement in at least one dimension (i.e., microplasmas) [7–15]. Strategies based on high-frequency plasma excitation are also utilized as in the case of radiofrequency (RF) or microwave (MW) driven discharges [6,9]; while, recently, nanosecond pulsed power supplies have been proposed to achieve strong and stable non-equilibrium plasma conditions [11].

The distinctive feature of plasma jets resides in the fact that the plasma, generated remotely within the device, can be launched outside its physical boundaries, extending in the open space in the form of a so-called "plasma plume" (see the general plasma source scheme in Fig. 1). The adequate choice of the source design, the electric field geometry and gas flow conditions can allow the plasma plume to propagate through the external environment as far as a few tens of millimeters from the device exit [1,3,4].

Atmospheric pressure plasma jets were firstly developed as thermal arc-based plasma sources (i.e., arc jets and plasma torches) [6,8,16], with application in propulsion, cutting, welding and other high-temperature inorganic material processing technologies [8]. Non-equilibrium plasma jet devices began to emerge in the 1990s [2,17,18], benefiting from both the technological advances in the field of non-equilibrium plasma generation at atmospheric pressure, and the rising industrial demand for cold plasma technology in surface processing. Since then a large variety of devices have been developed, differing in the strategy utilized for

non-equilibrium plasma generation, in the electrode arrangement and overall architecture as well as in the shape, size and dynamics of the plasma plume ejected from the device [3,4,6].

Over the years, AP non-equilibrium plasma jets have demonstrated to be very promising in a plethora of cold plasma-based processes which allow the surface modification of a large variety of materials, without affecting their bulk properties [19]. These processes can be broadly divided into three main classes [20]:

(i) *Plasma etching* allows the removal of either the substrate material (in both isotropic and anisotropic fashion) or surface contaminants (i.e., *plasma cleaning*) to form volatile products.

(ii) *Plasma-assisted deposition* affords the preparation of organic, inorganic and hybrid multicomponent thin films (average thickness ranging from some nanometers to a few microns) as well as localized structures (width ranging from a few tens to a few hundreds microns and height up to several hundred microns). Different approaches can be used such as the plasma-enhanced chemical vapor deposition (PECVD), the aerosol-assisted plasma deposition (AAPD) and various evaporation- and/or sputtering-based techniques [11,15,21].

(iii) *Plasma treatment* consists in the modification of the outermost layers of the substrate through chemical grafting of specific functional groups and/or increase of the crosslinking degree and/or variation of the surface roughness. It includes a wide range of processes utilizing plasmas generally fed with noble gases (e.g., helium or argon) and/or molecular gases (e.g., nitrogen, oxygen, hydrogen, ammonia, etc.), operated under experimental conditions that are not able to induce considerable etching and appreciable polymerization.

In addition to the benefits offered by the atmospheric pressure operation, such as the potential cost reduction of plasma reactors as well as the easier handling and maintenance of apparatuses, beyond doubts the main advantage of plasma jets utilization in surface

processing is related to their distinctive remote operation. Plasma jets give, in fact, the unique possibility of placing the substrate outside the source physical boundaries, since they are able to bring the plasma, and therefore the reactive plasma species (e.g., radicals, metastables, ions, etc.), in the external environment and even in open air. Consequently, the processing of complex three-dimensional (3D) objects and the integration in existing production lines are much easier. It is worth highlighting that the source physical boundaries are very often mainly dictated by the geometric constraints for the generation of non-equilibrium plasmas at atmospheric pressure. Specifically, typical electrode assemblies utilize narrow gas gaps which are often limited to a few mm (for instance in the case of DBD and RF discharges-based plasma jets) because of the relatively high breakdown voltage of gases at atmospheric pressure [3,5,7–9]. Microplasma jets impose even more stringent geometric restrictions; however, as miniaturized devices they offer a unique tool towards localized and spatially resolved surface processing at atmospheric pressure [13–15,22–24]. On the other hand, strategies for uniform surface modification over large areas have been also implemented and are currently available in the realm of plasma jet technology [15,25].

However, while appealing, plasma jet technology has the drawback that great efforts are required for process optimization, since many factors can affect the physical and chemical proprieties of the plasma plume propagating in the external environment towards the substrate to be treated. The interaction of the plasma emerging from the device with the surrounding atmosphere and the substrate (Fig. 1) can be responsible for several phenomena that, while predictable in principle, are very difficult to be handled in practice. Indeed, the control of chemical reactions occurring under non-equilibrium plasma conditions can require more effort when dealing with plasma jets.

Different reviews have been published on plasma jet technology so far [3,4,6,19]. Laroussi and coauthors classified atmospheric pressure non-equilibrium plasma jets according to the power supply frequency range [3], the operational parameters [3] and the type of gas used to

ignite the discharge [4]; they also focused on the understanding of the nature and dynamics of plasma propagating in the surrounding environment [4]. The recent review by Weltmann and coworkers [6] gives an overview of jet devices and specifically provides an update of new designs and novel research achievements. Papers by Belmonte *et al.* [22,23] outline the localized and large area deposition processes by means of both millimetric plasma jets and microplasma jets; while the review papers by Mariotti and Sankaran [15] and by Lin and Wang [24] are focused on nanomaterials synthesis by microplasmas technology and, among others, include examples on the utilization of microplasma jets for the surface modification of materials.

The aim of this paper is to provide a critical literature review on the utilization of AP non-equilibrium plasma jets in surface modification of materials. Both the novelty and distinctive character of this review mainly reside in the fact that it presents the most relevant aspects to be taken into account in the optimization of plasma jets operation to obtain reliable and reproducible processes. First, the multitude of devices developed so far for use in surface processing will be classified and briefly described (Section 2). Then, the attention will be focused on some important issues to be faced in process optimization and strictly related to the remote operation of the plasma sources, such as the propagation dynamics of the plasma plume in open space, its interaction with the surrounding atmosphere and the substrate (Fig. 1); the localized surface modification of materials will be discussed and possible strategies for the large area processing will be presented (Section 3). Finally, a brief overview will be given of the available applications in surface engineering with special focus on specific advances that have been recently made in the field of plasma etching, deposition and treatment (Section 4).

2. Atmospheric pressure non-equilibrium plasma jets used in surface processing

Many different atmospheric pressure plasma jets have been developed so far to be utilized in surface modification of materials. Over the last two decades, technological advances in the design of this class of plasma sources have been boosted by the growing research interests for AP non-equilibrium plasmas in various areas of study including medicine and healthcare [26,27], nanomaterials synthesis [15,22–24] and surface engineering [12,15,22,23]. Without doubt, the progress made in the emerging field of plasma medicine has significantly contributed to the development of new plasma sources and, *inter alia*, to the understanding of their operation in open air [26–28]. Indeed, AP non-equilibrium plasma jets are among the most utilized plasma devices in the treatment of living cells, tissues, and even organs, since they operate under ambient conditions and may allow, for instance, the direct interaction of the plasma with the human (or animal) body to realize therapeutic effects [26–28]. On the other hand, due to their distinctive remote operation, AP non-equilibrium plasma jets have also offered new and exciting opportunities in materials science, pushing the plasma community to properly optimize plasma sources for nanomaterials synthesis and surface modification.

This section proposes a brief overview of AP non-equilibrium plasma jets, the use of which falls within the realm of surface processing. First, some basic concepts on the architecture and operation of plasma jet systems will be illustrated (subsection 2.1). Then, the attention will be focused on the various strategies adopted to obtain non-equilibrium plasmas conditions, with specific reference to the designs, power supplies and operational conditions used in various etching, deposition and treatment processes (subsection 2.2). A brief comparison between atmospheric pressure and low pressure non-equilibrium plasmas will be

also presented. Although this review is focused on non-equilibrium plasma sources operating far away from thermodynamic equilibrium (also referred to as cold or non-thermal plasmas) for the sake of completeness, it will include a few examples of arc plasma jets (i.e., equilibrium or hot or thermal plasma sources) characterized by relatively low operating temperatures (subsection 2.3). When properly handled, these sources can be utilized in surface modification without causing thermal damage to the treated materials.

It is worth mentioning that in the literature the term "plasma jet" is commonly used interchangeably to mean both the remote source able to generate the plasma and to launch a plasma plume in the external environment, and the plasma plume itself. Therefore, to avoid any confusion, in this review the term "plasma jet" is used to refer only to the remote plasma source.

2.1. Basic concepts on architecture and operation of plasma jets

As already mentioned in the introduction, the main feature of plasma jets is that the plasma, ignited and sustained remotely within the plasma source, extends well beyond the region where it is generated and can, finally, be launched outside the device in the form of a so called "plasma plume" (Fig. 1). Specifically, in the case of atmospheric pressure non-equilibrium plasma jets, the adequate choice of the source design, the electric field geometry and gas flow conditions can favor the propagation of the plasma plume through the external environment, as far as a few tens of millimeters from the device outlet to intersect the substrate to be treated. However, when very mild plasma treatments are needed, the plasma source can be kept far enough from the substrate, so that the plasma can decay prior to reaching the substrate surface. In this case the substrate interacts only with the long-living species produced by plasma and transported outside the source by the gas flow [29].

Many different plasma jet devices have been developed so far, differing in the strategy exploited for non-equilibrium plasma generation, in the geometry of the electrode

arrangement as well as in the shape and dimensions of the plasma plume ejected from the device [3,4,6,23,24]. However, despite the large variety of configurations used in surface processing, it is possible to identify some common architectural features, that will be briefly described below and are schematized in Fig. 1 as well as in the various plasma jet systems reported in Fig. 2-7.

First of all, almost all plasma jets structurally integrate both the electrode assembly for the generation of the discharge and the channel (or duct) through which the feed gas flows and in which the plasma generates and propagates (Fig. 1). Notable exceptions to this exist are, for instance, the inductively coupled plasma sources (Fig. 4e and f) or the electrode-less microwave plasma jets (Fig. 6a) which have, however, to integrate the resonant cavity to generate the plasma [10,30].

The plasma propagates through the channel, along the gas flow direction, towards the outlet where it can be ejected outside the device (Fig. 1). The channel usually has circular (or round-shaped) or annular (or ring-shaped) or rectangular cross-section perpendicular to the gas flow direction (see, for instance, the plasma jets in Fig. 3). The cross-sectional shape and dimensions of the channel are generally identical to the shape and dimensions of the source outlet. An exception to this can be found in Fig 3b showing a plasma jet featuring an annular channel and a circular outlet. In some cases, the device outlet can present a restriction or a convergent nozzle (Fig. 4f, 5a and 7a) which reduces the gas channel cross-section to favor the focusing of the plasma plume or to promote the reactions occurring within the source [31–35]. It is worth mentioning that, as a function of the device outlet shape and dimensions, different denominations can be used for plasma jets. Devices characterized by very narrow circular outlets are broadly considered zero-dimensional plasma sources and often referred to as “point plasma sources” [5]. Plasma jets featuring high aspect-ratio rectangular outlet (i.e., high length-to-width ratio) are considered one-dimensional sources generally known as

"linear plasma jets" because the plasma plume emerging from the source resembles a "plasma line" [36–39].

Round-shaped gas channels can have diameter ranging from a few hundreds of microns to a few millimeters [32,40]; while ring-shaped channels can in principle present inner and outer diameters of up to a few centimeters, and annular space thickness up to a few millimeters [41–43]. Finally, the cross-section of rectangular gas channels generally presents length ranging between a few centimeters and some tens of centimeters, and width of up to a few millimeters [36,44].

The critical dimensions of the gas channel cross-section (i.e., the circle diameter in round-shaped cross-sections, the annular region thickness in ring-shaped cross-sections, the rectangle width in rectangular cross-sections) are mainly dictated by the geometric constraints associated to the generation of non-equilibrium plasmas at atmospheric pressure. In fact, since the atmospheric operation implies high gas breakdown voltages, narrow gas gaps are generally used; they are limited, for instance, to a few millimeters in the case of DBD and RF discharges. This, *inter alia*, prevents the utilization of very high voltages to ignite and sustain the discharge [4,5,7–9]. Even more stringent geometric constraints are associated with microplasmas where at least one dimension needs to be reduced to the sub-millimeter scale [13–15].

Regarding the materials in direct contact with the feed gas and the discharge within the plasma sources, metals are often used, and this is the case of plasma jets featuring bare metal electrodes (Fig. 2a, Fig. 3b, Fig. 4a, c and d, Fig. 4, Fig. 7a). Dielectric inorganic materials (e.g., alumina, glass, quartz, fused silica) are also utilized when, for instance, the gas channel consists of a tube of dielectric material (e.g., Fig. 2a, Fig. 4a, b, e and f) and/or when dielectric-covered electrodes are used (see the DBD jets in Fig. 3). On the other hand, the use of polymers is rarely reported [45].

Additionally, plasma jet systems can present single or multiple inlets for feed mixture introduction within the source and even independent inlets can be used for the different components of the mixture. Specific examples can be made regarding the introduction of the thin film precursors (in vapor or aerosol form) in plasma jets used in deposition processes. A first approach utilizes a single inlet (see Fig. 3a) and consists of injecting the precursor together with the so called "discharge gas" (e.g., a pure gas such as helium, argon, nitrogen, or gas mixtures not containing polymerizing species) into the plasma source, upstream of the plasma generation region. This favors the precursor activation and fragmentation in the discharge, but causes deposition inside the device. In a second approach the discharge is fed only by the "discharge gas", while the precursor is separately introduced, downstream of the plasma generation region (Fig. 3b, Fig. 5c, Fig. 6), through an independent inlet located before or after the source outlet [12,46]. In case of coaxial cylindrical systems, very often, hollow central electrodes are used for precursor injection directly in the plasma plume (Fig. 3b and 6). The vapor or aerosol of the precursor is commonly introduced in the source in mixture with a carrier gas which is usually the same as the discharge gas. The role of the carrier gas is dual, since it assists both the formation of the precursor vapor or aerosol (when bubblers and pneumatic atomizers are respectively used) as well as its transportation and injection in the plasma source. The downstream injection of the precursors prevents deposition inside the gas channel and, therefore, renders the periodic maintenance and cleaning of the devices less frequent and even unnecessary.

It is worth mentioning that for deposition of thin films and nanostructures, even solid precursors can be used in the form, for instance, of consumable metal wires integrated within the plasma source and directly exposed to the discharge (Fig. 4f) [32].

Finally, regarding the overall architecture of apparatuses integrating plasma jet sources, it is important to have in mind that:

(i) Depending on needs, plasma jets can be operated either in open air or in controlled environments. In the latter case the plasma sources are located into airtight chambers [41].

(ii) The substrate is commonly placed onto a sample holder located below the source exit, while the source axis is commonly perpendicular to the sample holder [41].

(iii) The source-to-substrate distance, taken to mean as the distance between the plasma source exit and the substrate, can be generally varied from less than 1 mm to a few tens of mm. The holder can be also heated during the process, as can be required to assist the deposition of dense inorganic coatings [31,46].

(iv) The apparatuses can be also equipped with displacement systems of the plasma source and/or the sample holder (Fig. 1), to improve the final uniformity of the treated surfaces and/or to enlarge the treated area (Section 3.3).

2.2. Strategies for atmospheric pressure non-equilibrium plasma generation

When working at atmospheric pressure, due to the high collisional frequency between electrons and neutrals (e.g., gas atoms or molecules), it is very challenging to mantain non-equilibrium plasma conditions keeping the electron temperature (T_e) much higher than the gas temperature (T_g), and the latter at or near room temperature [47,48]. Strategies must be implemented to avoid the thermalization (i.e., the transition to equilibrium plasma conditions) and, therefore, to reduce the risk of gas heating and arc formation. These strategies exploit, for instance, special electrode shapes and geometries, dielectric barriers, plasma confinement in small cavities, high-frequency alternated-current (AC), high gas flow rates [9,12]. The gas temperature of the different types of AP non-equilibrium plasma jets can range between room temperature and some hundreds degrees Celsius (roughly 700-1000°C as indicated in ref. [6,9]) and, therefore, remains at least one order of magnitude lower than the electron temperature [6]. The fact that in some cases the gas temperature rises significantly above

ambient temperature can make challenging the utilization of some types of AP non-equilibrium plasmas in the surface treatment of thermolabile materials (e.g., polymers) as well as in the deposition of polymeric coatings.

Authoritative review papers propose classifications of AP non-equilibrium plasma jets based on the frequency range of the power supply [3,6] and on the type of gas used to ignite the discharge [4]. In this paper, AP non-equilibrium plasma jets currently used in surface processing of materials are classified according to the approach adopted to obtain thermal non-equilibrium plasma conditions at atmospheric pressure [5,9,10]. Broadly, each approach allows identifying a specific type of AP non-equilibrium plasma and can be assigned to one of the two following proposed classes:

– *class 1*: strategies based on the design of the discharge cells;

– *class 2*: strategies based on high-frequency plasma excitation.

Approaches exploiting highly asymmetric electrode geometries, dielectric barriers, sub-millimeter plasma confinement in at least one dimension belong to class 1 and allow the generation of corona discharges, dielectric barrier discharges, and microplasmas, respectively [7–9,11,15]. While class 2 includes radiofrequency or microwave driven discharges [5,6,9]. However, it is important to keep in mind that the proposed classification is not exhaustive and very often boundaries between some discharge types are blurred.

For each approach reported below, the most common electrode configurations and power supplies will be presented, along with the typical designs and operational conditions (e.g., feed gas, gas flow rates, etc.) of plasma jets utilized in surface processing.

2.2.1. Strategies based on the design of the discharge cells

Corona discharges (CDs) utilize highly asymmetric electrode configurations and high-curvature electrodes (i.e., sharp electrodes) such as in point-to-plane, wire-to-plane and wire-to-cylinder geometries. They consist of a small metal electrode, in the form of a sharp point

(e.g., pin or needle) or of a thin wire and a large electrode that can be a flat metal plate, a cylinder or a tube. By applying a high voltage to the small electrode, a strong electric field is produced around it. Therefore, gas breakdown occurs in close proximity to this small electrode, where the corona discharge ignites and remains localized in the form of a weakly ionized non-equilibrium plasma. However, the careful increase of the applied voltage can allow the discharge to extend towards the larger electrode (i.e., the counter-electrode), without reaching it in order to avoid the corona-to-arc transition and the increase of the ionization degree.

CDs can be generated by using both DC and AC power supplies at voltages up to several tens of kV (e.g., DC voltages with both positive and negative polarity, audiofrequency AC voltages). Also pulsed power supplies can be used and, interestingly, it has been shown that nanosecond pulsing can render the stabilization of non-equilibrium conditions easier. In particular it has been shown that pulses with 100–300 ns duration are sufficiently short to avoid the corona-to-spark transition [7,8,39] because arcs do not have sufficient time to develop within one pulse.

Several plasma jets based on corona discharges fed with air and nitrogen have been commercialized for plasma treatments and, in particular, for wettability and adhesion enhancement of the polymeric surfaces [49–52] through grafting of polar groups.

Fig. 2a shows the schematic diagram of the PlasmaStream^{TM} plasma jet, developed by Dow Corning, utilized for the open-air deposition of thin films by aerosol-assisted processes [40,45,53–56]. The system consists of a dielectric head housing two needle electrodes connected to a power supply operating in the audiofrequency (AF) range (15–25 kHz, sinusoidal excitation signal). The electrodes are located either side of a central pneumatic nebulizer through which the aerosol of the precursor is introduced; independent inlets are present for the He-N_2 gas mixtures (total flow rate of about 5 slm) and the thin film precursor. This arrangement is positioned at one end of a quartz or polytetrafluoroethylene (PTFE) tube

which acts as guide for the gas flow and in which the corona discharge develops extending towards the substrate (Fig. 2b). In ref. [40] the substrate is placed on a grounded metal plate (counter-electrode) covered by a polymeric sheet, while in ref. [45] no counter-electrode is used.

The spectroscopic investigation of the helium-fed corona discharge generated in this plasma jet, revealed a gas temperature of about 130°C (deduced from the rotational temperature of N_2, present as impurity due to the open air operation). Whereas thermographic imaging revealed that the surface temperature of the quartz tube ranges between about 50 and 80°C [40]. Interestingly, thermographic measurements carried out during the thin films deposition, demonstrated that the temperature of the quartz tube, measured after 20 min of discharge operation, is significantly lower when the aerosol of the precursor (e.g., hexamethyldisiloxane, HMDSO) is added to the He/N_2 discharge (i.e., about 90° and 50°C without and with aerosol addition, respectively) [53]. This is likely due to the fact that a significant amount of total thermal energy is imparted to precursors droplets and enable their evaporation in the discharge. Interaction between the liquid precursor droplets and the non-equilibrium cold plasma was studied in more detail by Iqual *et al.* [56].

Colombo and coworkers developed a linear corona plasma jet for the treatment of polymeric substrates (i.e., electrospun poly(L-lactic acid) scaffolds) [39]. The plasma source is composed of a housing made of dielectric material and a sharp stainless steel blade (36 mm wide and 0.1 mm thick) operated as high-voltage electrode. The housing is provided with a gas inlet (N_2 gas flow rate of 5 slm) and two parallel gas channels to obtain a uniform gas flow in the electrode region. In order to generate a uniform discharge, the plasma source is driven by a nanosecond pulsed generator (peak voltage of 7–20 kV range, pulse repetition frequency of 83–1050 Hz, pulse width of 12 ns and rise time of 3 ns) [39].

Dielectric barrier discharges exploit the presence of at least one dielectric layer located in the current path between the electrodes to achieve non-equilibrium plasma conditions at atmospheric pressure. The dielectric material has the key role of limiting the discharge duration, preventing arc formation since the discharge is stopped before thermalization occurs. DBDs are generated by using AC power supplies operating at frequencies generally between 50 Hz and a few hundreds of kHz, both in continuous and pulsed mode. Different feed gases can be used (e.g., He, Ar, N_2 and air) at flow rates ranging from a few slm to some tens of slm, as a function of the characteristics and dimensions of the apparatus. One of the main features of DBDs resides in their possible operation in completely different discharge regimes. In most cases DBDs operate in filamentary regime (i.e., filamentary dielectric barrier discharges, FDBDs) characterized by many microdischarges of short duration (~40 ns) and narrow diameter (~200 μm) [7,8], which evenly and randomly distribute in the discharge gap over the dielectric surface. However, homogeneous microdischarge-free regimes can be also obtained under particular experimental conditions mainly linked to the power supply (e.g., excitation frequency range and applied voltage, utilization of power matching and discharge stabilization network [11,57]) and of the feed gas mixtures. Different homogeneous regimes may exist (e.g., glow, glow-like and Tonwsend-like regimes) and Massines *et al.* summarized their main characteristics in ref. [11].

Numerous plasma jets based on DBDs have been reported in the literature so far [41,58,59] and also commercialized systems exist [36,43]. Applications in surface processing mainly include surface treatment and thin film deposition. Fig. 3 shows three of the many possible electrode configurations used in DBD jets. As previously discussed, the geometry and dimensions of the electrode assemblies inevitably determine the shape and dimensions of the jet canal cross-section perpendicular to the gas flow direction. Two different coaxial geometries are reported in Fig. 3a and b: the first one shows external ring electrodes on a dielectric tube (circular channel), while the second consists of an inner high voltage

cylindrical electrode, a dielectric tube and an external grounded tube (annular channel). As reported in Fig.3b, the inner electrode can be a hollow cylinder to accomplish the injection of the precursor in the downstream region. Finally, Fig. 3c reports a DBD jet with a parallel plate electrode geometry (rectangular channel), in which both electrodes are covered by a dielectric layer.

Microplasmas are defined as plasmas confined within sub-millimeter cavities in at least one dimension [15]. Different studies highlighted that thermodynamic non-equilibrium conditions are stably achieved at atmospheric pressure for sub-millimeter plasmas. Mariotti in ref. [60] reported experimental evidences of non-equilibrium in atmospheric microplasmas and, specifically, showed that the increase of the pressure to the atmospheric level does not imply the loss of non-equilibrium and the thermalization. Moreover, under atmospheric pressure conditions, the reduction of the size of the plasma results in an increase of the electron temperature and a concomitant decrease of the gas temperature, enhancing the non-equilibrium characteristics of the discharge.

Fundamentals and applications of microplasmas are reviewed in reff. [13–15,61]. As far as the technological applications in nanomaterials synthesis are concerned, it is worth mentioning that microplasmas have been widely utilized for the fabrication of free-standing nanomaterials (e.g., nanoparticles as powders or colloidal dispersions) [15,22–24]. This application is beyond the scope of this review, that will remain focused on the utilization of microplasma jets for surface modification of materials generally carried out as local etching, treatment and deposition of nanostructured thin films.

Fig. 4 reports a selection among all the available microplasma jet designs. Numerous devices employ corona [62–64] and DBD [65] configurations as those reported in Fig. 4a and b, which show respectively a typical needle-to-plane corona geometry and a coaxial DBD geometry with external ring electrodes on a dielectric tube. Fig.4c reports a hollow cathode

microjet consisting of a stainless steel capillary tube (holes size of a few hundreds of microns) used as the cathode and a metal plate or grid as the anode [66,67]. This design was utilized by Sankaran *et al.* [66] for the deposition of diamond films; in this study the discharge was operated using a negative DC power supply with current-limiting resistor in series.

Many radiofrequency-driven microplasma jets have been also developed [14]. In particular a RF capacitively coupled plasma source with coaxial cylindrical electrodes is shown in Fig. 4d, while Fig. 4e reports a RF inductively coupled plasma source using a coil looped around an alumina or quartz tube with sub-millimeter internal diameter [14,68]. The design shown in Fig. 4f can be considered as a variation of the configuration of Fig. 4e. In this case the RF inductively coupled microplasma jet is provided with a consumable metal wire inserted into a restricted quartz nozzle. This design was used for the localized deposition of metal or metal oxide nanostructures by evaporating or sputtering the sacrificial metal electrode [15,24,32].

Regarding microplasma generation, as it can be also deduced from the above descriptions, a wide range of power supplies can be used as a function of the device configuration, e.g., both DC and pulsed DC power supplies, AC power supplies operating in the AF, RF and MW range. Discharges are usually fed with nobles gases such as argon or helium (low flow rates up to a few hundreds of sccm), in mixture with reactive gases when needed.

2.2.2. Strategies based on high-frequency plasma excitation

The approaches here reported exploit high-frequency alternated-current electric fields (i.e., from MHz to GHz frequency range) for the generation of stable and uniform arc-free non-equilibrium plasmas at atmospheric pressure.

The study of RF non-equilibrium plasmas at atmospheric pressure has started in the late nineties, when the so called “atmospheric pressure plasma jet” (APPJ) operating at 13.56

MHz was developed at the Los Alamos Laboratories in USA [18]. Since then different AP RF plasma jets have been designed and utilized in surface processing [2,5].

Atmospheric pressure RF plasma jets operate in a capacitive electrode configurations using RF power (usually at 13.56 MHz) which produce stable, very uniform glow discharge between two bare metallic electrodes, without any dielectric in between [5].

Briefly, AP RF glow discharges can operate in two modes, known as α-mode and γ-mode. In the α-mode a stable uniform discharge forms; it is sustained by volumetric (or bulk) ionization, while cathode secondary electron contribution is negligible. In the γ-mode the discharge is sustained by secondary electron emission from the electrode surface, similar to DC discharges, and covers only a small fraction of the electrode surface [5]. Various studies pointed out that the uniform discharge observed in case of AP RF plasma jets operates in the α-mode [5,69,70]. This mode is commonly obtained at current densities up to approximately 500 $A \cdot m^{-2}$, otherwise the transition to a localized γ-mode can occur. It is worth mentioning that, in the case of He-fed RF discharges, gas ionization can be considerably enhanced by the Penning ionization of gas impurities or additives (such as nitrogen and oxygen) by He metastables [71]. Penning ionization can contribute to achieve adequate electron production in the sheath region promoting the transition from the α-mode and γ-mode [71]. In the α-mode stable and uniform glow discharges can be sustained over a wide range of RF powers at interelectrode distances ranging from 0.5 to 2.5 mm, in noble gases such as helium and argon (flow rates ranging from a few slm [70] to some tens of slm [69]), with only small additions of molecular gases. Gas temperatures lower than about 200°C are reported for these discharge [2,5,11,69].

Three basic bare electrodes configurations are schematized in Fig. 5: the first utilizes concentric electrodes, while the second and the third present parallel electrodes which can be solid or perforated. The coaxial jet in Fig. 5a represents the first AP RF plasma jet developed and used for etching and deposition [31,72,73]. It consists of two concentric electrodes made

of stainless steel; RF power is applied to the inner electrode. Water cooling can be used to prevent excessive heating; in ref. [73] it was found that the effluent temperature of a jet equipped with cooling jacket varied from 100 to 150°C, depending on the RF power. In reff. [31,72] the etching of polymeric materials is carried out by using a He-O_2 mixture fed into the annular space between the two electrodes at about 50 slm. The effluent exits the device through a restricted nozzle at a velocity of 30 m s^{-1}. When the deposition of SiO_2-like coatings is carried out, a mixture of He and vapors of tetraethoxysilane (TEOS) is injected downstream, through an independent inlet located before the jet outlet [73].

Fig. 5b shows a RF plasma jet with a classical parallel plate electrode geometry [5,70]; the gas flows along the electrodes through the rectangular channel. Fig. 5c reports a most recently developed jet, commercialized by SurfX technologies LLC [37]. It consists of two parallel circular electrodes which are perforated (by 126 holes with 0.6 mm diameter [38]) allowing the feed gas (He or Ar) to flow through them (flow rate of a few tens of slm). The upper electrode is connected to the RF power supply, while the lower electrode is grounded. A third perforated metallic plate is installed beneath the lower electrode. It contains an internal network of channels and holes that allow to inject and mix thin film precursors downstream of the plasma generation region. This plasma source is commonly called "showerhead plasma jet" since it is provided with a showerhead outlet consisting of a circular honeycomb array of sub-millimeter holes. Several works reported the use of this source for surface treatment [38,74,75] and deposition of both organic and inorganic coatings [76–81].

Microwave discharges at atmospheric pressure can benefit from the stabilizing effect of microwave excitation (usually at 2.45 GHz) on volumetric ionization [9]. Microwaves are, in fact, often utilized to generate non-equilibrium plasma columns as well as moving and extended plasmas proposed for instance for the treatment of the inner surfaces of tubular structures of heat sensitive materials [9,82,83]. To date, few studies have been published on

atmospheric pressure microwave-driven non-equilibrium plasma jets and, in particular, on their utilization in surface processing [30,84,85].

A MW electrode-less jet, using a surfatron as excitation source, was presented by Schäfer *et al.* [30] (Fig. 6a) for the deposition of SiO_2-like coatings. The surfatron source is powered by a microwave magnetron generator (2.45 GHz) connected via ferrite circulator, waveguide and coaxial cable; the cable and the coaxial connectors limit the supplied power to 300 W. The surfatron excitation source consists of a tuned coaxial resonant cavity, through which a fused silica discharge tube (80 mm long, 6 mm and 8 mm inner and outer diameter, respectively) is inserted. Another silica coaxial capillary with 1 mm diameter, located at the center of the discharge tube, allows the downstream injection of a mixture composed by Ar and the vapors of an organosilicon precursor (tetrakis(trimethylsilyloxy)silane, TTMS). The discharge is fed with Ar (2.6 slm) which flows through the annular region between the two tubes. The deposited coatings were characterized by O/Si atomic ratios between 1.6 and 2 and very low carbon content (as determined by energy dispersive X-ray spectroscopy), while the deposition rate varied between 600 and 1020 $nm \cdot min^{-1}$. The cross-sectional scanning electron microscopy (SEM) image in Fig. 6a evidences the presence of dendritic nanostructures. These results were compared with the ones obtained by means of a RF plasma jet with similar coaxial geometry (Fig. 6b), consisting of two external ring electrodes on a silica tube, operated 27.12 MHz and at a lower power (6-15 W). A comparable chemical composition of the films was achieved, but, as evident from the SEM image in Fig. 6b, smooth and dense films were obtained at much lower deposition rate (6-24 $nm \cdot min^{-1}$). The largely different film morphologies and deposition rates obtained with the two approaches were mainly ascribed to the different power densities. In particular, the higher power densities in the MW discharge seemed to promote oligometization and nucleation in the volume of the plasma, allowing the formation of porous and nanostructured coatings at high deposition rates.

2.2.3 Atmospheric pressure vs. low pressure non-equilibrium plasma operation.

Over the last decades, surface processing of materials by using low pressure (LP) non-equilibrium plasmas has become strongly consolidated in a wide range of applications including the areas of microelectronics, photovoltaics, optics, packaging, biomaterials. In recent years, research efforts have increasingly shifted towards the development of atmospheric pressure non-equilibrium plasma technologies. The main motivation in exploring such field has lied in the benefits offered by the absence of vacuum systems, i.e., the reduced cost of plasma reactors, the easier handling of apparatuses, the possible open-air operation. However, the technological expectations have been accompanied by the growing awareness of the specific features of AP non-equilibrium plasmas that differentiate them from low pressure ones and can even restrict their utilization in surface processing.

A detailed comparison of low pressure and atmospheric pressure non-equilibrium plasmas is beyond the scope of this review, however to better enlighten limitations and opportunities of using AP non-equilibrium plasma jet technology in surface processing, in this subsection some critical issues will be discussed.

Firstly, as already reported, due to the higher collisional frequency, it is by far more challenging to maintain non-equilibrium plasma conditions at atmospheric pressure than at low pressure. AP non-equilibrium plasmas face, in fact, a range of instabilities (e.g., thermal instabilities [5,7]) which can cause discharge contraction, arcing and gas heating. Plasma filamentation is often observed (as for instance in filamentary DBDs) and it can have negative effects on the homogeneity of the surface treatment or of the deposited layers [11,12].

AP non-equilibrium plasmas used in surface processing are often fed by a main gas (or dilution gas) and additives at generally low concentrations, as a function of the process to be performed (i.e., etching, deposition, treatment) [11]. The careful selection of the feed mixture composition can contribute to maintain non-equilibrium conditions and suppress gas heating

at atmospheric pressure [7,9,11,12]. The discharge physics is primarily dictated by the main gas, however the presence of additives can significantly affect the discharge regime [11]. Nobles gases, and in particular helium and argon (i.e., the less expensive noble gases), are the most frequently utilized main gases. As reported by Fridman [8], noble gas fed plasmas operate at significantly lower voltage and, therefore, lower power density, which helps to avoid thermal instability. Helium is extensively for various reasons including (i) the low breakdown voltage, (ii) the fact that homogeneous (filament-free) discharges are rather easily obtained, (iii) the high thermal conductivity allowing a quick dissipation of local gas heating [11]. Molecular gases, such as nitrogen and air, are sometimes also used as main gas, but unfortunately, they are characterized by much higher breakdown voltages. In particular, the presence of oxygen results in electron attachment, which causes higher operating voltage, higher power, leading to thermal instability. The utilization of noble gases has important implications in the running costs of atmospheric pressure plasmas since, differently from LP plasmas, high main gas flow rates (up to several tens of slm) are very often needed to reduce the residence time and limit gas heating as well as for cooling purposes [9]. Moreover, in case of AP plasma jets, the high main gas flow rate can favor the plasma plume propagation in the surrounding environment (see section 3.1.1).

The high collisional frequency is also responsible for the limited kinetic energy of ions in AP non-equilibrium plasmas. At AP the kinetic energy of ions impinging on the surfaces is very low because ions lose most of their kinetic energy in elastic collisions with the surrounding gas, in the volume of the discharge as well as in the sheaths [11]. Consequently, in contrast to what commonly obtained at low pressure, in AP non-equilibrium plasmas ion bombardment does not consistently contribute to surface activation and etching. As far as thin film deposition is concerned, the lack of an effective ion bombardment in AP plasmas makes the production of dense and crystalline films very challenging at room temperature and also precludes the utilization of the classical LP sputtering-based techniques. On the other hand, at

atmospheric pressure, the defects generally induced on the treated surfaces and on the deposited coatings by the ion bombardment are not observed [11].

An important advantage of atmospheric pressure operation that deserves to be discussed is the possibility of igniting non-equilibrium plasmas into millimeter and submillimeter gaps and cavities [14,15,86,87]. This is unlikely to occur under low pressure plasma conditions since to achieve plasma ignition cavity dimensions should be consistently greater than the Debye length. For instance, in case of a low pressure glow discharge, characterized by electron temperature and density of 4 eV and 10^{10} cm^{-3}, respectively, the Debye length is estimated to be 0.14 mm [47]. As a consequence, AP non-equilibrium plasmas offer unique opportunities for the processing of the inner surfaces of tubes and channels having inner diameter or width ranging between a few hundred microns and a few millimeters [86,88]. The atmospheric operation can also simplify the processing of porous materials and, more specifically, the interior of sponges and scaffolds [87].

2.3. Low temperature arc jets used in surface processing

For the sake of completeness this review includes examples of arc-based plasma jets successfully utilized for the surface treatment of polymers as well as for the deposition of both organic and inorganic thin films. In principle, arc jets are plasma sources operating under thermodynamic equilibrium and, therefore, characterized, by high gas temperatures. However, recently, it has been shown that the adequate choice of the power supply and of the operating conditions allows these sources to eject in the external environment a plasma characterized by relatively low gas temperatures [89–104]. For instance, pulsed power supplies are used to reduce the discharge current, while high speed vortex flows permit to spatially stabilize the arc and associated downstream plasma [8].

To this class of plasma jets belongs the plasma source commercialized by Plasmatreat® [94–104] reported in Fig. 7a [95]. The discharge is generated by applying a high frequency (19–23

kHz) pulsed voltage to two tubular electrodes separated by a dielectric material. The generator delivers a pulse-pause modulated current controlled by adjusting the plasma cycle time (PCT); a PCT of 100% corresponds to a pulse duration equal to the pause duration. The plasma jet is fed with air or nitrogen at flow rates ranging approximately between 30 slm and 80 slm [95,102]; a vortex flow is produced within the device to promote the rotation of the electric arc and prevent an irregular erosion of the metal housing. Thin film deposition can be accomplished by injecting the precursor in the downstream region (to avoid thermal decomposition of the precursors inside the source), before the source outlet nozzle (Fig.7a) [95]; alternatively, the precursor can be injected below the source outlet [97].

Arefi and coworkers widely characterized this type of plasma source and optimized the operational conditions for surface treatment of polymers (e.g., polyamide-6, polydimethylsiloxane) [99,101] and deposition of various coatings (e.g., SiO_2-like, TiO_2-like coatings, acrylic coatings) [95–98,100]. Optimization of these sources in surface processing requires a great care to reduce the heat loading on the exposed surfaces, in particular when polymeric substrates need to be treated or organic thin layers are deposited [99,102]. Parameters to be optimized include the input power (depending on both the excitation frequency and the plasma cycle time), the treatment duration, the source outlet-to-substrate distance. Various methods were used to measure the gas temperature of the plasma exiting from the source (e.g., optical methods and thermocouples measurements), the temperature of the surfaces exposed to the discharge (e.g., thermal infrared imaging), the heat flux from the plasma jet to the treated substrate (e.g., calorimetric probes measurements) [95,97,102,105]. In ref. [95] a thermocouple was introduced below the outlet nozzle, in the axis of symmetry of the plasma source, to measure the gas temperature as a function of the distance from the outlet and of the power transferred to the plasma (i.e., the PCT at fixed frequency). These measurements permitted to obtain the response surface reported in Fig. 7c which shows the increase of the gas temperature from about 200 to about 850°C by increasing the PCT from 30

to 100% as well as by decreasing the distance from the exit from 22 to 12 mm. Under the investigated conditions, the plasma plume ejected from the device has a length of about 21-22 mm, as estimated by using a CCD camera (Fig.7b). The fluid dynamic behavior of the jet was also studied and calculations showed that the gas flow regime (air flow rate of 40 slm) at the source exit is initially laminar, while it becomes partially turbulent with the distance, because of the reduction of the air viscosity upon cooling (see Fig 7c).

3. Features and specificities of AP plasma jets utilization in surface processing

While offering the possibility of bringing reactive plasma-generated species into the external environment and even in open air, AP non-equilibrium plasma jets require considerable efforts to be reliably and effectively utilized in surface modification of materials.

This section is aimed at presenting a range of general and specific aspects very important to be taken into consideration in process optimization. First, the discussion will be dealing with basic concepts and peculiarities associated with the remote operation of AP plasma jets, including the characteristics and propagation of the plasma plume outside the device, the influence of both the external environment and the substrate (section 3.1.). Then, the focus will shift on issues related to localized small area surface processing of materials (section 3.2). Finally, the implementation of apparatuses and plasma sources for large area surface processing will be discussed (section 3.3.). Examples will be selected from the scientific literature to address a range of issues and challenges, which may arise in the optimization of etching, deposition and treatment processes. For ease of understanding and comparability of

results, the examples given in this section mainly concern plasma jets with coaxial geometry and round-shaped exit, i.e., the most frequently used devices in surface processing.

3.1. Remote plasma processing of materials

Broadly, surface modification by non-equilibrium plasmas both at low and atmospheric pressure can be accomplished by using two different approaches, i.e., the "direct" and the "remote" approach. In the direct approach the substrate to be treated is located in the plasma generation region, where it is directly exposed to the plasma [11,29]. In contrast, when the remote approach is used, the substrate is located downstream of the plasma generation region and , in the case of AP plasma jets, it is placed outside the plasma source, in front of the source outlet (Fig. 1). It is important to specify that the contact between the plasma and the substrate is not mandatory when AP non-equilibrium plasma jets are used and, in fact, it is possible, to distinguish between two basic operation modes:

(i) The "contact" or "touch" mode, in which the plasma plume extends well beyond the source outlet and physically touches the substrate. This approach is the most commonly utilized in surface processing and exploits plasma source designs and operational conditions allowing the plasma plume to extend as necessary to actually intersect the substrate surface [29].

(ii) The "non-contact" or "non-touch" mode, in which the plasma decays prior to reaching the substrate surface which is, consequently, exposed only to the long lifetime species formed by plasma and transported by the gas flow out of the source [29]. This approach can be used when soft reactive conditions are needed to process very sensitive substrates or to obtain mild surface modifications. It would be also preferable when discharge localization and filamentation at the substrate surface induce the undesired local overgrowth of a thin film or the formation of damaged areas due to localized substrate etching [106]. The non-contact operation mode can be implemented, for instance, by

keeping the plasma source far enough from the substrate or by using designs and/or experimental conditions able to reduce the propagation of the plasma, that in some cases does not even exit out of the device [107,108].

It is important to point out that the above classification is generally based on naked-eye evaluations or imaging investigations (e.g., high-speed imaging techniques) of the plasma during device operation. Therefore, the accuracy with which it is possible to distinguish between the "contact" or "non-contact" operation modes strictly depends on the method used. It follows that, in case of naked-eye observations of weakly luminous plasma plumes, the confident identification of the operation mode can be tricky and the use of high-sensitivity, high-speed imaging techniques is definitely recommended.

The remote operation of AP non-equilibrium plasma jets offers different advantages. First of all, it affords the surface modification of complex and/or big 3D objects [109–111]. This is very often practically unfeasible by using the direct approach, because the narrow gas gaps, typically needed for non-equilibrium plasma generation at atmospheric pressure, impose strict limitations to the shape and dimension of the substrates that can be located in the plasma generation region. The remote approach is generally acknowledged to greatly simplify the surface modification of curved (e.g., cylindrical or tubular objects) or very thick substrates [88,106,112,113]. The direct processing of such types of substrates can, in fact, be trickier because it can imply important changes to the electrode assemblies and/or to the experimental conditions. By using the direct approach, the surface modification of curved objects can require purposely designed electrode assemblies [114]; while, an excessive increase of the applied voltage can be needed for plasma generation when DBDs are used for the direct processing of very thick dielectric substrates. In contrast, curved and thick substrates can be processes by using AP plasma jets without the need of changing either the plasma ignition conditions or the device geometry.

Promising results have been recently reported on the plasma penetration into narrow tubes suggesting possible applications of AP plasma jets for the processing of the inner surfaces of tubes and, more generally, of cavities. Onyshchenko *et al.* [88] used an AP plasma jet to explore the plasma plume penetration inside narrow tubes (inner diameter in the range 0.28-3.00 mm) and the treatment of their inner surfaces to impart hydrophilic character. The plasma penetration was affected by the inner diameter of the tube and that the maximum plasma propagation of 25 cm was obtained for a diameter of 1.02 mm. Indeed, unique opportunities are offered for the surface modification of both the inner and outer surfaces of tubular substrates as very recently reported by Chen *et al.* [112], which used an Ar fed AP plasma jet to modify the outer surfaces of a polymeric tube and, meanwhile, to induce a "transferred" plasma inside the tube to modify its inner surfaces [112,113,115]. Unfortunately, to our best knowledge, no comprehensive studies on etching and deposition into narrow tubes and cavities have been published so far. Moreover, as far as the AP plasma jet processing of complex-shapes objects is concerned, there are not examples in the literature reporting a detailed investigation of the uniformity of deposition processes as well as showing results on coatings conformity.

In addition, due to their remote operation, plasma jets offer a valid plasma tool for the maskless local surface processing of materials (subsection 3.2). They are in fact able to modify only the region of the substrate surface, actually interacting with the plasma plume or, more generally, with the reactive species formed by plasma and present in the gaseous effluent. Unfortunately, this peculiarity highlights the well known limits of plasma jets for the uniform treatment of large area surfaces; however, strategies can be implemented to circumvent this problem, for instance, through the displacement of the plasma jet and/or of the substrate, as well as by using arrays of plasma jets (subsection 3.3).

It follows from all these considerations that, beyond doubt, from the technological point of view, AP plasma jets are among the most compatible plasma sources with continuous

automated production; indeed, offering remote operation in combination with atmospheric pressure and even open-air conditions, they can be also more easily integrated into existing production lines.

However, while appealing, surface processing of materials by using AP non-equilibrium plasma jets can suffer some inevitable disadvantages associated with their peculiar remote operation. Great care and attention are, in fact, required in process optimization, since many factors can affect the characteristics and behavior of the plasma launched outside the device, and interacting with both the surrounding atmosphere and the substrate. All these issues will be addressed in the following subsections.

3.1.1. Plasma plume characteristic features and propagation behavior

The reliable utilization of an AP non-equilibrium plasma jet device in surface processing requires, first of all, the basic knowledge of the main features and general behavior of the so called "free plasma plume". This can be defined as a plasma plume launched into a stagnant gas at atmospheric pressure and room temperature, while no substrate is located downstream of the device outlet, neither a front plate or side walls are present at the source exit or around the source, respectively. This basic knowledge can allow, in a second moment, the better understanding of the influence of both the external environment and the nature of the substrate on the plasma plume characteristics and dynamics.

Since both the composition of the plasma jet feed gas and of the surrounding atmosphere can play an important role in defining the general behavior of the plasma plume in open space [116], it seems important to point out that the examples discussed in this subsection specifically relate to AP non-equilibrium plasma jets fed with helium or argon and operated in open air. Aspects more closely linked to the influence of the surrounding gas composition will be discussed in detail in the next subsection (section 3.1.2).

Some preliminary considerations can be made to highlight that both controlling and handling the plasma outside the physical boundaries of the jet are not trivial tasks:

- The jet device launches the plasma plume in the open space, where the applied field is normally quite low and where, therefore, the plasma can be hardly sustained.
- The atmospheric pressure operation promotes the rapid recombination of the charged species, which can even cause plasma extinction immediately beyond the source exit.
- The inevitable diffusion and mixing of the surrounding gas with the gaseous effluent of the device can significantly alter the plasma plume characteristics and propagation behavior.
- The utilization of high gas flow rates, very often associated with AP plasma jets operation, does not necessarily enhance the plasma plume propagation through the external environment. High velocity gas injection into a stagnant (or still) gaseous medium can induce various phenomena related, for instance, to the formation of turbulent flow regimes, which can severely destabilize and reduce the plasma propagation as well as cause significant entrainment of the surrounding gas.

The primary issue generally taken into account when dealing with a free plasma plume concerns its overall appearance and dimension. Images in Fig. 8a and b allow appreciating the roughly conical shape of the plasma plumes emitted in ambient air by two different devices fed with helium [117]. This is the typical appearance of plasma plumes produced by plasma jets featuring a circular outlet, fed with noble gas and operated in open air. However, different and more complex shapes have been very often reported as in the case of multidart, brush-like and crockscrew-like plumes which may form as a function of the plasma source and the experimental conditions utilized [118−121].

Broadly, the shape and dimensions of the plasma plume can be affected by the jet design, the electric field geometry, as well as by the experimental conditions such as the gas flow rate, the feed gas composition and the discharge excitation parameters (e.g., excitation frequency, applied voltage, input power, discharge pulsing parameters) [118−127]. The scientific

literature shows that many efforts have been made to find strategies to increase the length of the plasma plumes [124] as well as to enlarge or narrow their cross-section perpendicular to the plasma propagation direction [33−35,128].

Among the various operational parameters of an AP non-equilibrium plasma jet, the gas flow rate has undoubtedly a key role in the propagation dynamics of the plasma outside the source and, significantly affects both the shape and length of the plasma plume, as very often revealed by simple naked eye observations. Depending on the device, the length of the plasma plume emerging from the jet outlet can be varied from a few mm to several cm as a function of the gas flow rate, keeping constant all other experimental parameters. The variation of the gas flow rate can also induce changes of the plasma plume shape which often verify when discontinuities occur in the variation of the plume length with increasing the gas flow rate [118−122,127]. In most cases, the plasma plume exits the device with conical shape and its length increases as a function of the gas flow rate until a critical value is reached. Above this flow rate value the plume length starts decreasing, and a more complex plume shape can appear (e.g., brush-like shape or a corkscrew-like shape) [118−122,127]. These evidences generally indicate the occurrence of a transition from a laminar to a turbulent gas flow regime. For any given plasma jet device, the critical flow rate value at which this transition occurs can vary as a function of the discharge electrical parameters (excitation frequency, applied voltage, pulsing parameters, etc.). Structural changes in the plasma source architecture (involving the design of the gas canal and of the source outlet, the position of the electrodes, etc.) can also significantly alter the gas flow regime.

For illustrative purposes, Fig. 9 reports the influence of both the gas flow rate and the pulse repetition frequency on the shape and length of a plasma plume as well as on the gas flow regime of an AP non-equilibrium plasma jet [121]. Results are obtained using a device operated with a HV pulsed power supply and characterized by a coaxial geometry consisting of a single HV electrode (i.e., a stainless steel needle with a diameter of 100 μm), inserted in

the center of the quartz tube (1 mm inner diameter). The distance between the tip of the HV electrode and the exit of the quartz tube is 15 mm. A digital camera is utilized to capture plasma plume photographs with exposure time of 1/10 s, while Schlieren imaging is used to investigate the gas flow dynamics [121] and, more specifically, to reveal refractive index variations due to density gradients in the gaseous medium. In the specific case of a He fed plasma jet operating in open air [121], these density gradients are associated to the presence of air rich and helium rich regions [118].

The pictures of the plasma plume reported in Fig. 9 indicate that, at 8 kHz, the length of the roughly conical plasma plume increases when the gas flow rate is increased up to 2 slm; at 2.5 slm plume shortening occurs and some disturbances are evident at the plume tip [121]. The flow rate value at which plume shortening and disturbances appear decreases with decreasing the frequency from 8 kHz to 3 kHz. Schlieren images show that without plasma, turbulence appears at gas flow rates above 2 slm; in fact, at 2.5 slm (Fig. 9d) a transition from a laminar to turbulent flow regime can be appreciated at a certain distance from the outlet of the quartz tube. In particular, the gas flow exits the device in laminar regime and a laminar region establishes near the device outlet; this region has a certain length (also referred to as laminar length) after which the transition to a turbulent regime occurs [121]. The turbulence, and more specifically the formation of large and small eddies, is responsible of both entrainment and mixing of the surrounding medium (air in this case). When plasma is ignited at 8 kHz, instabilities in the laminar flow regime and turbulences appear at gas flow rates above 1.5 slm; the laminar length decreases by increasing the flow rate, namely the laminar to turbulent regime transition occurs closer to the source outlet. Moreover, keeping constant the flow rate, the laminar length decreases by decreasing the frequency. Interestingly, in all cases, the disturbance at the tip of the plasma plume seems to verify approximately where the turbulent regions begins. It can be, in fact, observed for experimental conditions in which the plasma plume tip reaches the transition region between laminar and the turbulent flow regime (e.g.,

for a flow rate of 2 slm this occurs only at 3 kHz and 5 kHz, because at 8 kHz the plume length is shorter than the laminar length).

The understanding of the above described evolution of the shape and length of the plasma plume as a function of the gas flow rate, first of all, requires the knowledge of the flow characteristic of free gas jets formed into a constant pressure region downstream of a nozzle with a circular exit (i.e., circular gas jets). The observed gas flow regime (or pattern) primarily depends on the initial conditions of the gas jet, namely on the Reynolds number which, in turns, depends on the nozzle exit diameter and the gas velocity at the nozzle exit (i.e., the initial gas velocity). Transitions between different flow regimes can be observed as a function of the Reynolds number for any given nozzle [129−131]. For instance, several publications on gas jets agree that if the Reynolds number is less than 500 the gas jet is laminar (i.e., dissipated laminar jet or fully laminar jet); while at Reynolds number greater than about 500, the gas jet is semiturbulent, i.e., it is characterized by a laminar length after which it becomes turbulent. This laminar length decreases with increasing the Reynolds number and, for Reynolds number greater than about 2000, the flow regime becomes turbulent very close to the exit.

It is very important to emphasize that the above reported threshold values should be considered as indicative only, because a certain dependence on the nozzle geometry and length (profiled nozzle, pipe nozzle, etc.) has been observed. Moreover, gas buoyancy (e.g., in case of a helium jet in air [132,133]) and heating can also influence the characteristics of the flow regime and favor the entrainment and mixing of the surrounding gas [95,133].

Moreover, as evident in Fig. 9, in case of AP plasma jets it is extremely important to be aware that plasma ignition can induce changes or instabilities in the gas flow regimes. Plasma ignition can, in fact, promote the transition from laminar to turbulent regime (see Fig. 9b and c) or affect the transition from the two regimes causing either a decrease (as shown in Fig. 9d) [118,121,134] or increase [118] of the laminar length. Moreover, as shown in a recent study

on high-speed Schlieren imaging of a nanosecond pulsed non-equilibrium plasma jet [127], plasma ignition can cause fluid dynamic instabilities (i.e., a transient turbulent structure) correlated with the high voltage pulses and moving in the direction of the jet flow. These examples allow to understand why, considering the wide range of plasma jets configurations and power supplies utilized, several singularities and deviations from the most common trends can be found in the literature on the propagation behavior of plasma plumes emitted by AP non-equilibrium plasma jets.

Interestingly, the experimental study reported in ref. [117] revealed that, in plasma jets, a fruitful interplay may exist between the gas flow field and the electric field. This study was carried out by using the two different plasma jets reported in Fig. 8 and enlightened that the electric and gas flow fields can act synergistically to enhance the propagation and characteristics of the plasma plume as well as the efficiency in the etching of polymeric materials. The first plasma jet (Fig. 8a) had a coaxial electrode configuration with a central powered electrode of 1 mm diameter and a grounded outer electrode wrapped around a 4 mm diameter quartz tube. This jet had, therefore, a cross-field configuration with its electric field perpendicular to the feed flow field (i.e., electric field being in radial direction and gas flowing in axial direction). The second device (Fig. 8b) consisted of a single powered electrode wrapped around an identical quartz tube (4 mm) and presented a linear-field configuration having parallel electric and flow fields (i.e., both electric and flow fields in axial direction). Both jets were fed with He (flow rate of 10 slm) and operated with a fixed input RF power of 15 W (4 MHz). In the cross-field jet the discharge appeared very intense in the interelectrode region and much weaker outside the quartz tube (plume length of 8.9 mm from the source exit). In contrast, in the linear-field jet the discharge was less intense inside the quartz tube, but its intensity remained high over a longer plume length (12.6 mm outside the tube). The continuous decay of the plasma plume ejected by the cross-field plasma jet indicated that in this device the rapid oscillation of the RF excitation voltage imparts a

radially directed momentum on electrons, making difficult for electrons to be transported axially toward the downstream region. In the linear-field jet, however, the electric field is largely in the axial direction and, hence, imparts an axially directed momentum to electrons. Consequently, in the linear-field device, axial electron transportation to the downstream region is enhanced and this results in a longer and more reactive plasma plume. These evidences are corroborated by results on the etching of polyamide by using He-O_2 feed mixtures. Fig. 8c shows that, for both jet devices, the etch rate increases with the oxygen concentration in the feed and is higher in the case of the linear-field jet. At 0.1% O_2 etch rates of 118 $\mu m \cdot min^{-1}$ and 9 $\mu m \cdot min^{-1}$ were obtained with the linear- and cross-field jets, respectively. The linear-field jet is, therefore, able to achieve 13-fold greater etch rates than the cross-field one, as well as higher ozone concentrations in the plasma plume.

Lastly, in the context of this subsection, mention should be made to the fact that, as revealed by high-speed imaging investigations, the plasma plumes emanated from AP non-equilibrium plasma jets excited by AC or pulsed power supplies have a discrete nature. In fact, although they typically appear as a luminous continuum to the naked eye, they are actually formed by propagation of a series of ionization waves (IWs) travelling with velocities in the range 10^4-10^6 $m \cdot s^{-1}$, much greater than the gas velocity (some tens of $m \cdot s^{-1}$) [4,58,135−138]. The ionization wave fronts are typically characterized by a ring-shaped structure [4,58,137]. They propagate, first, through the device canal and, then, through the gas channel formed in the surrounding atmosphere by the gas flow exiting the device, until the ionization wave dies.

3.1.2. Influence of the surrounding atmosphere

Beyond doubts, the possible influence of the surrounding environment on the final performances of the plasma processes remains one of the most critical issues in surface modification by using AP non-equilibrium plasma jets in both contact and non-contact mode. The remote operation of plasma jets inevitably implies the interaction of the plasma plume

and, more generally, of the gaseous effluent with the surrounding gas. In particular, species from the surrounding atmosphere can diffuse into the effluent inducing changes in its chemical composition which, in turn, can significantly affect both the propagation of the plasma plume and the nature and concentration of reactive species formed in the plasma. Moreover, the formation of turbulent flow regimes and associated eddies (see subsection 3.1.1) can cause significant entrainment and mixing of the surrounding gaseous medium, enhancing the interaction of the plasma plume with the external atmosphere.

Basically, as far as the conditions of the external environment are concerned, when used in surface processing, AP non-equilibrium plasma jets can be operated either in controlled atmosphere or in open air:

(i) The controlled atmosphere plasma processing requires the utilization of an airtight chamber in which the plasma jet device is located [41,108]. Before each plasma process, the chamber is evacuated [108] or purged with high flow rates of a gas (which usually corresponds to the discharge gas) [41], to reduce air and water vapor contaminations. This approach allows having a good control of both the composition and pressure of the atmosphere surrounding the jet during the plasma processes, however, it generally involves an increased cost of apparatuses and processes, associated with the utilization of either vacuum pumps or high purging gas flow rates.

(ii) The open air plasma processing involves merely the operation of the plasma jet in humid ambient air. Open air operation undoubtedly implies less expensive apparatuses and processes; however, additional efforts may be required for process optimization to reduce air entrainment and to obtain reliable and reproducible results. This is especially true in the case of plasma processes suffering from the inevitable compositional fluctuations of ambient air due to relative humidity variations. Strategies have been implemented to protect the plasma from the surrounding air; for instance, plasma jets can be equipped with a shielding gas device able to produce a gas curtain (or shroud) with a defined gas

composition around the plasma plume. This permits to control the atmosphere surrounding the active effluent region of the plasma jet during its operation [139] and minimizes the mixing between the central plasma plume and the ambient air.

As expected and evident from the scientific literature, most processes utilizing AP plasma jets for surface modification are carried out in ambient air. However, open air operation can induce undesirable effects especially when the plasma jet devices are fed with a gas different than air, such as a noble gas (i.e., helium or argon), and/or used in processes particularly sensitive to oxygen, nitrogen and water vapor. Broadly, diffusion and entrainment of these species can lead to undesired oxygen and nitrogen uptake [140] at the plasma-treated surface as well as adversely affect the efficiency of plasma processes in terms, for instance, of deposition and etching rates [141]. Therefore, to better address the main critical issues and challenges associated with open air operation in surface processing, in this subsection the discussion will remain focused on the scientific literature on AP plasma jets fed with a noble gas, also containing low concentrations of reactive additives.

The first point that needs to be examined concerns the key role played by the surrounding air in determining the propagation behavior of the plasma plume in open space [116]. Due to the mixing with ambient air, the gas composition inside the plasma plume emitted by a plasma jet varies both in axial and radial directions [29,123,138,142,143]. This, first of all, can reduce the propagation of the ionization wave front [29,115,142] and the lateral spreading of the plasma plume [142]. In general, it can be said that there is a finite distance of propagation of the ionization wave in open space [29]. For instance, since helium has a lower self-sustaining E/N (electric field/gas number density) than N_2 and O_2, air mixing in He causes an increase of the self-sustaining E/N which is larger in locations where air concentration is larger. As a consequence, an ionization wave propagating through a He plume in ambient air dies as the air contamination within the plume increases the self-sustaining E/N at values greater than the local E/N [29]. Moreover, the He plasma plume does not spread laterally

because the ionization wave are guided through the gas channel formed by the He flow exiting the device and in which the self-sustaining E/N is inevitably lower [142]. Recent results from experimental and computational investigations of He-fed plasma jets allowed proposing that negative ions formed from O_2 in the mixing layer between the He stream exiting the device and air contribute to a focusing of electrons towards the jet axis (i.e., electrostatic focusing mechanism) [144]. They consequently promote to the propagation of guided ionization waves through the helium channel [144].

The diffusion and entrainment of humid air into the plume is also accompanied by the formation of various highly reactive oxygen and nitrogen species (RONS) such as oxygen atoms, *singlet molecular oxygen molecules (*O_2 ($^1\Delta_g$)), hydroxyl radicals (OH), hydrogen peroxide (H_2O_2), ozone (O_3), various nitrogen oxides (NO, NO_2, N_2O, N_2O_5), nitric acid (HNO_3). Oxygen atoms and radicals, for instance, have very short lifetimes and, therefore, are effective only inside or in close vicinity of plasma [8]; while ozone, hydrogen peroxide and nitrogen oxides are long-living reactive species and thus can react even far from the plasma zone where they are generated. The formation of RONS was reported in numerous spectroscopic studies of the plasma phase, in which the evolution of the chemical composition of the plasma plume propagating in open air was investigated [140,145–147].

Experimental studies on the utilization of AP non-equilibrium plasma jets fed with noble gases for the treatment of polymeric materials revealed that oxygen and nitrogen species formed in the gas phase due to air mixing can react at the surface of the substrates affecting their final chemical composition and, specifically, producing nitrogen and oxygen-bearing functional groups [104,137,145–147]. These can be very informative about the specific RONS active at the surface [108,140,148–150].

For instance, Vogelsang *et al.* [140] investigated the treatment of polystyrene substrates by using an argon-fed microplasma jet, focusing on the effects of air entrainment. X-ray photoelectron spectroscopy (XPS) analyses confirmed that the plasma treatment leads to the

uptake of both oxygen and nitrogen at the polymer surface. Interestingly, the high resolution N 1s XPS spectrum of the plasma-treated polymer revealed the presence of oxime (C=N-OH), nitroso (C-NO) and nitrate (C-O-NO_2) functional groups, whose formation was ascribed to the reaction of nitrogen monoxide (NO) with alkyl radicals produced on the polymer surface.

Examples in the literature show that the surrounding atmosphere can significantly alter the final performances of plasma processes. This was reported in the case of the PECVD of fluorocarbon coatings [141] carried out by using a RF plasma jet fed with argon and octafluorocyclobutane (c-C_4F_8) and operated in either nitrogen or air atmosphere. XPS analyses revealed that the chemical composition of the coatings does not change appreciably for the two different atmospheres; however, a significant decrease of the deposition rate from 2 to 0.5 μg s^{-1} was observed passing from the nitrogen to the air atmosphere indicating the detrimental effect of oxygen.

The influence of the surrounding atmosphere was evaluated in a recent study regarding the decomposition of platinum (II) acetylacetonate ([$Pt(acac)_2$]) to form Pt nanoparticles on carbon black (CB) by using an Ar-fed RF plasma jet (Fig. 5c) operated in open air [75]. A mixture of the organometallic precursor and carbon black powder was pressed onto a copper tape and treated using two different configurations: (i) in the "open configuration" the tape was fixed on a glass slide placed at a distance from the jet of 3 or 10 mm; (ii) in the "confined configuration" the tape was placed at the bottom of a 10 mm high crucible, positioned against the plasma jet. XPS analysis showed that the platinum, oxygen and carbon surface atomic concentrations of the as prepared [$Pt(acac)_2$]/CB mixture were about 0.3%, 6% and 93%, respectively. The plasma treatment increased the platinum and oxygen atomic concentrations, and reduced the carbon content. For processes performed in the open configuration, by increasing the distance from 3 mm to 10 mm, the XPS Pt percentage decreased from 9.9% to 3.5%, the C concentration increased from about 72 to about 78% and the oxygen

concentration remained constant at about 18%. No metallic platinum was present in the sample placed at 10 mm distance from the jet; the high resolution XPS Pt 4f spectrum showed, in fact, only the Pt(II) and Pt(IV) components. The minor degradation of the [$Pt(acac)_2$] organic component and the Pt(II) oxidation to Pt(IV) at 10 mm of distance from the jet were correlated with the optical emission spectroscopy (OES) measurements that indicated a consistent drop of the excited Ar species due to collisions with molecules of the surrounding atmosphere. In contrast, in the confined configuration, the Pt content reached 11.4%, the oxygen content was lower than in the open configuration (13%) and a higher amount of metallic platinum was present (75% of Pt was under metallic form). Therefore, it was concluded that the confined configuration is able to minimize the influence of the air contamination, reducing the reaction between the oxygen present in the external environment and the excited species formed by plasma.

Liu *et al.* [151] examined the influence of environmental humidity on the chemical composition, roughness and wettability of ultra-high-modulus polyethylene (UHMPE) fibers treated by an He-fed RF plasma jet (Fig. 5c). With increasing the relative humidity from 5% to 100%, an increase of both oxygen containing groups grafted on the surface and roughness was observed, leading to a higher wettability of the plasma-treated fibers.

3.1.3. Influence of the nature of the substrate

The characteristics and the propagation behavior of the free plasma plume can change significantly when a substrate is placed in front of the device outlet. It is, in fact, essential to be aware that, although not located in the plasma generation region, the substrate cannot be considered as a passive object, especially when plasma jets are operated in contact mode.

Both experimental and modelling studies [141,152–160] demonstrated that the electrical properties of the substrate play a prominent role in determining the dynamics of the plasma-substrate interaction. More specifically, the conductivity and permittivity of the substrate

material can significantly influence the properties of the impinging plasma plume and can affect the plasma propagation towards the substrate, its spreading on the substrate surface as well as the gas flow characteristics [127,141,153,156,158]. Numerous studies highlighted that the plasma plume sensitivity to the electrical properties of the surface being treated derives, firstly, from the fact that when touched by the plasma the surface becomes an element of the electrical circuit of the plasma jet [141,153,155,156,160].

As shown by published works reporting the experimental investigation of the plasma plume/substrate interaction through high-speed time-resolved imaging, discharge localization and formation of intense and constricted discharge channels commonly occur on metal substrates [152,156,158,160]. In contrast, the plasma generally spreads on the surface of dielectric substrates, remaining less intense and more [152,155–158,160]. Bornholdt *et al.* [152] investigated the interaction of the plasma plume, emitted by a coaxial RF plasma jet with a dielectric and a metal substrate, i.e., a glass and copper plate, respectively. The plasma jet utilized in this work is a commercially available device known under the name kINPen and developed by the Leibnitz Institute for Plasma Science and Technology (INP, Greifswald, Germany) and neoplasm tools GmbH. In ref. [152] the device was operated at 1.7 MHz, input power of 65 W, and peak-to-peak voltage in the range 2.5-3.5 kV. High speed imaging allowed the region of interaction between the plasma and the substrate to be observed. In the case of the copper substrate, significant fluctuations of the intensity and position of the discharge were observed and associated to the formation of intense discharge channels (i.e., filaments). In contrast, in the case of the glass plate there was no evidence of filaments formation and the discharge appeared less intense and more homogeneous.

Hofmann *et al.* [156] utilized time and spatial resolved optical and electrical methods to characterize RF driven plasma jets operated in contact (i.e., contact operation mode)with substrates of different conductivity and permittivity (i.e., water, aluminum and glass). Typical electrical conductivity values for are water, aluminum and glass are 0.025, $1 \cdot 10^{7}$ and $1 \cdot 10^{-13}$

$S \cdot m^{-1}$, respectively; while, water and glass permittivity are respectively 80 (at 1 GHz and 20°C, distilled water) and 4.9 (at 1MHz). Two different electrode configurations were studied, i.e., a linear-field and cross-field configuration; for the former the effect of both continuous RF and kHz pulsed excitation was examined. In all investigated cases a significant increase of both the dissipated power and gas temperature was observed when the plasma interacted with water and aluminium. More specifically, the time resolved plasma imaging and the power dissipated measurements indicated that the increase of power is only starting the moment the plasma touches the conductive substrate (power increase up to a factor of 3). The increase of power was attributed to a change of the equivalent electrical circuit, leading to a more favorable matching between the power supply and the plasma source. In addition, when in contact with a conductive substrate, in all cases the gas temperature of the plasma jet increased by up to 80°C.

Ref. [153] reported the computational investigation of a plasma plume ejected from an AP plasma jet (coaxial configuration similar to that of the above mentioned kINPen) sustained in a He/O_2 mixture, flowing into humid air, and impinging onto a surface in contact with ground and whose electrical properties were varied. In particular, dielectric surfaces with relative permittivity ranging from 2 (typical for polymers) to 80 (typical for liquid water) were taken into consideration, along with a grounded metal surface. Results showed that the relative permittivity of the surface significantly affects the discharge dynamics as well as the production of charged and reactive species. The increase of the relative permittivity enhances the speed of the ionization wave towards to the surface, increases the electron temperature as well as the electron and ion density in the plasma column. Therefore, a more conductive channel is formed between the inner pin electrode and the treated surface. The higher electron density and temperature in the conduction channel and at the surface increase the production of reactive neutrals (e.g., atoms, radicals, metastable species) that can be of interest in surface processing. In contrast, a lower permittivity of the substrate results in a

weaker ionization wave with lower production of charged species and reactive neutrals within the conductive channel and on the surface. However, low values of relative permittivity promotes the penetration of the electric field into the treated material, as well as the formation and propagation of a surface ionization wave, which enables greater spreading of the plasma along the surface [153,159].

These findings complement with the experimental evidences reported by Vogelsang *et al.* [141] regarding the deposition of fluorocarbon coatings on substrates with different permittivity by using a RF plasma jet fed with argon-octafluorocyclobutane mixtures. Specifically, an aluminum foil, a silicon wafer and a polystyrene (PS) sheet were selected as conductor, semiconductor and dielectric substrates, respectively. In case of the Al substrate, thin film deposition occurred only when the input power was greater than 30 W, which corresponded to the minimum power required to allow the discharge to come into contact with the substrate. Under these conditions a strong localization of the discharge was observed in the form of three constricted and intense discharge channels. As a consequence, the deposition on the metal substrate was found to be very inhomogeneous and showed a distinctive pattern consisting of three deposited patches where a high local growth rate (2.4 $\mu m \cdot min^{-1}$) was obtained. When the Si wafer was used under the same experimental conditions, the deposition rate decreased while the deposited area appeared to be more homogeneous. In contrast, in case of the PS substrate, no deposition could be achieved at all. The authors rationalized these results hypothesizing that at the input power of 30 W, when the discharge comes into contact with the Al or Si substrate, a transition from a α-mode to a γ-mode occurs in the discharge zone between the orifice of the jet and substrate surface. The prerequisite for the formation of the γ-mode appeared to be the utilization of a conductive substrate, that touched by the discharge can enter to be an element in the electrical circuit of the plasma jet, specifically acting as second grounded electrode. The deposition of the fluoropolymer occurred only on metallic and semiconductor substrates which allowed the

formation of the constricted and localized γ-mode able to produce an increase of the concentration CF_x radicals in the close vicinity of the substrate. In the paper a simplified equivalent circuit diagram of the jet–substrate system is presented to clarify the observed dependence of the discharge regime on the choice of substrate material conductivity.

Very recently, Wang *et al.* [160] reported an experimental study on the temporal and spatial evolution of the interaction between the plasma plume emitted by a He-O_2 fed plasma jet and samples consisting of a 4 μm thick parylene-C film deposited on three different substrates, i.e., Si, Cu and glass substrates. It was found that the conductivity of the substrate material significantly influences the interaction of the plasma with the sample and determines different etching mechanisms of the parylene-C film. In particular, as clearly evident in the discharge pictures taken at different etching times in Fig. 10a-c, when the parylene-C film is deposited onto a glass substrate discharge spreading occurs. The optical microscope images of the etched holes and the corresponding depth profiles (Fig. 10d-f) show that the diameter of the circular etched region (about 900 μm) remains constant with increasing the etching time, confirming that the polymer is gradually etched with a layer-by-layer mechanism. In contrast, when the polymer is deposited on Si or Cu substrates, initially the plasma spreads on the surface and a layer-by-layer etching occurs (Fig. 10g corresponding to a Si substrate). Then at a certain treatment time (12 s for a Si substrate) the film is completely removed at a point near the center of the plasma plume on the surface, as evident from the optical microscope image and "V" shape depth profile in Fig. 10h. From then on, the plasma remains confined in the etched hole, directly coupled to the conductive substrate, and its luminous intensity and the dissipated power increase. Under these conditions the plasma starts to etch the film in radial direction producing a progressive enlargement of the etched hole diameter up to about 600 μm (Fig. 10i).

Finally, another very important aspect to be considered is the influence of the substrate relative permittivity on the flow dynamics of the impinging plasma plume, that has been

experimentally investigated through Schlieren imaging by various authors. Boselli *et al.* [127] reported the critical role of the substrate nature on the gas flow regime of a He fed nanosecond pulsed plasma jet with single-electrode geometry. As reported in Fig. 11a and b, they observed a drastic decrease of the turbulent behavior of the gas flow of the plasma jet at the impinging region passing from a bare metallic substrate to one covered by a dielectric layer. They were also able to track turbulent front propagating along the metal substrate surface by using high speed Schlieren imaging. On the other hand, in case of a He fed microsecond pulsed plasma jet device with coaxial DBD electrode configuration, Robert *et al.* [118,132] observed a significant modification of the helium flow behavior when the plasma was ignited in the presence of a metal target downstream of the source outlet, resulting in a channeling of the He flow towards the target (Fig. 12a and b) [132]. Gas flow channeling after plasma ignition (Fig. 12b) was able also to reduce buoyancy effects associated to the low density of helium, which can diffuse in the ambient air, flowing preferably in upwards direction without plasma (Fig. 12a) [132]. More pronounced channeling was observed when the metal substrate was grounded rather than floating. These experimental results suggest a more effective transport of reactive plasma-generated species to the substrate during plasma processes and allow envisaging the possibility of tuning the plasma-substrate interaction through substrate biasing.

3.2. Localized small area surface processing

The localized surface modification of materials is considered one of the most peculiar applications of AP non-equilibrium plasma jet technology. As already mentioned in the previous sections, plasma jets are able to modify only a small area of an unmasked surface, corresponding to the region of the substrate surface interacting directly with the plasma plume or, more generally, with the reactive plasma-generated species present in the gaseous effluent of the device.

The localized surface modification can be, for instance, realized by using plasma jets with circular outlet in two basic operation modes: (i) keeping both the source and the sample in fixed position to obtain, generally, plasma-treated circular spots (i.e., static operation mode) [35,107]; (ii) moving either the plasma source or the sample at a controlled scan speed along a line to obtain a plasma-treated track (i.e., dynamic operation mode) [161,162]. The diameter of the treated spots and the width of the treated tracks can vary from a few microns [34,35] to a few millimeters (very often less than 10 mm) [41,163] and are roughly dictated by the diameter of the device outlet. It is, in fact, widely acknowledged that they can be considerably greater than the device outlet diameter and vary significantly with the experimental conditions such as the source-to-sample distance, the gas flow rate, the discharge electrical excitation parameters, the process duration, the displacement speed. Also the substrate material can influence the final dimensions of the treated area since discharge localization and spreading are often observed in the case of conductive and non-conductive substrates, respectively (subsection 3.1.3.) [141,160]. Therefore, a careful optimization of the device design and operation conditions is needed to achieve a precise control of the treated area dimension as well as good repeatability and uniformity in terms, for instance, of thickness of the deposited/etched layer, chemical composition, wettability, etc..

As evident from the scientific literature, over the years, the localized surface processing has been investigated with various objectives and perspectives: (i) to address specific applications which strictly require the precise and localized small area surface modification (e.g., surface patterning) [33–35,65]; (ii) to optimize the operation conditions of plasma jet devices also in view of the large area surface processing through plasma source/sample displacement [41,53,91,164–166]; (iii) to investigate in more detail the plasma plume-surface interaction as well as to gain insights into etching/deposition mechanisms [57,160,164,165]. The aim of this section is to summarize what has been done on this subject so far; various examples on the

localized etching, deposition and treatment will be reported with particular focus on the optimization of the plasma source design and of the process conditions.

Localized etching

Various studies investigated the localized etching of silicon [167,168] and of different polymers (e.g., polyethylene, polystyrene, photoresist) [17,169]. Line etching experiments showed that the depth and width of the etched tracks are significantly affected by the source-to-substrate distance and the scan speed of the source over the substrate (i.e., the etching time) [17,167]. In the case of photoresist etching by using an O_2-fed corona microplasma jet (hollow needle with inner diameter of 0.40 mm connected to a RF power supply), the full width at half maximum of the etched profile was found to decrease from about 1.1 mm to about 0.2 mm with increasing the scan rate of the jet from 1 to 20 $mm \cdot s^{-1}$ [17].

Polymer etching experiments in static mode operation allowed enlightening that the shape of the depth profiles across the etched area can depend on the feed mixture composition. Fig. 13a shows results on the etching of a poly(ether ether ketone) (PEEK) substrate by using a RF plasma jet operated in ambient air and fed with pure Ar or with Ar-O_2 mixtures (etching time of 20 min, device outlet diameter of 1.6 mm) [169]. In case of a pure Ar plasma a ring-shaped profile can be observed, i.e., the etching takes place mainly off the jet axis (maximum depth of about 10 μm, corresponding to a etch rate of about 0.5 $\mu m \cdot min^{-1}$), while at the jet axis almost no etching occurs. This depth profile could be ascribed to the formation of eddies which cause air entrainment and hence lead to the production of reactive oxygen species capable of polymer etching. The special shape of this profile shows the main role of chemical etching by oxygen containing species, while physical etching due to ion bombardment (e.g., Ar ions formed in the Ar-fed plasma impinging on the PEEK substrate) seems to be not effective. At low O_2 concentration in the feed (0.2%), the etch depth increases but the two off-axis depth minima are still present likely because the contribution of entrained ambient air

to polymer etching is still remarkable. If the O_2 is increased to 1%, the etch rate has its maximum at the jet axis, the profile is almost symmetric and can be described by a single Gauss function. The maxiumum depth is 67 μm and corresponds to a etch rate of about 3.4 $\mu m \cdot min^{-1}$.

Moreover, as discussed in detail in section 3.1.3, the investigation of the localized etching in static operation mode of thin polymeric films deposited on different substrates revealed that the etching mechanism can change depending on the substrate conductivity [160]. Also the diameter of the etched hole varies as a function of the substrate materials and appears larger when the polymeric film is deposited onto a dielectric substrate (Fig. 10f and i).

Localized deposition

Numerous published studies reported the localized deposition of organic and inorganic thin films by using various AP non-equilibrium plasma jets operated in static mode. Very often these studies are not motivated by the precise intent of depositing a thin film in a small localized area, but, on the contrary, they are carried out to optimize the plasma source design and operating conditions in view of the uniform large area deposition [53,91]. Deposits with circular shape and diameter ranging from a few hundreds of microns to several mm (e.g., 10-20 mm) are obtained [41,53,91,170]. Coating thickness profiles are generally symmetrical respect to the jet axis, with maximum at the center of the deposited spot [41,91,166,171 – 173], as shown in Fig. 13b reporting the thickness profile of a polymeric deposit obtained by using a cylindrical coaxial DBD jet fed with helium, acrylic acid and ethylene mixtures (outlet diameter of the source of 6 mm) [41].

However, axisymmetric thickness profiles showing a minimum at the center were also reported; they correspond to annular deposits or to circular deposits with a central thickness minimum that can be obtained with decreasing the source-to-substrate distance [164] or increasing the gas flow rate [165]. Schäfer *et al.* [165] reported the experimental and

theoretical investigation of thin film deposition from Si-containing precursors using a RF plasma jet. The flux of precursor fragments onto the target surface was calculated through a two-dimensional axisymmetric fluid model. Results showed that, in agreement with measured profiles of the film thickness, the radial profile of the particle flux strongly changes with the flow rate and ring-shaped radial profiles are more evident with increasing the flow rate.

On the other hand, asymmetric deposition profiles were obtained due to misalignments of the plasma source assembly (e.g., in case of concentric electrode configurations) [171], to too short source-to-sample distance [91,171] or to turbulences and large vortices that can form at the source outlet when the admission of the thin film precursor downstream of the plasma source is not adequately optimized (see plasma jets in Fig. 3b with a hollow inner electrode for downstream injection of the precursor) [174].

Another important aspect taken into consideration in process optimization is the chemical uniformity of the deposited coating. Different studies [41,163] reported the possibility to achieve a uniform chemical composition over the deposited area, even if the film thickness is not constant. Fig. 13b shows that, in case of polymeric coatings deposited from acrylic acid-containing plasma, the percentage of carboxylic groups in C1s XPS spectra does not change significantly as a function of the position across the deposited spot [41]. However, studies regarding the thin film deposition from organosilicon precursors [164] revealed that an evolution of the chemical composition of the coating (e.g., of the organic character of the coating) can be observed across axisymmetric deposited spots.

The potential of microplasma jets for the localized deposition of thin films and nanostructured materials on small areas was demonstrated by numerous published works [32,68,161,170,175]. A short overview of microplasma utilization in this field is provided in ref. [15]. For instance, mound-shaped and tower-shaped deposits composed of tungsten oxide nanoparticles were obtained at high growth rates [32,161] by using a ultrahigh-frequency (450 MHz) inductively coupled microplasma jet in which a sacrificial tungsten wire was

inserted (Fig. 4f). Fig. 13c reports the scanning electron microscopy (SEM) image of a typical tower-shaped deposit (base diameter and height of about 100 μm and 500 μm, respectively) obtained within a few seconds at a growth rate of 50 $\mu m \cdot s^{-1}$ [161]. The deposition of stripes of nanostructured metal oxides was also demonstrated with line widths of 30 μm by using a microplasma jet with outlet diameter of 50 μm [161].

Localized treatment

Significant results have been reported on the maskless localized surface treatment of various polymers [35,65,107,140,162,176,177] and inorganic materials [34,179,180], for the grafting of oxygen and nitrogen-containing groups. Microplasma jets appear to be very promising in this field and numerous studies report their utilization for generating hydrophilic circular spots and linear tracks on various surfaces [65,162]. Considerable efforts have been directed to obtain a fine control of the spatial distribution of the plasma treatment as well as to reduce the treated area closer to the size of the device outlet.

Doherty *et al*. [65] reported the spatially resolved surface modification of PS substrates by using a He-fed microplasma jet with DBD electrode configuration and 100 μm outlet diameter. The device was operated in static mode, at the source-to-sample distances of 1 and 10 mm, for a treatment time of 20 s. The plasma was generated at 10 kHz and 8 kV, varying the helium flow rate (25-200 sccm). The plasma treatment was able to produce a defined reduction of the WCA (from about 80° to less than 30° for the untreated and plasma-treated regions, respectively) in a circular area with a diameter of 1.5 mm or more, markedly larger than the size of the device outlet and of the visible plasma plume. WCA profiles revealed the dependence of the treated spot diameter on both the source-to-sample distance and the gas flow rate. The sharper decrease of the WCA and the narrower spot were obtained at 1 mm and low flow rates. Spatially resolved XPS analyses confirmed that the decrease in WCA corresponds to a local increase in the surface oxygen content.

Szili *et al.* [107] investigated the localized surface treatment of PS substrates by using a neon-fed microplasma jet operated in static mode and equipped with an outlet capillary glass tube with length and internal diameter of 50 mm and 0.7 mm, respectively. They were able to effectively reduce the size of the treated area by decreasing the applied voltage in order to contain the discharge within the capillary tube. Keeping constant the discharge excitation frequency (10 kHz), at 4.5 kV the visible glow of the microplasma jet was confined within the capillary tube and produced narrower treated areas (Fig. 13d) compared to when the visible glow extended 3 mm into the ambient atmosphere at 8.0 kV. An enlargement of the treated area was observed with increasing the treatment time (WCA profiles in Fig. 13d). It is worth mentioning that, since the source outlet-to-sample distance was 5 mm, plasma treatments were carried out in non-contact operation mode. The optimized parameters were then applied to produce smaller treated areas of 200 μm in diameter using a microplasma jet equipped with a 142 μm inner diameter capillary tube.

In agreement, with results obtained in static mode operation, studies carried out in dynamic mode operation showed that the increase of the scan speed (corresponding to a decrease of the treatment time) and of the source-to-sample distance can produce narrower plasma-treated tracks [162,176,177]. Typical scan rates ranged between a few hundred microns to a few tens of millimeters per second.

Promising results have been reported on the micrometer scale surface patterning by using AP non-equilibrium plasma jets with outlet diameter variable from a few microns down to 100 nm, which allow the precise control of the resolution of the plasma-treated dots. In particular, very recently, nanocapillary atmospheric pressure plasma jets [33–35,178] were proposed for the ultra fine maskless surface functionalization of polymers [35,178] and carbon nanotubes dot arrays [34] for biosensing and related biomedical applications. Motrescu *et al.* [35] reported the chemical patterning of polymeric surfaces though localized grafting of amine groups. The plasma source presented a DBD coaxial geometry and consisted of two copper

ring electrodes on a quartz tube with internal diameter of 4 mm (electrode configuration similar to Fig. 3a). The tip of the quartz tube had an aperture size of 1 μm and 100 nm; a functionalized dotted matrix was obtained by using as sample holder a computer controlled x-y stage. The plasma process consisted of two steps: (i) the pretreatment for surface activation by using a pure helium plasma, and (ii) the treatment for grafting of amine groups by using helium-ammonia fed plasma. During the pretreatment, negative DC bias (-500 V) was applied on a metal grid placed under the samples; the bias application during the pretreatment was mandatory to ensure the grafting of amine groups in the treatment. The visualization of the patterns was done by fluorescence microscopy after reaction of the surface-grafted amine moieties with a fluorescent dye. It was observed that, going from the 1 μm to the 100 nm tip aperture, the diameter of the patterned dots decreases almost ten times for the same processing conditions. In fact, at the fixed He-NH_3 plasma treatment duration of 1.5 s, the increase of the pretreatment time from 0.1 to 3 s caused an increase of the diameter of the treated dots from about 20 μm to 100 μm and from about 2 μm to 10 μm by using the tip apertures of 1 μm and 100 nm, respectively. Fig. 13e reports fluorescence images examples of the dotted patterns obtained for the two tip apertures at the shorter pretreatment time [35].

3.3. Towards large area surface processing

Without doubt, the small size of the treated areas inevitably associated with the utilization of single plasma jets in static mode operation is considered one of the major drawbacks of AP non-equilibrium plasma jet technology in the perspective of large scale applications. As discussed in the two following subsections, proposed strategies towards large area surface processing involve the displacement of either the plasma source or the sample holder and/or the utilization of arrays of plasma jets. Critical aspects related to the utilization of these two

strategies will be discussed, with particular focus on the uniformity of the surface modification.

3.3.1. Plasma source/sample holder displacement

The most utilized approach to enlarge the treated area in plasma jet technology exploits the displacement of the plasma source and/or of the sample holder [91,181,182]. In principle, this strategy is easy to implement, however careful optimization is required to achieve an adequate control of the final uniformity of the treated surface. To treat large areas by using plasma jets, successive scans of the source are performed over the sample surface, at a specific distance from each other. Otherwise keeping fixed the plasma jet, the sample can be scanned under the source by using a xy-motorized stage (Fig. 1).

Displacement speeds up to some tens of meters per minute were reported [95,97,101,184,185]. Different studies showed the influence of the scan parameters (e.g., the displacement speed, the distance between two consecutive tracks) on the extent of the surface modification. For instance, regarding the plasma treatment of polymeric surfaces for wettability improvement, it was shown that, as expected, the decrease of the scan speed (i.e., the increase of the treatment time) results in a decrease of the WCA of the treated surfaces [184]. In the case of deposition processes, the coating thickness generally decreases with increasing the scan speed [185]; interestingly, thin films characterized by superior retention of the precursor structure can be obtained at high scan speeds, due to the reduced interaction of the plasma with the growing layer [96].

Considerable efforts are required to obtain coatings with a uniform thickness and chemical composition over large areas. It was enlightened that the knowledge of the static deposition profile of the plasma source is a fundamental prerequisite for the dynamic thin film deposition [164]. On the other hand, the investigation of the deposition of a single track is essential for the optimization of the scan parameters in the track-by-track deposition over

larger areas. Merten *et al.* [183] reported a comprehensive study on the single tracks deposition of organosilicon coatings deposited by using a low temperature arc jet (section 2.3). The deposition profile of the track perpendicular to the source displacement direction is symmetrical respect to the jet axis and shows a central maximum; an axisymmetric evolution of the chemical composition of the coatings was also revealed at different positions across the deposition profile. On the basis of this knowledge it was possible to optimize the track-by-track deposition and in particular the optimum distance between two consecutive tracks to obtain a large area deposition with an overall inhomogeneity in layer thickness of less than 3.5%.

3.3.2. Arrays of plasma jets

The utilization of one-dimensional (1D) [66,111,186,187] or two-dimensional (2D) [25,188–192] arrays of plasma jets has been also proposed to enlarge the treated area. Very often this strategy is reported in combination with source/sample holder displacement to improve the uniformity of the process and further enlarge the treated area [187].

Recent studies have shown that the unique challenge of scaling plasma jet arrays is that individual plasma jets tend to interact with each other through various mechanisms (electrostatic, hydrodynamic, photolytic and chemical interactions [29,189,193–195]). Jet-to-jet interactions can lead to non-uniformity, instabilities, and even to quenching of some individual plasma plumes in the array [29,189]. Therefore, careful optimization is required to obtain simultaneous operation of all the jets of the array with good jet-to-jet uniformity both in time and in space [189]. Jet-to-jet interactions can also result in the merging of the plasma plumes, as observed in the case of densely packed arrays in which the spacing between the jets is reduced [29].

Fig. 14 shows the photographs of a jet array device consisting of seven quartz glass tubes densely packed in a honeycomb configuration, with a single tube in the center of the array and

the remaining six quartz tubes surrounding the centered one [190]. As a function of the gas flow conditions, this device can operate in two different modes, i.e., an intense plasma mode (Fig. 14a) and a well-collimated plasma mode (Fig. 14b). In particular, when the He gas velocity ranged between 4.6 and 10.6 $m \cdot s^{-1}$ (corresponding to a flow rate of 1.5–3.5 slm), due to jet-to-jet coupling, the formation of an intense plasma plume highly concentrated at the center quartz tube was observed (Fig. 14a). A further increase in the He linear velocity resulted in seven well-collimated plumes (Fig. 14b).

4. Plasma jet technology applications in surface modification of materials

Over the last two decades, the interest of both the academic and industrial communities has considerably expanded to the utilization of atmospheric pressure non-equilibrium plasmas in surface processing of materials. In particular, intense efforts have been made to adapt the classical plasma etching, deposition and treatment processes to the distinctive remote operation of plasma jets as well as to open air conditions.

The aim of this section is to give the general sense of what has been accomplished so far, and where the research is going. Therefore, a brief overview of the available applications and recent developments of plasma jet technology in surface modification will be given, with special focus on studies published from 2010 onwards in the field of plasma etching, deposition and treatment. For the sake of completeness, this section includes also examples on surface on plasma processes using low temperature arc-based jets (section 2.3).

4.1 Etching

First examples on dry etching of various materials with AP non-equilibrium plasma jets date back to the nineties; in particular, they refer to the utilization RF driven jet devices fed with He and reactive additives such as CF_4 and O_2 for the etching of inorganic materials (e.g., Si, SiO_2, W, Ta [17,31] and polymers (e.g., polyimide) [31,72], respectively. Nowadays, fundamental research in this field is still active and, in fact, in the last few years, comprehensive studies were published on the etching mechanism [160,168,169,197] as well as on the evolution of the chemistry and morphology of the etched surfaces in case of both polymers (parylene-C, PEEK, PE, photoresist etc.) and inorganic materials (Si [168] and fused silica [197]).

As far as inorganic materials etching is concerned, recently, a plasma jet-based machining technology was proposed for ultra-precision surface finishing of optical elements made of silicon and silicon-containing materials like fused silica and silicon carbide [198,199]. More

specifically the shaping and the shape correction of optical surfaces with high material removal rate and high spatial resolution was reported.

Plasma jets are currently utilized for surface cleaning [110,200–203], e.g., for the removal of carbon layers from flat surfaces and inside deep and narrow gaps [110]. These processes appear very efficient and cost effective when carried out using air as feed gas. Various commercial devices have been developed for the surface cleaning of metals, glass and ceramics; they are used, for instance, for the removal of organic residues on printed circuit boards before the next steps of production [51,94,204–206].

As it will be also evident from the following subsections, nowadays, AP non-equilibrium plasma jets are by far less used in etching than in thin film deposition and treatment. This may reflect the limited utilization of plasma jet sources and, more generally, of AP non-equilibrium plasmas for microelectronics applications. A possible explanation could reside in the fact that under atmospheric pressure conditions, the kinetic energy of ions impinging the surfaces is very low (see section 2.2.3). The lack of an effective ion bombardment intrinsically makes anisotropic etching with high aspect ratio very challenging, and, therefore, definitely reduces the potential of atmospheric pressure non-equilibrium plasma processes in microelectronic manufacturing as compared to the low pressure counterpart. The material removal by using AP plasma jets and, more generally, AP non-equilibrium plasmas, remains dominated by an isotropic purely chemical etching mechanism [168,169,198,199].

4.2 Deposition

AP plasma jets are currently widely utilized for the preparation of inorganic, organic and hybrid multicomponent thin films as well as of localized structures [15,19,22,23]. The research is very rapidly evolving in this direction and, over the last few years, many papers have been published on the optimization of a plethora of plasma jet devices for thin film deposition as well as on the exploration of new processes. Different deposition strategies have

been used such as the plasma-enhanced chemical vapor deposition (PECVD), the aerosol-assisted plasma deposition (AAPD) [45,207] and evaporation/sputtering-based techniques [15]. In particular, aerosol-assisted processes have appeared to be particularly convenient, and can even offer the only possible solution, when non-volatile (and eventually thermolabile) precursors, solution or dispersions need to be injected in the atmospheric plasma [11,21]. It is worth mentioning that aerosols are scarcely utilized in combination with low pressure plasmas. This is due to fact that the handling of aerosols at low pressure is very difficult and problematic (e.g., for the risk of contamination of the vacuum chamber with liquids) in particular if deposition processes need to be carried out at room temperature. On the other hand, evaporation/sputtering-based approaches are, for instance, associated to the utilization of microplasma jets in which a sacrificial metal wire electrode is directly exposed to the discharge. Heating of the wire electrode during the process is believed to be responsible of metal evaporation or sputtering of surface atoms at lower ion energies [15,175]. Recent developments in thin film deposition by using AP plasma jets are reported below and grouped as a function of the chemical nature of the deposited coatings.

Inorganic thin films

In the last years, the deposition of SiO_x thin film has been widely investigated by using many different plasma jet devices and organosilicon precursors (e.g., hexamethyldisiloxane, tetraethoxysilane, octamethylcyclotetrasiloxane, and tetrakis(trimethylsilyloxy)silane) [30,95,164,165,172,181,208,209]. Growth rates as high as 60 $\mu m \cdot min^{-1}$ have been reported for smooth SiO_x coatings by using the low temperature arc jet of Fig. 7a [95].

The deposition of various metal oxides (e.g., titanium oxide, zinc oxide and various doped and mixed oxides) has been also widely reported [77,98,175,210,211]. For instance, Collette *et al.* [210] deposited TiO_2 coatings using a RF atmospheric plasma jet (configuration similar to Fig. 5c) fed with argon, oxygen and vapors of titanium isopropoxide. Anatase TiO_2

structure was observed by Raman spectroscopy after annealing at 450°C. The crystallization of the coating induced an improvement of the photocatalytic activity evaluated investigating the degradation of the methylene blue.

As far as metal coatings are concerned, recently, the deposition of highly conductive Cu thin films [212–215] have attracted growing attention due for instance to their high conductivity [12,214] and bactericidal properties [215].

Organic thin films

A plethora of polymeric thin films have been deposited over the last few years, e.g., hydrocarbon [173,209,216], organosilicon [53,182,217–221], fluorocarbon [166,207,221], polyethyleneoxide-like thin films [55,80,223] and polymeric coatings containing carboxylic acid [41,81,96,97,100,103,224–226] or amine[163] functional groups.

Much attention has been devoted to the deposition of various fluorocarbon and organosilicon coatings due to their final hydrophobic properties [53,166,207,221]; superhydrophobic behavior has been obtained in case of nanostructured coatings [53,218]. Organosilicon coatings have been also widely studied due to their corrosion protection, wear resistance and antifrictional properties [42,217,220]. Múgica-Vidal *et al.* [227] reported the deposition of hydrophobic and wear resistant coatings on glass substrates by using a DBD plasma jet fed with nitrogen and the aerosol of mixtures of heptadecafluoro-1,1,2,2-tetrahydrodecyl)trimethoxysilane (FLUSI) and aminopropyltriethoxysilane (APTES). Since it was observed that coatings based on FLUSI are hydrophobic but exhibit a low wear resistance, while those obtained from APTES are able to enhance the wear resistance but have a hydrophilic character, the aim of the work was to determine the optimal mixture of precursors able to produce a satisfactory coating in both characteristics.

The study of deposition of polyethyleneoxide-like thin films [55,80,223] and of various polymeric coatings containing carboxylic acid groups [81,96,97,100,103,226] have been

mainly intended for biomedical applications. In particular, efforts have been recently devoted to the preparation of coatings containing carboxylic groups and stable in water [41,97,100,224]; enhanced water stability was obtained through codeposition of acrylic acid with methylene-bis-acrylamide [97,100] and ethylene [41,224].

Hybrid nanocomposite coatings

Organic-inorganic nanocomposite coatings consisting of inorganic nanoparticles (NPs) embedded in an organic matrix have been recently deposited by atmospheric pressure plasma jets [228–231]. Commonly, the deposition process involves the injection of preformed inorganic nanoparticles in the atmospheric pressure plasma along with the precursor of the organic matrix. The first study on this approach was published in 2011 [228] and reported the deposition of organosilicon polymer/TiO_2 NP nanocomposite coatings by injecting in a corona plasma jet dispersions of TiO_2 NPs in tetramethoxysilane (TMOS). Different alcohols (i.e., methanol, pentanol and octanol) were added to the dispersions, even at high concentration (i.e. 50 %), to improve their stability and, therefore, to enhance the homogeneity and thickness of the plasma-deposited coating. Very recently, Liguori *et al.* [231] presented the deposition of nanocomposite coatings consisting of silver NPs embedded in a plasma-polymerized polyacrylic acid matrix obtained using a feed mixture composed of argon, vapors of acrylic acid and a dispersion of Ag NPs in ethanol. The most appealing advantage of this deposition approach is the fact that, due to the aerosol utilization, in principle any type of preformed NPs can be injected in the plasma and incorporated in the coating, provided that a good dispersion of the NPs in a suitable solvent is obtained [21]. This strategy seems very different from the numerous low pressure plasma processes (e.g., sputtering-based processes) in which the formation of both the matrix and the inorganic particles of the nanocomposite coating occurs in situ and in a single step [21].

Contrary to the previously examples in which preformed NPs were used, Beier *et al.* [230] reported a deposition process in which Ag nanoparticles were synthesized in situ in the atmospheric pressure plasma. Specifically, in this process the plasma jet was fed with air, vapors of hexamethyldisiloxane (HMDSO) and the aerosol of a silver nitrate ($AgNO_3$) solution in water and isopropanol, to obtain in a single step and at atmospheric pressure an inorganic NC coating consisting of Ag NPs embedded in a SiO_x matrix.

4.3 Treatment

The utilization of AP plasma jets for the treatment of a large variety organic and inorganic materials has received enormous attention and a wide range of processes has been proposed for many different applications since the late nineties [232–239]. In particular, in the last decades, AP plasma jets have been primarily used for the treatment of polymeric surfaces to increase their surface energy and, therefore, to improve their wettability as well as their adhesion to inks, glues, adhesives and metal coatings [232–237], etc.; many commercial devices have been also developed for this purpose [49,51,52,94,240,241]. The studies on the subject published before 2010 widely showed that the plasma jet treatment is able to effectively modify the surface chemical composition (i.e., through the grafting of polar oxygen- and nitrogen-containing chemical functionalities and the change of the crosslinking degree) as well as to induce a variation in the surface roughness (e.g., an increase of the roughness [99]).

Although wettability and adhesion enhancement represents a well-established application of plasma jets, the research in this field is still active nowadays, as demonstrated by the presence of many recent fundamental and applicative publications on the treatment of both synthetic polymers [38,65,101,107,112,113,184,242–252], natural organic materials (e.g., cellulosic materials such as paper and cotton) [253,254] and inorganic materials (e.g. metals) [255–257].

Particular attention is given to the optimization of the operation conditions of the plasma sources to reduce the treatment time as well as the aging of the treated surfaces predominantly due to the hydrophobic recovery mechanism [74,101,112,113,184,242–244] The latter involves the reorientation of plasma-grafted polar groups into the bulk of the material during air storage, therefore, causes a decrease of the hydrophilicity imparted by the plasma treatment with storage time [243].

In recent years, significant efforts have been directed both to improve the spatial resolution in localized plasma treatments [35,65,107] and to obtain uniform and fast treatments over large areas [184]. Plasma processes are commonly carried out using air or nitrogen as feed gas [101,184]. This is without doubt the less expensive option which renders atmospheric pressure technologies very attractive compared to low pressure plasmas processes in particular for in-line open-air processing. However, the use of noble gases (e.g., He and Ar) with eventual admixture of reactive additives (e.g., oxygen, water vapor, ammonia, nitrogen) is also widely reported [34,35,38,140]. Unfortunately, feed mixture dilution with noble gases increases the process cost, however it offers the advantages of a lower breakdown voltage and of a better control of the plasma chemistry.

The continuous research in this field is highly motivated by biomedical applications, where the presence of polar groups is required to promote the cell cultures and biomolecule immobilizations [34,35]. With this purpose, the processing of both polymers and inorganic materials (e.g., titanium surfaces, carbon nanotubes, silver nanowires) has been very recently reported [34,255,256]. Plasma jet treatments of polymers have been also investigated in the last few years for the fabrication of efficient devices in the field of flexible electronics, dye sensitized solar cells and litium-ion batteries [248,250,251].

It is worth mentioning that a few recent studies reported the utilization of plasma jet treatments for applications different than wettability and adhesion enhancement. Examples include the preparation of Pt nanoparticles on carbon supports through decomposition of

organometallic precursors for fuel cells applications [75] and the localized sacrificial oxidation of Si substrates before wet chemical etching of the oxide layer [179].

5 Conclusion

A critical literature review on the utilization of AP non-equilibrium plasma jets in surface processing of materials has been provided. Basic concepts on the architecture of the plasma sources have been summarized and the various strategies adopted to obtain non-equilibrium plasma conditions at atmospheric pressure have been presented. It has been shown that due to their distinctive remote operation, plasma jets require great care and attention to be reliably and effectively utilized in surface modification of materials. Many factors can affect the physical and chemical proprieties of the plasma propagating in the external environment towards the substrate to be treated. For instance, the inevitable diffusion and mixing of the surrounding gas with the gaseous effluent of the device can significantly alter the plasma plume characteristics and propagation behavior. Moreover, the substrate cannot be considered as a passive object especially when plasma jets are operated in contact mode; the substrate electrical properties can, in fact, significantly alter the plasma/surface interaction dynamics, leading also to very different final results when etching and deposition processes are carried out. While the most peculiar application of AP non-equilibrium plasma jet technology appears to be the maskless localized surface modification of materials, various studies report the large area surface processing through the source/sample holder displacement at scan speeds as high as some tens of meters per minute. Also plasma jet arrays have been proposed to enlarge the treated area, even if a careful optimization is required to obtain simultaneous operation of all the jets of the array with good jet-to-jet uniformity both in time and in space. The plethora of etching, deposition and treatment processes investigated in the last few years confirms the growing interest of both the academic and industrial communities in AP plasma jet technology. This interest is expected to motivate further investigation of plasma jets operation, fundamental prerequisite to obtain reliable and reproducible processes.

Acknowledgements

This research was supported by Regione Puglia Regione Puglia under grant "ATTIV'AZIONE" (grant code S8R8930, call "Aiuti a Sostegno Cluster Tecnologici Regionali") and grant "LIPP" (grant no. 51) within the Framework Programme Agreement APQ "Ricerca Scientifica", II atto integrativo - Reti di Laboratori Pubblici di Ricerca. The financial support of the Italian Ministry for Education, University and Research (MIUR) under grant PONa3_00369 is also acknowledged.

Dedication. Fiorenza Fanelli dedicates this paper to the memory of her father.

References

[1] M. G. Kong, B. N. Ganguly, R. F. Hicks, Plasma jets and plasma bullets (Editorial), Plasma Sources Sci. Technol. 21 (2012) 030201.

[2] A. Schütze, J. Y. Jeong, S. E. Babayan, J. Park, G. S. Selwyn, R. F. Hicks, The atmospheric-pressure plasma jet: a review and comparison to other plasma sources, IEEE Trans. Plasma Sci. 26 (1998) 1685–1694.

[3] M. Laroussi, T. Akan, Arc-free atmospheric pressure cold plasma jets: a review, Plasma Process. Polym. 4 (2007) 777–788.

[4] X. Lu, M. Laroussi, V. Puech, On atmospheric-pressure non-equilibrium plasma jets and plasma bullets, Plasma Sources Sci. Technol. 21 (2012) 034005.

[5] J. Laimer, H. Störi, Recent advances in the research on non-equilibrium atmospheric pressure plasma jets, Plasma Process. Polym. 4 (2007) 266–274.

[6] J. Winter, R. Brandenburg, K. D. Weltmann, Atmospheric pressure plasma jets: an overview of devices and new directions, Plasma Sources Sci. Technol. 24 (2015) 064001.

[7] A. Fridman, A. Chirokov, A. Gutsol, Non-thermal atmospheric pressure discharges, J. Phys. D: Appl. Phys. 38 (2005) R1–R24.

[8] A. Fridman, Plasma Chemistry, Cambridge University Press, New York, 2008.

[9] L. Bárdos, H. Baránková, Cold atmospheric plasma: sources, processes, and applications, Thin Solid Films 518 (2010) 6705–6713.

[10] C. Tendero, C. Tixier, P. Tristant, J. Desmaison, P. Leprince, Atmospheric pressure plasmas: A review, Spectrochim. Acta B 61 (2006) 2–30.

[11] F. Massines, C. Sarra-Bournet, F. Fanelli, N. Naudé, N. Gherardi, Atmospheric pressure low temperature direct plasma technology: status and challenges for thin film deposition, Plasma Process. Polym. 9 (2012) 1041–1073.

[12] D. Mariotti, T. Belmonte, J. Benedikt, T. Velusamy, G. Jain, V. Švrček, Low-temperature atmospheric pressure plasma processes for ‘‘green’’ third generation photovoltaics, Plasma Process. Polym. 13 (2016) 70–90.

[13] R. Foest, M. Schmidt, K. Becker, Microplasmas, an emerging field of low-temperature plasma science and technology, Int. J. Mass Spectrom. 248 (2006) 87–102.

[14] F. Iza, G. J. Kim, S. M. Lee, J. K. Lee, J. L. Walsh, Y. T. Zhang, M. G. Kong, Microplasmas: sources, particle kinetics, and biomedical applications, Plasma Process. Polym. 5 (2008) 322–344.

[15] D. Mariotti, R. M. Sankaran, Microplasmas for nanomaterials synthesis, J. Phys. D: Appl. Phys. 43 (2010) 323001.

[16] G. M. Giannini, A. C. Ducati, Plasma steam apparatus and methods, US Patent No. 2922869 A (1960).

[17] H. Koinuma, H. Ohkubo, T. Hashimoto, K. Inomata, T. Shiraishi, A. Miyanaga and S. Hayashi, Development and application of a microbeam plasma generator, Appl. Phys. Lett. 60 (1992) 816–817.

[18] G. S. Selwyn, Atmospheric-pressure plasma jet, US Patent No. 5961772 (1999).

[19] O. V Penkov, M. Khadem, W. S. Lim, D. E. Kim, A review of recent applications of atmospheric pressure plasma jets for materials processing, J. Coat. Technol. Res. 12 (2015) 225–235.

[20] R. d'Agostino (Ed.), Plasma Deposition, Treatment and Etching of Polymers, Academic Press, New York, 1990.

[21] F. Fanelli, F. Fracassi, Aerosol-assisted atmospheric pressure cold plasma deposition of organic–inorganic nanocomposite coatings, Plasma Chem. Plasma Process. 34 (2014) 473–487.

[22] T. Belmonte, G. Henrion, T. Gries, Nonequilibrium atmospheric plasma deposition, J. Therm. Spray Techn. 20 (2011) 744–759.

[23] T. Belmonte, G. Arnoult, G. Henrion, T. Gries, Nanoscience with non-equilibrium plasmas at atmospheric pressure, J. Phys. D: Appl. Phys. 44 (2011) 363001.

[24] L. Lin, Q. Wang, Microplasma: a new generation of technology for functional nanomaterial synthesis, Plasma Chem. Plasma Process. 35 (2015) 925–962.

[25] Q. Y. Nie, Z. Cao, C. S. Ren, D. Z. Wang, M. G. Kong, A two-dimensional cold atmospheric plasma jet array for uniform treatment of large-area surfaces for plasma medicine, New J. Phys. 11 (2009) 115015.

[26] M. Laroussi, A Fridman, Plasma medicine (editorial), Plasma Process. Polym. 5 (2008) 501–502.

[27] T. von Woedtke, S. Reuter, K. Masur, K.D. Weltmann, Plasmas for medicine, Phys. Rep. 530 (2013) 291–320.

[28] G. Y. Park, S. J. Park, M. Y. Choi, I. G. Koo, J. H. Byun, J. W. Hong, J. Y. Sim, G. J. Collins, J. K. Lee, Atmospheric-pressure plasma sources for biomedical applications, Plasma Sources Sci. Technol. 21 (2012) 043001.

[29] N. Y. Babaeva, M. J. Kushner, Interaction of multiple atmospheric-pressure micro-plasma jets in small arrays: He/O_2 into humid air, Plasma Sources Sci. Technol. 23 (2014) 015007.

[30] J. Schäfer, J. Hnilica, J. Šperka, A. Quade, V. Kudrle, R. Foest, J. Vodák, L. Zajíčková, Tetrakis(trimethylsilyloxy)silane for nanostructured SiO_2-like films deposited by PECVD at atmospheric pressure, Surf. Coat. Technol. 295 (2016) 112–118.

[31] J. Y. Jeong, S. E. Babayan, V. J. Tu, J. Park, I. Henins, R. F. Hicks, G. S. Selwyn, Etching materials with an atmospheric-pressure plasma jet, Plasma Sources Sci. Technol. 7 (1998) 282–285.

[32] Y. Shimizu, A. C. Bose, D. Mariotti, T. Sasaki, K. Kirihara, T. Suzuki, K. Terashima, N. Koshizaki, Reactive evaporation of metal wire and microdeposition of metal oxide using atmospheric pressure reactive microplasma jet, Jap. J. Appl. Phys. 45 (2006) 8228–8234.

[33] R. Kakei, A. Ogino, F. Iwata, Ma. Nagatsu, Production of ultrafine atmospheric pressure plasma jet with nano-capillary, Thin Solid Films 518 (2010) 3457–3460.

[34] T. Abuzairi, M. Okada, Y. Mochizuki, N. R. Poespawati, R. W. Purnamaningsih, M. Nagatsu, Maskless functionalization of a carbon nanotube dot array biosensor using an ultrafine atmospheric pressure plasma jet, Carbon 89 (2015) 208–216.

[35] I. Motrescu, M. Nagatsu, Nanocapillary atmospheric pressure plasma jet: a tool for ultrafine maskless surface modification at atmospheric pressure, ACS Appl. Mater. Interfaces 8 (2016) 12528−12533.

[36] VITO - Flemish Institute for Technological Research, The Plasma Technology Group, PlasmaLine, http://www.vitoplasma.com/en/plasmaline (accessed on 31 January 2017).

[37] Surfx® Technologies LLC, http://www.surfxtechnologies.com/surfx-products/plasma-sources/ (accessed on 31 January 2017).

[38] S. A. Rich, T. Dufour, P. Leroy, F. Reniers, L. Nittler, J.-J. Pireaux, LDPE surface modifications induced by atmospheric plasma torches with linear and showerhead configurations, Plasma Process. Polym. 12 (2015) 771–785.

[39] L. S. Dolci, S. D. Quiroga, M. Gherardi, R. Laurita, A. Liguori, P. Sanibondi, A. Fiorani, L. Calzà, V. Colombo, M. L. Focarete, Carboxyl surface functionalization of poly(L-lactic acid) electrospun nanofibers through atmospheric non-thermal plasma affects fibroblast morphology, Plasma Process. Polym. 11 (2014) 203–213.

[40] C. E. Nwankire, V. J. Law, A. Nindrayog, B. Twomey, K. Niemi, V. Milosavljevic, W. G. Graham, D. P. Dowling, Electrical, thermal and optical diagnostics of an atmospheric plasma jet system, Plasma Chem. Plasma Process. 30 (2010) 537–552.

[41] P. Bosso, F. Fanelli, and F. Fracassi, Deposition of water-stable coatings containing carboxylic acid groups by atmospheric pressure cold plasma jet, Plasma Process. Polym. 13 (2016) 217–226.

[42] F. Alba-Elías, E. Sainz-García, A. González-Marcos, J. Ordieres-Meré, Tribological behavior of plasma-polymerized aminopropyltriethoxysilane films deposited on thermoplastic elastomers substrates, Thin Solid Films 540 (2013) 125–134.

[43] VITO - Flemish Institute for Technological Research, The Plasma Technology Group, PlasmaSpot, http://www.vitoplasma.com/en/plasmatorch (accessed 31 January 2017).

[44] A. J. Wagner, D. Mariotti, K. J. Yurchenko, T. K. Das, Experimental study of a planar atmospheric-pressure plasma operating in the microplasma regime, Phys. Rev. 80 (2009) 065401.

[45] L. O'Neill, P. A. F. Herbert, C. Stallard, D. P. Dowling, Investigation of the effects of gas versus liquid deposition in an aerosol-assisted corona deposition process, Plasma Process. Polym. 7 (2010) 43–50.

[46] M. D. Barankin, T. S. Williams, E. Gonzalez II, R. F. Hicks, Properties of fluorinated silica glass deposited at low temperature by atmospheric plasma-enhanced chemical vapor deposition, Thin Solid Films 519 (2010) 1307–1313.

[47] M. A. Lieberman, A. J. Lichtenberg, Principles of Plasma Discharges and Materials Processing, John Wiley & Sons, Inc., second ed., Hoboken, New Jersey, 2005.

[48] Y. P. Raitzer, Gas Discharge Physics, first ed., Springer-Verlag, Berlin-Heidelberg, 1991.

[49] Corotec Corporation, 3D treaters, http://www.corotec.com/corotec/3d-treaters (accessed on 31 January 2017)

[50] Tantec, SpotTEC, http://www.tantec.com/high-frequency-spot-system.html (accessed on 31 January 2017)

[51] Tigres GmbH, T-jet, http://www.tigres-plasma.de/en/oberflaechentechnik-2/t-jet-technology (accessed on 31 January 2017).

[52] Dyne Technology Ltd, Corona treatment and surface modification, http://www.dynetechnology.co.uk/applications/corona/ (accessed on 31 January 2017).

[53] C. P. Stallard, M. M. Iqbal, M. M. Turner, D. P. Dowling, Investigation of the formation mechanism of aligned nano-structured siloxane coatings deposited using an atmospheric plasma jet, Plasma Process. Polym. 10 (2013) 888–903.

[54] J. Albaugh, C. O'Sullivan, L. O'Neill, Controlling deposition rates in an atmospheric pressure plasma system, Surf. Coat. Technol. 203 (2008) 844–847.

[55] C. P. Stallard, P. Solar, H. Biederman, D. P. Dowling, Deposition of non-fouling PEO-like coatings using a low temperature atmospheric pressure plasma jet, Plasma Process. Polym. 13 (2016) 217–226.

[56] M. M. Iqbal, C. P. Stallard, D. P. Dowling, M. M. Turner, Two-dimensional integrated model for interaction of liquid droplets with atmospheric pressure plasma, Plasma Process. Polym. 12 (2015) 1256–1270.

[57] S. Starostine, E. Aldea, H. de Vries, M. Creatore, M. C. M. van de Sanden, Atmospheric pressure barrier discharge deposition of silica-like films on polymeric substrates, Plasma Process. Polym. 4 (2007) S440–S444.

[58] M. Teschke, J. Kedzierski, E. G. Finantu-Dinu, D. Korzec, J. Engemann, High-speed photographs of a dielectric barrier atmospheric pressure plasma jet, IEEE Trans. Plasma Sci. 33 (2005) 310–311.

[59] Y. L. Wu, J. Hong, Z. Ouyang, T. S. Cho, D. N. Ruzic, Electrical and optical characteristics of cylindrical non-thermal atmospheric-pressure dielectric barrier discharge plasma sources, Surf. Coat. Technol. 234 (2013) 100–103.

[60] D. Mariotti, Nonequilibrium and effect of gas mixtures in an atmospheric microplasma, Appl. Phys. Lett. 92 (2008) 151505.

[61] K. H. Becker, K. H. Schoenbach, J. G. Eden, Microplasmas and applications, J. Phys. D: Appl. Phys. 39 (2006) R55–R70.

[62] H. Yoshiki, K. Taniguchi, Y. Horiike, Localized removal of a photoresist by atmospheric pressure micro-plasma jet using rf corona discharge, Jap. J. Appl. Phys. 41 (2002) 5797–5798.

[63] R. E. J. Sladek, T. A. Baede, E. Stoffels, Plasma-needle treatment of substrates with respect to wettability and growth of escherichia coli and streptococcus mutans, IEEE Trans. Plasma Sci. 34 (2006) 1325–1330.

[64] D. B. Kim, J. K. Rhee, S. Y. Moon, W. Choe, Feasibility study of material surface modification by millimeter size plasmas produced in a pin to plane electrode configuration, Thin Solid Films 515 (2007) 4913–4917.

[65] K. G. Doherty, J. S. Oh, P. Unsworth, A. Bowfield, C. M. Sheridan, P. Weightman, J. W. Bradley, R. L. Williams, Polystyrene surface modification for localized cell culture using a capillary dielectric barrier discharge atmospheric-pressure microplasma jet, Plasma Process. Polym. 10 (2013) 978–989.

[66] R. M. Sankaran, K. P. Giapis, Hollow cathode sustained plasma microjets: characterization and application to diamond deposition, J. Appl. Phys. 92 (2002) 2406–2411.

[67] B. Barwe, A. Stein, O. E. Cibulka, I. Pelant, J. Ghanbaja, T. Belmonte, J. Benedikt, Generation of silicon nanostructures by atmospheric microplasma jet: the role of hydrogen admixture, Plasma Process. Polym. 12 (2015) 132–140.

[68] Y. Shimizu, K. Koga, T. Sasaki, D. Mariotti, K. Terashima, N. Koshizaki, Localized deposition of metallic molybdenum particles in ambient air using atmospheric-pressure microplasma, Digest of Papers-Microprocesses and Nanotechnology 2007 (20th International Microprocesses and Nanotechnology Conference), 174–175.

[69] J. Park, I. Henins, H. W. Herrmann, G. S. Selwyn, R. F. Hicks, Discharge phenomena of an atmospheric pressure radio-frequency capacitive plasma source, J. Appl. Phys. (2001) 20–28.

[70] J. Laimer, H. Störi, Glow discharges observed in capacitive radio-frequency atmospheric-pressure plasma jets, Plasma Process. Polym. 3 (2006) 573–586.

[71] J. J. Shi, M. G. Kong, Mechanisms of the a and g modes in radio-frequency atmospheric glow discharges, J. Appl. Phys. 97 (2005) 023306

[72] J. Y. Jeong, S. E. Babayan, A. Schutze, V. J. Tu, Etching polyimide with a nonequilibrium atmospheric-pressure plasma jet, J. Vac. Sci. Technol. A 17 (1999) 2581–2585.

[73] S. E. Babayan, J. Y. Jeong, V. J. Tu, J. Park, G. S. Selwyn, R F Hicks, Deposition of silicon dioxide films with an atmospheric-pressure plasma jet, Plasma Sources Sci. Technol. 7 (1998) 286–288.

[74] E. Gonzalez II, M. D. Barankin, P. C. Guschl, R. F. Hicks, Surface activation of poly(methylmethacrylate) via remote atmospheric pressure plasma, Plasma Process. Polym. 7 (2010) 482–493.

[75] D. Merche, T. Dufour, J. Baneton, G. Caldarella, V. Debaille, N. Job, F. Reniers, Fuel cell electrodes from organometallic platinum precursors: an easy atmospheric plasma approach, Plasma Process. Polym. 13 (2016) 91–104.

[76] R. A. Sailer, A. Wagner, C. Schmit, N. Klaverkamp, D. L. Schulz, Deposition of transparent conductive indium oxide by atmospheric-pressure plasma jet, Surf. Coat. Technol. 203 (2008) 835–838.

[77] K. W. Johnson, S. Guruvenket, R. A. Sailer, S. P. Ahrenkiel, D.L. Schulz, Atmospheric pressure plasma enhanced chemical vapor deposition of zinc oxide and aluminum zinc oxide, Thin Solid Films 548 (2013) 210–219.

[78] M. D. Barankin, E. Gonzalez II, S, B. Habib, L. Gao, P. C. Guschl, R. F. Hicks, Hydrophobic films by atmospheric plasma curing of spun-on liquid precursors, Langmuir 25 (2009) 2495–2500.

[79] D. Merche, C. Poleunis, P. Bertrand, M. Sferrazza, F. Reniers, Synthesis of polystyrene thin films by means of an atmospheric-pressure plasma torch and a dielectric barrier discharge, IEEE Trans. Plasma Sci. 37 (2009) 951–960.

[80] B. Nisol, G. Oldenhove, N. Preyat, D. Monteyne, M. Moser, D. Perez-Morga, F. Reniers, Atmospheric plasma synthesized PEG coatings: non-fouling biomaterials showing protein and cell repulsion, Surf. Coat. Technol. 252 (2014) 126–133.

[81] B. Nisol, A. Batan, F. Dabeux, A. Kakaroglou, I. De Graeve, G. Van Assche, B. Van Mele, H. Terryn, F. Reniers, Surface characterization of atmospheric pressure plasma-

deposited allyl methacrylate and acrylic acid based coatings, Plasma Process. Polym. 10 (2013) 564–571.

[82] M. Nagatsu, Y. Zhao, I. Motrescu, R. Mizutani, Y. Fujioka, A. Ogino, Sterilization method for medical container using microwave-excited volume-wave plasma, Plasma Process. Polym. 9 (2012) 590–596.

[83] J. Ehlbeck, A. Ohl, M. Maaß, U. Krohmann, T. Neumann, Moving atmospheric microwave plasma for surface and volume treatment, Surf. Coat. Technol. 174–175 (2003) 493–497.

[84] J. A. S. Ting, L. M. D. Rosario, H. V. Lee Jr., H. J. Ramos, R. B. Tumlos, Hydrophobic coating on glass surfaces via application of silicone oil and activated using a microwave atmospheric plasma jet, Surf. Coat. Technol. 259 (2014) 7–11.

[85] J. Hnilica, J. Schäfer, R. Foest, L. Zajíčková , V. Kudrle, PECVD of nanostructured SiO_2 in a modulated microwave plasma jet at atmospheric pressure, J. Phys. D: Appl. Phys. 46 (2013) 335202.

[86] M. Eichler, K. Nagel, P. Hennecke, C.-P. Klages, Area-selective microplasma treatment in microfluidic channels for novel fluid phase separators, Plasma Process. Polym. 9 (2012) 1160–1167.

[87] F. Fanelli, F. Fracassi, Thin film deposition on open-cell foams by atmospheric pressure dielectric barrier discharges, Plasma Process. Polym. 13 (2016) 13, 470–479.

[88] I. Onyshchenko, N. De Geyter, A. Y. Nikiforov, R. Morent, Atmospheric pressure plasma penetration inside flexible polymeric tubes, Plasma Process. Polym. 12 (2015) 271–284.

[89] J. Toshifuji, T. Katsumata, Hirofumi Takikawa, T. Sakakibara, I. Shimizu, Cold arc-plasma jet under atmospheric pressure for surface modification, Surf. Coat. Technol. 171 (2003) 302–306

[90] Y.-H. Choi, J.-H. Kima, K.-H. Paek, W.-T. Ju, Y. S. Hwang, Characteristics of atmospheric pressure N_2 cold plasma torch using 60-Hz AC power and its application to polymer surface modification, Surf. Coat. Technol. 193 (2005) 319–324.

[91] M. H. Han, J. H. Noh, T. I. Lee, J. H. Choi, K. W. Park, H. S. Hwang, K. M. Song, H. K. Baik, High-rate SiO_2 deposition by oxygen cold arc plasma jet at atmospheric pressure, Plasma Process. Polym. 5 (2008) 861–866.

[92] C.-C. Hsu, C.-Y. Wu, Electrical characterization of the glow-to-arc transition of an atmospheric pressure pulsed arc jet, J. Phys. D: Appl. Phys. 42 (2009) 215202.

[93] Y.-W. Hsu, Y.-J. Yang, C.-Y. Wu, C.-C. Hsu, Downstream characterization of an atmospheric
pressure pulsed arc jet, Plasma Chem Plasma Process 30 (2010) 363–372.

[94] Plasmatreat - Openair® Plasma Technology, http://www.plasmatreat.com/plasma-technology/openair-atmospheric-plasma-technique.html (accessed on 31 January 2017)

[95] J. Pulpytel, V. Kumar, P. Peng, V. Micheli, N. Laidani, F. Arefi-Khonsari, Deposition of organosilicon coatings by a non-equilibrium atmospheric pressure plasma jet: design, analysis and macroscopic scaling law of the process, Plasma Process. Polym. 8 (2011) 664–675.

[96] O. Carton, D. B. Salem, S. Bhatt, J. Pulpytel, F. Arefi-Khonsari, Plasma polymerization of acrylic acid by atmospheric pressure nitrogen plasma jet for biomedical applications, Plasma Process. Polym. 9 (2012) 984–993.

[97] D. B. Salem, O. Carton, H. Fakhouri, J. Pulpytel, F. Arefi-Khonsari, Deposition of water stable plasma polymerized acrylic acid/MBA organic coatings by atmospheric pressure air plasma jet, Plasma Process. Polym. 11 (2014) 269–278.

[98] H. Fakhouri, D. B. Salem, O. Carton, J. Pulpytel, Arefi-Khonsari, Highly efficient photocatalytic TiO_2 coatings deposited by open air atmospheric pressure plasma jet with aerosolized TTIP precursor, J. Phys. D: Appl. Phys. 47 (2014) 265301.

[99] D. B. Salem, J. Pulpytel, F. Pillier, A. Pailleret, F. Arefi-Khonsari, Amorphization and polymorphism modification of polyamide-6 films via open-air non-equilibrium atmospheric pressure plasma jet treatment, Plasma Process. Polym.11 (2014) 961–973.

[100] O. Carton, D. B. Salem, J. Pulpytel, F. Arefi-Khonsari, Improvement of the water stability of plasma polymerized acrylic acid/MBA coatings deposited by atmospheric pressure air plasma jet, Plasma. Chem. Plasma Process. 35 (2015) 819–829.

[101] J. A. Jofre-Reche, J. Pulpytel, F. Arefi-Khonsari, J. M. Martín-Martínez, Increased adhesion of polydimethylsiloxane (PDMS) to acrylic adhesive tape for medical use by surface treatment with an atmospheric pressure rotating plasma jet, J. Phys. D: Appl. Phys. 49 (2016) 334001.

[102] D. P. Dowling, F. T. O'Neill, S. J. Langlais, V. J. Law, Influence of dc pulsed atmospheric pressure plasma jet processing conditions on polymer activation, Plasma Process. Polym. 8 (2011) 718–727.

[103] M. Donegan, D. P. Dowling, Protein adhesion on water stable atmospheric plasma deposited acrylic acid coatings, Surf. Coat. Technol. 234 (2013) 53–59.

[104] S. Farhat, M. Gilliam, M. Rabago-Smith, C. Baran, N. Walter, A. Zand, Polymer coatings for biomedical applications using atmospheric pressure plasma, Surf. Coat. Technol. 241 (2014) 123–129.

[105] T. Kewitz, M. Fröhlich, J. von Frieling, H. Kersten, Investigation of a commercial atmospheric pressure plasma jet by a newly designed calorimetric probe, IEEE Trans. Plasma Sci. 43 (2015) 1769–1773.

[106] A. J. Knoll, P. Luan, E. A. J. Bartis, C. Hart, Y. Raitses, G. S. Oehrlein, Real time characterization of polymer surface modifications by an atmospheric pressure plasma jet: electrically coupled versus remote mode, Appl. Phys. Lett. 105 (2014) 171601.

[107] E. J. Szili, S. A. Al-Bataineh, P. M. Bryant, R. D. Short, J. W. Bradley, D. A. Steele, Controlling the spatial distribution of polymer surface treatment using atmospheric-pressure microplasma jets, Plasma Process. Polym. 8 (2011) 38–50.

[108] E. A. J. Bartis, D. B. Graves, J. Seog, G. S. Oehrlein, Atmospheric pressure plasma treatment of lipopolysaccharide in a controlled environment, J. Phys. D: Appl. Phys. 46 (2013) 312002.

[109] P. R. Gandhiraman, V. Jayan, J.W. Han, B. Chen, J. E. Koehne, M. Meyyappan, Plasma jet printing of electronic materials on flexible and nonconformal objects, ACS Appl. Mater. Interfaces 6 (2014) 20860−20867.

[110] C. Stancu, D. Alegre, E.R. Ionita, B. Mitu, C. Grisolia, F. L. Tabares, G. Dinescu, Cleaning of carbon materials from flat surfaces and castellation gaps by an atmospheric pressure plasma jet, Fusion Eng. Design 103 (2016) 38–44.

[111] Z. Cao, J. L. Walsh, M. G. Kong, Atmospheric plasma jet array in parallel electric and gas flow fields for three-dimensional surface treatment, Appl. Phys. Lett. 94 (2009) 021501.

[112] F. Chen, J. Song, S. Huang, S. Xu, G. Xia, D. Yang, W. Xu, J. Sun, X. Liu, Simultaneous and long-lasting hydrophilization of inner and outer wall surfaces of polytetrafluoroethylene tubes by transferring atmospheric pressure plasmas, J. Phys. D: Appl. Phys. 49 (2016) 365202.

[113] F. Chen, S. Liu, J. Liu, S. Huang, G. Xia, J. Song, W. Xu, J. Sun, X. Liu, Surface modification of tube inner wall by transferred atmospheric pressure plasma Appl. Surf. Sci. 389 (2016) 967–976.

[114] M. Polak, J. Winter, U. Schnabel, J. Ehlbeck, K.-D. Weltmann, Innovative plasma generation in flexible biopsy channels for inner-tube decontamination and medical applications, Plasma Process. Polym. 9 (2012) 67–76.

[115] Z. Xiong, E. Robert, V. Sarron, J.-M. Pouvesle, M. J Kushner, Atmospheric-pressure plasma transfer across dielectric channels and tubes, J. Phys. D: Appl. Phys. 46 (2013) 155203.

[116] W.-C. Zhu, Q. Li, X.-M. Zhu, Y.-K. Pu, Characteristics of atmospheric pressure plasma jets emerging into ambient air and helium, J. Phys. D: Appl. Phys. 42 (2009) 202002.

[117] J. L. Walsh, M. G. Kong, Contrasting characteristics of linear-field and cross-field atmospheric plasma jets, Appl. Phys. Lett. 93 (2008) 111501.

[118] E. Robert, V. Sarron, T. Darny, D Riès, S. Dozias, J. Fontane, L. Joly, J.-M. Pouvesle, Rare gas flow structuration in plasma jet experiments, Plasma Sources Sci. Technol. 23 (2014) 012003.

[119] T. Darny, E. Robert, D. Riès, S. Dozias, J. M. Pouvesle, Unexpected plasma plume shapes produced by a microsecond plasma gun discharge, IEEE T. Plasma Sci. 42 (2014) 2504−2505.

[120] X. Pei, M. Ghasemi, H. Xu, Q. Hasnain, S. Wu, Y. Tu, X. Lu, Dynamics of the gas flow turbulent front in atmospheric pressure plasma jets, Plasma Sources Sci. Technol. 25 (2016) 035013.

[121] M. H. Qaisrani, Y. Xian, C. Li, X. Pei, M. Ghasemi, X. Lu, Study on dynamics of the influence exerted by plasma on gas flow field in non-thermal atmospheric pressure plasma jet, Phys. Plasmas 23 (2016) 063523.

[122] V. Sarron, E. Robert, J. Fontane, T. Darny, D. Riès, S. Dozias, L. Joly, J.M. Pouvesle, Plasma plume length characterization, in: A. von Keudell, J. Winter, M. Böke, V. Schutz-von der Gathen (Eds.), Proc. 19th International Symposium of Plasma Chemistry, Bochum, Germany, July 25-31, 2009.

[123] Q. Xiong, X. Lu, K. Ostrikov, Z. Xiong, Y. Xian, F. Zhou, C. Zou, J. Hu, W. Gong, Z. Jiang, Length control of He atmospheric plasma jet plumes: effects of discharge parameters and ambient air, Phys. Plasmas 16 (2009) 043505.

[124] E. Robert, V. Sarron, D. Riès, S. Dozias, M. Vandamme, J.-M. Pouvesle, Characterization of pulsed atmospheric-pressure plasma streams (PAPS) generated by a plasma gun, Plasma Sources Sci. Technol. 21 (2012) 034017.

[125] J. L.Walsh, P. Olszewski, J. W. Bradley, The manipulation of atmospheric pressure dielectric barrier plasma jets, Plasma Sources Sci. Technol. 21 (2012) 034007.

[126] M. T. Benabbas, S. Sahli, A. Benhamouda, S Rebiai, Effects of the electrical excitation signal parameters on the geometry of an argon-based non-thermal atmospheric pressure plasma jet, Nanoscale Res. Lett. 9 (2014) 697.

[127] M. Boselli, V. Colombo, E. Ghedini, M. Gherardi, R. Laurita, A. Liguori, P. Sanibondi, A. Stancampiano, Schlieren high-speed imaging of a nanosecond pulsed atmospheric pressure non-equilibrium plasma jet, Plasma Chem. Plasma Process. 34 (2014) 853–869.

[128] S. Wu, Z. Wang, Q. Huang, X. Lu, K. Ostrikov, Open-air direct current plasma jet: scaling up, uniformity, and cellular control, Phys. Plasmas 19 (2012) 103503.

[129] J. W. Gauntner, J. N. Livingood, P Hrycak, Survey of literature on flow characteristics of a single turbulent jet impinging on a flat plate, NASA Technical Note D-5652, National Aeronautics and Space Administration, Washington, D.C., 1970.

[130] T. L. Labus, E. P. Symons, experimental investigation of an axisymmetric free jet with an initially uniform velocity profile, NASA Technical Note D-6783, National Aeronautics and Space Administration, Washington, D.C., 1972.

[131] A. Abdel-Rahman, A Review of effects of initial and boundary conditions on turbulent, WSEAS Trans. Fluid Mech. 5 (2010) 257–275.

[132] E. Robert, T. Darny, S. Dozias, S. Iseni, J. M. Pouvesle, New insights on the propagation of pulsed atmospheric plasma streams: from single jet to multi jet arrays, Phys. Plasmas 22 (2015) 122007.

[133] S. Zhang, A. Sobota, E. M. van Veldhuizen, P. J. Bruggeman, Gas flow characteristics of a time modulated APPJ: the effect of gas heating on flow dynamics, J. Phys. D: Appl. Phys. 48 (2015) 015203.

[134] H. Yamada, Y. Yamagishi, H. Sakakita, S. Tsunoda, J. Kasahara, M. Fujiwara, S. Kato, H. Itagaki, J. Kim, S. Kiyama, Y. Fujiwara, Y. Ikehara, S. Ikehara, H. Nakanishi, N. Shimizu. Bending and turbulent enhancement phenomena of neutral gas flow containing an atmospheric pressure plasma by applying external electric fields measured by schlieren optical method, Jap. J. Appl. Phys. 55 (2016) 01AB08.

[135] X. Lu, M. Laroussi, Dynamics of an atmospheric pressure plasma plume generated by submicrosecond voltage pulses, J. Appl. Phys. 100 (2006) 063302.

[136] J. L.Walsh, F. Iza, N. B. Janson, V. J. Law, M. G. Kong, Three distinct modes in a cold atmospheric pressure plasma jet, J. Phys. D: Appl. Phys. 43 (2010) 075201.

[137] N. Mericam-Bourdet, M. Laroussi, A. Begum, E. Karakas, Experimental investigations of plasma bullets, J. Phys. D: Appl. Phys. 42 (2009) 055207.

[138] G. V. Naidis, Modelling of plasma bullet propagation along a helium jet in ambient air, J. Phys. D: Appl. Phys. 44 (2011) 215203.

[139] S. Reuter, J. Winter, A. Schmidt-Bleker, H. Tresp, M. U. Hammer, K.-D. Weltmann, Controlling the ambient air affected reactive species composition in the effluent of an argon plasma jet, IEEE Trans. Plasma Sci. 40 (2012) 2788–2794.

[140] A. Vogelsang, A. Ohl, H. Steffen, R. Foest, K. Schröder, K.-D. Weltmann, Locally resolved analysis of polymer surface functionalization by an atmospheric pressure argon microplasma jet with air entrainment, Plasma Process. Polym. 7 (2010) 16–24.

[141] A. Vogelsang, A. Ohl, R. Foest, K. Schröder, K. D. Weltmann, Hydrophobic coatings deposited with an atmospheric pressure microplasma jet, J. Phys. D: Appl. Phys. 43 (2010) 485201.

[142] S. A. Norberg, E. Johnsen, M. J. Kushner, Formation of reactive oxygen and nitrogen species by repetitive negatively pulsed helium atmospheric pressure plasma jets propagating into humid air, Plasma Sources Sci. Technol. 24 (2015) 035026.

[143] A. Sobota, O. Guaitella, G. B. Sretenović, I. B. Krstić, V. V. Kovačević, A. Obrusník, Y. N. Nguyen, L. Zajíčková, B. M. Obradović, M. M. Kuraica, Electric field measurements in a kHz-driven He jet—the influence of the gas flow speed, Plasma Sources Sci. Technol. 25 (2016) 065026.

[144] A. Schmidt-Bleker, S. A. Norberg, J. Winter, E. Johnsen, S. Reuter, K. D. Weltmann, M. J. Kushner, Propagation mechanisms of guided streamers in plasma jets: the influence of electronegativity of the surrounding gas, Plasma Sources Sci. Technol. 24 (2015) 035022.

[145] A. Schmidt-Bleker, J. Winter, A. Bösel, S. Reuter, K.-D. Weltmann, On the plasma chemistry of a cold atmospheric argon plasma jet with shielding gas device, Plasma Sources Sci. Technol. 25 (2016) 015005.

[146] S. Reuter, J. Winter, S. Iséni, A. Schmidt-Bleker, M. Dünnbier, K. Masur, K. Wende, K.-D. Weltmann, The influence of feed gas humidity versus ambient humidity on atmospheric pressure plasma jet-effluent chemistry and skin cell viability, IEEE Trans. Plasma Sci. 43 (2015) 3185–3192.

[147] S. Reuter, J. Winter, A. Schmidt-Bleker, D. Schroeder, H. Lange, N. Knake, V. Schulz-von der Gathen, K.-D. Weltmann, Atomic oxygen in a cold argon plasma jet: TALIF spectroscopy in ambient air with modelling and measurements of ambient species diffusion, Plasma Sources Sci. Technol. 21 (2012) 024005.

[148] E. A. J. Bartis, P. Luan, A. J. Knoll, C. Hart, J. Seog, G. S. Oehrlein, Polystyrene as a model system to probe the impact of ambient gas chemistry on polymer surface modifications using remote atmospheric pressure plasma under well controlled conditions, Biointerphases 10 (2015) 029512.

[149] E. A. J. Bartis, A. J. Knoll, P. Luan, J. Seog, G. S. Oehrlein, On the interaction of cold atmospheric pressure plasma with surfaces of bio-molecules and model polymers, Plasma Chem. Plasma Process. 36 (2016) 121–149.

[150] E. A. J. Bartis, P. Luan, A. J. Knoll, D. B. Graves, J. Seog, G. S. Oehrlein, Biodeactivation of lipopolysaccharide correlates with surface-bound NO_3 after cold atmospheric plasma treatment, Plasma Process. Polym. 13 (2016) 410–418.

[151] Y. Liu, H. Xu, L. Ge, C. Wang, L. Han, H. Yu, Y. Qiu, Influence of environmental moisture on atmospheric pressure plasma jet treatment of ultrahigh-modulus polyethylene fibers, J. Adhesion Sci. Technol. 21 (2007) 663–676.

[152] S. Bornholdt, M. Wolter, H. Kersten, Characterization of an atmospheric pressure plasma jet for surface modification and thin film deposition, Eur. Phys. J. D 60 (2010) 653–660.

[153] S. A. Norberg, E. Johnsen, M. J. Kushner, Helium atmospheric pressure plasma jets touching dielectric and metal surfaces, J. Appl. Phys.s 118 (2015) 013301.

[154] Y. Sakiyama, D. B. Graves, E. Stoffels, Influence of electrical properties of treated surface on RF-excited plasma needle at atmospheric pressure, J. Phys. D: Appl. Phys. 41 (2008) 095204.

[155] Q. Th. Algwari, D. O'Connell, Plasma jet interaction with a dielectric surface, IEEE Trans. Plasma Sci. 39 (2011) 2368–2369.

[156] S. Hofmann, K. van Gils, S. van der Linden, S. Iseni, P. Bruggeman, Time and spatial resolved optical and electrical characteristics of continuous and time modulated RF plasmas in contact with conductive and dielectric substrates, Eur. Phys. J. D 68 (2014) 56.

[157] O. Guaitella, A. Sobota, The impingement of a kHz helium atmospheric pressure plasma jet on a dielectric surface, J. Phys. D: Appl. Phys. 48 (2015) 255202.

[158] R. Zaplotnik, M. Bišćan, Z. Kregar, U. Cvelbar, M. Mozetič, S. Milošević, Influence of a sample surface on single electrode atmospheric plasma jet parameters, Spectrochim. Acta B 103–104 (2015) 124–130.

[159] L. Wang, Y. Zheng, S. Jia, Numerical study of the interaction of a helium atmospheric pressure plasma jet with a dielectric material, Phys. Plasmas 120 (2016) DOI: 10.1063/1.4963115

[160] T. Wang, B. Yang, X. Chen, X. Wang, C. Yang, J. Liu, Distinct modes in the evolution of interaction between polymer film and atmospheric pressure plasma jet, Plasma Process. Polym. (2016) DOI: 10.1002/ppap.201600067.

[161] Y. Shimizu, T. Sasaki, A. Chandra Bose, K. Terashima, N. Koshizaki, Development of wire spraying for direct micro-patterning via an atmospheric-pressure UHF inductively coupled microplasma jet, Surf. Coat. Technol. 200 (2006) 4251– 4256.

[162] J. West, A. Michels, S. Kittel, P. Jacob, J. Franzke, Microplasma writing for surface-directed millifluidics, Lab Chip 7 (2007) 981–983.

[163] A. Vogelsang, A. Ohl, R. Foest, K. Schroder, K.D. Weltmann, Deposition of thin films from amino group containing precursors with an atmospheric pressure microplasma jet, Plasma Process. Polym. 8 (2011) 77–84.

[164] J. Schäfer, R. Foest, A. Quade, A. Ohl, K. D. Weltmann, Local deposition of SiO_x plasma polymer films by a miniaturized atmospheric pressure plasma jet (APPJ), J. Phys. D: Appl. Phys. 41 (2008) 194010.

[165] J. Schäfer, R. Foest, F. Sigeneger, D. Loffhagen, K.-D. Weltmann, U. Martens, R. Hippler, Study of thin film formation from silicon-containing precursors produced by an RF non-thermal plasma jet at atmospheric pressure, Contrib. Plasma Phys. 52 (2012) 872–880.

[166] J. H. Yim, V. Rodriguez-Santiago, A. A. Williams, T. Gougousi, D. D. Pappas, J. K. Hirvonen, Atmospheric pressure plasma enhanced chemical vapor deposition of hydrophobic coatings using fluorine-based liquid precursors, Surf. Coat. Technol. 234 (2013) 21–32.

[167] H. M. L. Tan, T. Ikeda, T. Ichiki, 3 Dimensional silicon micromachining using a scanning microplasma jet source, J. Photopolym Sci. Technol. 18 (2005) 237–241.

[168] P. Piechulla, J. Bauer, G. Boehm, H. Paetzelt, T. Arnold, Etch mechanism and temperature regimes of an atmospheric pressure chlorine-based plasma jet process, Plasma Process. Polym. 13 (2016) 1128–1135.

[169] K. Fricke, H. Steffen, T. von Woedtke, K. Schroder, K.-D. Weltmann, High rate etching of polymers by means of an atmospheric pressure plasma jet, Plasma Process. Polym. 8 (2011) 51–58.

[170] Y. Shimizu, T. Sasaki, T. Ito, K. Terashima, N. Koshizaki, Fabrication of spherical carbon via UHF inductively coupled microplasma CVD, J. Phys. D: Appl. Phys. 36 (2003) 2940–2944.

[171] J. Benedikt, K. Focke, A. Yanguas-Gil, A. von Keudell, Atmospheric pressure microplasma jet as a depositing tool, Appl. Phys. Lett. 89 (2006) 251504.

[172] M. Janietz, T. Arnold, Surface figuring of glass substrates by local deposition of silicon oxide with atmospheric pressure plasma jet, Surf. Coat. Technol. 205 (2011) S351–S354.

[173] A. H. Ricci Castro, F. V.P. Kodaira, V. Prysiazhnyi, R. P. Mota, K. G. Kostov, Deposition of thin films using argon/acetylene atmospheric pressure plasma jet, Surf. Coat. Technol. 312 (2017) 13–18 .

[174] J. Benedikt, V. Raballand, A. Yanguas-Gil, K. Focke, A. von Keudell, Thin film deposition by means of atmospheric pressure microplasma jet, Plasma Phys. Control. Fusion 49 (2007) B419–B427.

[175] S. Stauss, Y. Imanishi, H. Miyazoe, K. Terashima, High rate deposition of ZnO thin films by a small-scale inductively coupled argon plasma generated in open air, J. Phys. D: Appl. Phys. 43 (2010) 155203.

[176] S. Yonson, S. Coulombe, V. Léveillé, R. L. Leask, Cell treatment and surface functionalization using a miniature atmospheric pressure glow discharge plasma torch, J. Phys. D: Appl. Phys. 39 (2006) 3508–3513.

[177] H. M. L. Tan, H. Fukuda, T. Akagi, T. Ichiki, Surface modification of poly(dimethylsiloxane) for controlling biological cells' adhesion using a scanning radical microjet, Thin Solid Films 515 (2007) 5172–5178.

[178] I. Motrescu, A. Ogino, M. Nagatsu, Micro-patterning of functional groups onto polymer surface using capillary atmospheric pressure plasma jet, J. Photopolym. Sci. Technol. 4 (2012) 529–534.

[179] H. Paetzelt, T. Arnold, G. Böhm, F. Pietag, A. Schindler, Surface patterning by local plasma jet sacrificial oxidation of silicon, Plasma Process. Polym. 10 (2013) 416–421.

[180] D. Ye, S.-Q. Wu, Y. Yu, L. Liu, X.-P. Lu, Y. Wu, Patterned graphene functionalization via mask-free scanning of micro-plasma jet under ambient condition, Appl. Phys. Lett. 104 (2014) 103105.

[181] J. Zeng, J. Lin, X. Zhang, Deposition of silicon oxide films by non-equilibrium, atmospheric-pressure plasma jet, Surf. Coat. Technol. 228 (2013) S416–S418.

[182] S. B. Said, F. Arefi-Khonsari, J. Pulpytel, Plasma polymerization of 3-aminopropyltrietoxysilane (APTES) by open-air atmospheric arc plasma jet for in-line treatments, Plasma Process. Polym. 13 (2016) 1025–1035.

[183] C. Merten, C. Regula, A. Hartwig, J. Ihde, R. Wilken, Track by track: the structure of single tracks of atmospheric pressure plasma polymerized hexamethyl disiloxane (HMDSO) analyzed by infrared microscopy, Plasma Process. Polym. 10 (2013) 60–68.

[184] J. A. Jofre-Reche, J. Pulpytel, H. Fakhouri, F. Arefi-Khonsari, J. Miguel Martín-Martínez, Surface treatment of polydimethylsiloxane (PDMS) with atmospheric pressure rotating plasma jet. Modeling and optimization of the surface treatment conditions, Plasma Process. Polym. 13 (2016) 459–469.

[185] P. Scopece, A. Viaro, R. Sulcis, I. Kulyk, A. Patelli, M. Guglielmi, SiO_x-based gas barrier coatings for polymer substrates by atmospheric pressure plasma jet deposition, Plasma Process. Polym. 6 (2009) S705–S710.

[186] W. J. Liu, X. J. Guo, C. L. Chang, J. H. Lu, Diamond-like carbon thin films synthesis by low temperature atmospheric pressure plasma method, Thin Solid Films 517 (2009) 4229–4232.

[187] C. Guang-Liang, Z. Xu, L. Guo-Hua, Z. Zhao-Xia, S. Massey, W. Smith, M. Tatoulian and Y. Si-Ze, Fabricating a reactive surface on the fibroin film by a room-temperature plasma jet array for biomolecule immobilization, Chin. Phys. B. 21(2012) 105201.

[188] E. Kedroňová, L. Zajíčková, D, Hegemann, M.Klíma, M. Michlíček, A. Manakhov, Plasma enhanced CVD of organosilicon thin films on electrospun polymer nanofibers, Plasma Process. Polym. 12 (2015) 1231–1243.

[189] Z. Cao, Q. Nie, D. L. Bayliss, J. L. Walsh, C. S. Ren, D. Z .Wang, M. G. Kong, Spatially extended atmospheric plasma arrays, Plasma Sources Sci. Technol. 19 (2010) 025003.

[190] J. Y. Kim, J. Ballato, S. O. Kim, Intense and energetic atmospheric pressure plasma jet arrays, Plasma Process. Polym. 9 (2012) 253–260.

[191] J. H. Kim, H.-J. Kim, J. Y. Kim, H.-S. Tae, Intense Ar plasma array jet with ring-type focusing electrode, IEEE Trans. Plasma Sci., 42 (2014) 2478–2479.

[192] Y. Xia, W. Wang, D. Liu, Y. Peng, Y. Song, L. Ji, Y. Zhao, Z. Qi, X. Wang, B. Li, An atmospheric-pressure microplasma array produced by using graphite coating electrodes, Plasma Process. Polym. (2016) DOI: 10.1002/ppap.201600132.

[193] M. Ghasemi, P. Olszewski, J. W. Bradley, J. L. Walsh, Interaction of multiple plasma plumes in an atmospheric pressure plasma jet array, J. Phys. D: Appl. Phys. 46 (2013) 052001.

[194] S. J. Kim, T. H. Chung, H. M. Joh, J.-H. Cha, I. S. Eom, H.-J. Lee, Characteristics of multiple plasma plumes and formation of bullets in an atmospheric-pressure plasma jet array, IEEE Trans. Plasma Sci. 43 (2015) 753–759.

[195] P. P. Sun, H. L. Chen, S.-J. Park, J. G. Eden, D. X. Liu, M. G. Kong, Off-axis chemical crosstalk in an atmospheric pressure microplasma jet array, J. Phys. D: Appl. Phys. 48 (2015) 425203.

[196] L. Wang, W. Ning, M. Fu, C. Wu, S. Jia, An experimental study of photoresist material etching by an atmospheric-pressure plasma jet with Ar/air mixed gas, J. Plasma Phys. 79 (2013) 683–689.

[197] H. Jin, Q. Xin, N. Li, J. Jin, B. Wang, Y. Yao, The morphology and chemistry evolution of fused silica surface after Ar/CF_4 atmospheric pressure plasma processing, Appl. Surf. Sci. 286 (2013) 405– 411.

[198] T. Arnold, G. Böhm, R. Fechner, J. Meister, A. Nickel, F. Frost, T. Hänsel, A. Schindler, Ultra-precision surface finishing by ion beam and plasma jet techniques—status and outlook, Nucl. Instrum. Methods Phys. Res. A 616 (2010) 147–156

[199] J. Meister, T. Arnold, New process simulation procedure for high-rate plasma jet machining, Plasma. Chem. Plasma Process. 31 (2011) 91–107.

[200] J. Ying, R. Chunsheng, Y. Liang, Z. Jialiang, W. Dezhen, Atmospheric pressure plasma jet in Ar and O_2/Ar mixtures: properties and high performance for surface cleaning, Plasma Sci. Technol. 15 (2013) 1203–1208.

[201] C. W. Kan, C. F. Lam, C. K. Chan, S. P. Ng, Using atmospheric pressure plasma treatment for treating grey cotton fabric, Carbohydr. Polym. 102 (2014) 167–173.

[202] T.S. Williams, R. F. Hicks, Aging mechanism of the native oxide on silicon (100) following atmospheric oxygen plasma cleaning, J. Vac. Sci. Technol. A 29 (2011) 041403.

[203] M. Boselli, C. Chiavari, V. Colombo, M. Gherardi, C. Martini, F. Rotundo, Atmospheric pressure non-equilibrium plasma cleaning of 19th century daguerreotypes, Plasma Process. Polym. 14 (2017) 1600027.

[204] Dyne Technology Ltd, Cleaning of ceramics, http://www.dynetechnology.co.uk/applications/cleaning-of-ceramics/ (accessed on 31 January 2017).

[205] Agaria AB, Plasma treatment for printed circuit boards, http://www.agaria.se/produkter/ytbehandling/atmosfarsplasma/applikationer/elektronik/tryckta-kretskort/ (accessed on 31 January 2017).

[206] MTI Corporation, http://www.mtixtl.com/AtomosphericPlasmaJet-Flowsystem-GSL1100X-PJF.aspx (accessed on 31 January 2017).

[207] P. A. F. Herbert, L. O'Neill, J. Jaroszynska-Wolinska, C. P. Stallard, A. Ramamoorthy, D. P. Dowling, A comparison between gas and atomized liquid precursor states in the deposition of functional coatings by pin corona plasma, Plasma Process. Polym. 8 (2011) 230–238.

[208] M. Bashir, S. Bashir, Hydrophobic–hydrophilic character of hexamethyldisiloxane films polymerized by atmospheric pressure plasma jet, Plasma Chem. Plasma Process. 35 (2015) 739–755.

[209] W. J. Liu, R. C. Wang, Novel low temperature atmospheric pressure plasma jet systems for silicon dioxide and poly-ethylene thin film deposition, Surf. Coat. Technol. 206 (2011) 925–928.

[210] S. Collette, J. Hubert, A. Batan, K. Baert, M. Raes, I. Vandendael, A. Daniel, C. Archambeau, H. Terryn, F. Reniers, Photocatalytic TiO_2 thin films synthesized by the post-discharge of an RF atmospheric plasma torch, Surf. Coat. Technol. 289 (2016) 172–178.

[211] K. M. Chang, S. H. Huang, C. J. Wu, W. L. Lin, W. C. Chen, C. W. Chi, J. W. Lin, C. C. Chang, Transparent conductive indium-doped zinc oxide films prepared by atmospheric pressure plasma jet, Thin Solid Films 519 (2011) 5114–5117.

[212] T. L. Koh, M. J. Gordon, Spray deposition of nanostructured metal films using hydrodynamically stabilized, high pressure microplasmas, J. Vac. Sci. Technol. A 31 (2013) 061312.

[213] P. Zhao, W. Zheng, Y. D. Meng, M. Nagatsu, Characteristics of high-purity Cu thin films deposited on polyimide by radio-frequency Ar/H_2 atmospheric-pressure plasma jet, J. Appl. Phys. 113 (2013) 123301.

[214] P. Zhao, W. Zheng, J. Watanabe, Y. D. Meng, M. Nagatsu, Highly conductive Cu thin film deposition on polyimide by RF-driven atmospheric pressure plasma jets under nitrogen atmosphere, Plasma Process. Polym. 12 (2015) 431–438.

[215] J. Kredl, J. F. Kolb, U. Schnabel, M. Polak, K.-D.Weltmann, K. Fricke, Deposition of antimicrobial copper-rich coatings on polymers by atmospheric pressure jet plasmas, Materials 9 (2016) 274.

[216] G. J. Han, S. N. Chung, B. H. Chun, C. K. Kim, K. H. Oh, B. H. Cho, 1,3-Butadiene as an adhesion promoter between composite resin and dental ceramic in a dielectric barrier discharge jet, Plasma Chem. Plasma Process. 33 (2013) 539–551.

[217] C. Regula, J. Ihde, U. Lommatzsch, R. Wilken, Corrosion protection of copper surfaces by an atmospheric pressure plasma jet treatment, Surf. Coat. Technol. 205 (2011) S355–S358.

[218] C. E. Nwankire, G. Favaro, Q.-H. Duong, D. P. Dowling, Enhancing the mechanical properties of superhydrophobic atmospheric pressure plasma deposited siloxane coatings, Plasma Process. Polym. 8 (2011) 305–315.

[219] X. Deng, A. Y. Nikiforov, N. De Geyter, R. Morent, C. Leys, Deposition of a TMDSO-based film by a non-equilibrium atmospheric pressure DC plasma jet, Plasma Process. Polym. 10 (2013) 641–648.

[220] E. Sainz-García, F. Alba-Elías, R. Múgica-Vidal, A. González-Marcos, Antifriction aminopropyltriethoxysilane films on thermoplastic elastomer substrates using an APPJ system, Surf. Coat. Technol. 310 (2017) 239–250.

[221] D. P. Dowling, C. E. Nwankire, M. Riihimäki, R. Keiski, U. Nylén, Evaluation of the anti-fouling properties of nm thick atmospheric plasma deposited coatings, Surf. Coat. Technol. 205 (2010) 1544–1551.

[222] W. C. Ma, C. Y. Tsai, C. Huang, Investigation of atmospheric-pressure plasma deposited hexafluorobenzene fluorocarbon film, Surf. Coat. Technol. 259 (2014) 290–296.

[223] S. Bhatt, J. Pulpytel, S. Mori, M. Mirshahi, F. Arefi-Khonsari, Cell repellent coatings developed by an open air atmospheric pressure non-equilibrium argon plasma jet for biomedical applications, Plasma Process. Polym. 11 (2014) 24–36.

[224] F. Fanelli, P. Bosso, A. M. Mastrangelo, F. Fracassi, Thin film deposition at atmospheric pressure using dielectric barrier discharges: advances on three-dimensional porous substrates and functional coatings, Jap. J. Appl. Phys. 55 (2016) 07LA01.

[225] F. Addou, T. Duguet, P. Bosso, A. Zhang, E. Amin-Chalhoub, F. Fanelli, C. Vahlas, Metallization of carbon fiber reinforced polymers: Chemical kinetics, adhesion, and properties, Surf. Coat. Technol. 308 (2016) 62–69.

[226] A. Liguori, A. Pollicino, A. Stancampiano, F. Tarterini, M. L. Focarete, V. Colombo, M. Gherardi, Deposition of plasma-polymerized polyacrylic acid coatings by a non-equilibrium atmospheric pressure nanopulsed plasma jet, Plasma Process. Polym. 13 (2016) 375–386.

[227] R. Múgica-Vidal, F. Alba-Elías, E. Sainz-García, J. Ordieres-Meré, Atmospheric plasma-polymerization of hydrophobic and wear-resistant coatings on glass substrates, Surf. Coat. Technol. 259 (2014) 374–385.

[228] A. Dembele, M. Rahman, I. Reid, B. Twomey, J. M. D. MacElroy D. P. Dowling, Deposition of hybrid organic–inorganic composite coatings using an atmospheric plasma jet system, J. Nanosci. Nanotechnol. 11 (2011) 8730–8737.

[229] X. Deng, C. Leys, D. Vujosevic, V Vuksanovic, U. Cvelbar, N. De Geyter, R. Morent, A. Nikiforov, Engineering of composite organosilicon thin films with embedded silver nanoparticles via atmospheric pressure plasma process for antibacterial activity, Plasma Process. Polym. 11 (2014) 921–93.

[230] O. Beier, A. Pfuch, K. Horn, J. Weisser, M. Schnabelrauch, A. Schimanski, Low temperature deposition of antibacterially active silicon oxide layers containing silver nanoparticles, prepared by atmospheric pressure plasma chemical vapor deposition, Plasma Process. Polym. 10 (2013) 77–87.

[231] A. Liguori, E. Traldi, E. Toccaceli, R. Laurita, A. Pollicino, M. L. Focarete, V. Colombo, M. Gherardi, Co-deposition of plasma-polymerized polyacrylic acid and silver nanoparticles for the production of nanocomposite coatings using a non-equilibrium atmospheric pressure plasma jet, Plasma Process. Polym. 13 (2016) 623–632.

[232] B. J. Lee, Y. Kusano, N. Kato, K. Naito, T. Horiuchi, H. Koinuma, Oxygen plasma treatment of rubber surface by the atmospheric pressure cold plasma torch, Jpn. J. Appl. Phys. 36 (1997) 2888–2891.

[233] M. Noeske, J. Degenhardt, S. Strudthoff, U. Lommatzsch, Plasma jet treatment of five polymers at atmospheric pressure: surface modifications and the relevance for adhesion, Int. J. Adhes. Adhes. 24 (2004) 171–177.

[234] Q. Chen, Y. Zhang, E. Han, Y. Ge, Atmospheric pressure DBD gun and its application in ink printability, Plasma Sources Sci. Technol. 14 (2005) 670–675.

[235] C. Cheng, Z. Liye, R. Zhan, Surface modification of polymer fibre by the new atmospheric pressure cold plasma jet, Surf. Coat. Technol. 200 (2006) 6659–6665.

[236] U. Lommatzsch, D. Pasedag, A. Baalmann, G. Ellinghorst, H.-E. Wagner, Atmospheric pressure plasma jet treatment of polyethylene surfaces for adhesion improvement, Plasma Process. Polym. 4 (2007) S1041–S1045.

[237] L. Liu, Q. Jiang, T. Zhu, X. Guo, Y. Sun, Y. Guan, Y. Qiu, Influence of moisture regain of aramid fibers on effects of atmospheric pressure plasma treatment on improving adhesion with epoxy, J. Appl. Polym. Sci. 102 (2006) 242–247.

[238] M.C. Kim, S.H. Yanga, J.-H. Boo, J.G. Han, Surface treatment of metals using an atmospheric pressure plasma jet and their surface characteristics, Surf. Coat. Technol. 174 (2003) 839-844.

[239] C.X. Wang, Y.P. Qiu, Two sided modification of wool fabrics by atmospheric pressure plasma jet: influence of processing parameters on plasma penetration, Surf. Coat. Technol. 201 (2007) 6273-6277.

[240] Maan Group, http://www.maangroup.nl/innovations/maan-plasma-treatment-en/plasmaanjet-system/?lang=en (accessed on 31 January 2017).

[241] PVA TEPLA AMERICA, http://www.pvateplaamerica.com/atmospheric/pen.php (accessed on 31 January 2017).

[242] T. Dufour, J. Minnebo, S. Abou Rich, E. C. Neyts, A. Bogaerts, F. Reniers, Understanding polyethylene surface functionalization by an atmospheric He/O_2 plasma through combined experiments and simulations, J. Phys. D: Appl. Phys. 47 (2014) 224007.

[243] S. A. Rich, T. Dufour, P. Leroy, L. Nittler, J. J. Pireaux, F, Reniers, Low-density polyethylene films treated by an atmospheric Ar–O_2 post-discharge: functionalization, etching, degradation and partial recovery of the native wettability state, J. Phys. D: Appl. Phys. 47 (2014) 065203.

[244] A. Van Deynse, P. Cools, C. Leys, R. Morent, N. De Geyter, Surface modification of polyethylene in an argon atmospheric pressure plasma jet, Surf. Coat. Technol. 276 (2015) 384–390.

[245] A. Sarani, A. Y. Nikiforov, N. De Geyter, R. Morent, C. Leys, Surface modification of polypropylene with an atmospheric pressure plasma jet sustained in argon and an argon/water vapour mixture, Appl. Surf. Sci. 257 (2011) 8737-8741.

[246] J. Sun, L. Yao, S. Sun, Y. Qiu, ESR study of atmospheric pressure plasma jet irradiated aramid fibers, Surf. Coat. Technol. 205 (2011) 5312–5317.

[247] K. Gotoh, Y. Nagai, Y. Yonehara and Y. Kobayashi, Surface hydrophilization of two polyester films by atmospheric-pressure plasma and ultraviolet excimer light exposures, J. Adhes. Sci. and Technol. 29 (2015) 473-486.

[248] C. Y. Li, Y. C. Liao, Adhesive stretchable printed conductive thin film patterns on PDMS surface with an atmospheric plasma treatment, ACS Appl. Mater. Interfaces 8 (2016) 11868−11874.

[249] C. Huang Y. C. Chang, S. Y. Wu, Contact angle analysis of low-temperature cyclonic atmospheric pressure plasma modified polyethylene terephthalate, Thin Solid Films 518 (2010) 3575–3580.

[250] C. Huang, P. J. Lin, C. Y. Tsai, R. S. Juang, Electrospun microfibrous membranes with atmospheric-pressure plasma surface modification for the application in dye-sensitized solar cells, Plasma Process. Polym. 10 (2013) 938–947.

[251] C. Huang, C. C. Lin, C. Y. Tsai, R. S. Juang, Tailoring surface properties of polymeric separators for lithium-ion batteries by cyclonic atmospheric-pressure plasma, Plasma Process. Polym. 10 (2013) 407–415.

[252] M. Gilliam, S. Farhat, A. Zand, B. Stubbs, M. Magyar, G. Garner, Atmospheric plasma surface modification of PMMA and PP micro-particles, Plasma Process. Polym. 11 (2014) 1037–1043.

[253] S. Sun, Y. Qiu, Influence of moisture on wettability and sizing properties of raw cotton yarns treated with He/O_2 atmospheric pressure plasma jet, Surf. Coat. Technol. 206 (2012) 2281–2286.

[254] J. Pawlat, P. Terebun, M. Kwiatkowski, J. Diatczy, RF atmospheric plasma jet surface treatment of paper, J. Phys. D: Appl. Phys, 49 (2016) 374001.

[255] T. Kawase, T. Tanaka, H. Minbu, M. Kamiya, M. Oda, T. Hara, An atmospheric-pressure plasma-treated titanium surface potentially supports initial cell adhesion, growth, and differentiation of cultured human prenatal-derived osteoblastic cells, J. Biomed. Mater. Res. 12 (2014) 1289–1296.

[256] J. Fang, I. Levchenko, A. Mai-Prochnow, M. Keidar, U.Cvelbar, G. Filipic, Z. J. Han, K. Ostrikov, Protein retention on plasma-treated hierarchical nanoscale gold-silver platform, Sci. Rep. 5 (2015) 13379.

[257] T. S. M. Mui, L. L. G. Silva, V. Prysiazhnyi, K. G. Kostov, Polyurethane paint adhesion improvement on aluminium alloy treated by plasma jet and dielectric barrier discharge, J. Adhes. Sci. Technol. 30 (2016) 218–229.

Figure captions

Fig. 1. Schematic diagram depicting a general plasma jet device that can be used in surface processing. Some of the most important issues addressed in this paper are summarized, e.g., the plasma generation and propagation, the plasma interaction with the surrounding environment and the substrate, the surface modification of a localized region of the substrate, the enlargement of the treated area through displacement of the sample holder.

Fig. 2. Corona discharge-based plasma jet developed by Dow Corning (PlasmaStream^{TM}) [40,53–55]: (a) schematic illustration of the plasma jet showing the two needle electrodes and the independent inlets for the gas and the thin film precursor; (b) photograph of the plasma source operating during deposition processes carried out by using a He/N_2 fed plasma with HMDSO addition [53]. Copyright 2013 WILEY–VCH Verlag GmbH & Co. KGaA, Weinheim.

Fig. 3. Schematic diagrams of DBD-based plasma jets differing in the electrode geometries and in the shape and dimensions of the canal cross-section perpendicular to the gas flow direction: (a) coaxial geometry with external annular electrodes (circular canal and outlet), (b) coaxial cylindrical geometry consisting of an internal high voltage hollow cylindrical electrode (allowing injection of the precursor in the downstream region), a dielectric tube and an external grounded tube (annular canal and circular outlet); (c) parallel plate electrode geometry (rectangular canal and outlet).

Fig. 4. Schematic diagrams of microplasma jets with circular outlet: (a) corona microplasma jet with a needle-to-plane electrode geometry (needle electrode inserted into a quartz tube and metal plate counter-electrode) [14,63,64], (b) coaxial dielectric barrier microdischarge jet with external ring electrodes on a dielectric tube [14,65], (c) hollow cathode microplasma jet in which the discharge is operated by using a negative dc power supply connected in series with a current-limiting resistor to a capillary stainless steel tube which acts as the cathode, while a metal plate serves as the anode [66]; (d) RF capacitively coupled microplasma with coaxial bare metal electrodes [17]; (e) RF inductively coupled microplasma using a coil on the outside of a quartz capillary tube [14,32]; (f) RF inductively coupled microplasma using a coil on the outside of a quartz capillary tube and provided with a consumable metal wire inserted into a restricted quartz nozzle; the consumable metal wire is used as solid precursor for the deposition of metal or metal oxide thin films and nanostructures [14,68].

Fig. 5. Schematic illustration of various RF plasma jets featuring different electrode configurations: (a) concentric electrodes (annular gas channel and circular exit) [5,31,72,73]; (b) solid parallel plate electrodes (rectangular channel and exit) [5]; (c) perforated parallel plate electrodes (showerhead plasma jet outlet) adopted in the Atmoflo^{TM} plasma jets commercialized by Surfx Technologies LLC [37,74–81].

Fig. 6. Schematic representation of the two plasma jets (annular canal and circular outlet) used in ref. [30] to compare the deposition of SiO_2-like thin films, and corresponding cross-sectional SEM images of thin films deposited on a Si substrate: (a) microwave electrode-less jet which utilizes a surfatron excitation source consisting of a tuned coaxial resonant cavity through which a fused silica tube is inserted; (b) RF jet with external ring electrodes on a fused silica tube. Copyright 2016 Elsevier.

Fig. 7. Arc jet commercialized by Plasmatreat [94] and used for thin film deposition in ref. [95]: (a) schematic illustration of the plasma source and (b) picture of the torch captured by a CCD camera; contrast has been increased by image processing. (c) Response surface of the gas temperature for different distances from the jet outlet nozzle and plasma cycle time (PCT) values (the increment between each curve is 25 K and the gas flow regime is also indicated) [95]. The discharge is fed by air and operated at 21 kHz with pulsed voltage; when PCT is 100% pulse duration is equal to the pause duration. Copyright 2011 WILEY–VCH Verlag GmbH & Co. KGaA, Weinheim.

Fig. 8. Images of (a) the cross-field plasma jet and (b) the linear-field jet characterized in ref. [117]; each image is obtained by overlaying the schematic of the electrode assembly on the photograph of the He-fed plasma jet captured by digital camera (1/30 s exposure time) during operation at the fixed input RF power of 15 W. (c) Etch rate of polyamide film and ozone concentration for the cross-field and linear-field jets fed with He-O_2 mixtures, as a function of the O_2 concentration in the feed mixture (fixed input power of 15 W, ozone concentration measured at z = 10 mm by using UV absorption spectroscopy). Copyright 2008 American Institute of Physics.

Fig. 9. He-fed AP non-equilibrium plasma jet operated with a HV pulsed power supply at the fixed pulse voltage and duration of 8 kV and 1 μs (pulse rise time of about 50 ns). Schlieren images of the gas flow and photographs of the plasma plume at the pulse repetition frequencies of 3, 5 and 8 kHz for different He gas flow rates: (a) 1 slm, (b) 1.5 slm, (c) 2 slm, (d) 2.5 slm [121]. Copyright 2016 American Institute of Physics.

Fig. 10. Evolution of the interaction between the plasma plume emitted from a He/O_2 jet and samples consisting of a 4 μm thick parylene-C film deposited on substrates of different conductivity, during the etching of the parylene-C film [160]. Glass substrate: (a-c) photographs of the discharge captured with a CCD camera, (d-f) optical microscope images and depth profiles of the etched hole at the etching times of 2, 12 and 50 s. Silicon substrate: (g-i) photographs of the discharge captured with a CCD camera, (l-n) optical microscope images and depth profiles of the etched hole at the etching times of 2, 12 and 45 s. Copyright 2016 WILEY–VCH Verlag GmbH & Co. KGaA, Weinheim.

Fig. 11. Schlieren images showing the gas flow behavior of a He-fed single-electrode plasma jet operating in open air in the presence of a flat substrate placed in front of the device outlet: (a) metallic substrate and (b) metallic substrate covered with a dielectric layer (He flow rate of 3 slm, positive nanosecond pulsed power supply, positive polarity voltage, pulse repetition frequency of 1 kHz, voltage pulse amplitude of 14 kV; images acquired when the voltage pulse occurs) [127]. Copyright 2014 Springer.

Fig. 12. Schlieren images showing the gas flow behavior of a He-fed DBD plasma jet (coaxial electrode geometry) operating in open air while a grounded flat metallic substrate is placed in front of the device outlet: (a) without plasma ignition, (b) after 50 ms of plasma operation (He flow rate of 1 slm, microsecond pulsed power supply, negative polarity voltage, pulse

repetition frequency of 2 kHz, voltage pulse amplitude of 16 kV) [132]. Copyright 2015 American Institute of Physics.

Fig. 13. Localized surface processing in static mode operation. (a) Depth profiles in PEEK substrates after 20 min etching with a RF driven plasma jet fed with pure Ar and Ar-O_2 mixtures at the O_2 concentration of 0.2% and 1% (jet diameter outlet of 1.6 mm) [169]. Copyright 2011 WILEY–VCH Verlag GmbH & Co. KGaA, Weinheim. (b) Profiles of the thickness and of the percentage of carboxylic groups in C1s XPS spectra of polymeric coatings deposited over a circular area by using a DBD jet fed with helium-ethylene-acrylic acid mixtures (jet outlet diameter of 6 mm) [41]. (c) SEM image of a typical tower-shaped deposit of tungsten oxide nanoparticles obtained by using an UHF inductively coupled microplasma jet (Fig. 4f) [161]. Copyright 2006 Elsevier. (d) Profiles of WCA measured across the circular treated spots obtained on PS substrates with a Ne-fed microplasma jet at different treatment durations (1, 15, 30 and 60 s). The device is equipped with an outlet capillary tube having length and internal diameter of 50 mm and 0.7 mm, respectively; the discharge is operated at 10 kHz and 4.5 kV, and remains confined within the capillary [107]. Copyright 2011 WILEY–VCH Verlag GmbH & Co. KGaA, Weinheim. (e) Fluorescence images of the amine functionalized dotted patterns obtained by using a nanocapillary plasma jet with outlet aperture of 1 μm and 100 nm [35]. Copyright 2016 American Chemical Society.

Fig. 14. Two different modes of operation observed as a function of the gas flow conditions for a plasma jet array device consisting of seven silica tubes arranged in a honeycomb configuration: (a) intense plasma mode consisting of a concentrated plasma plume, (b) well-collimated plasma mode consisting of seven well-collimated plasma plumes [190]. Copyright 2012 WILEY–VCH Verlag GmbH & Co. KGaA, Weinheim.

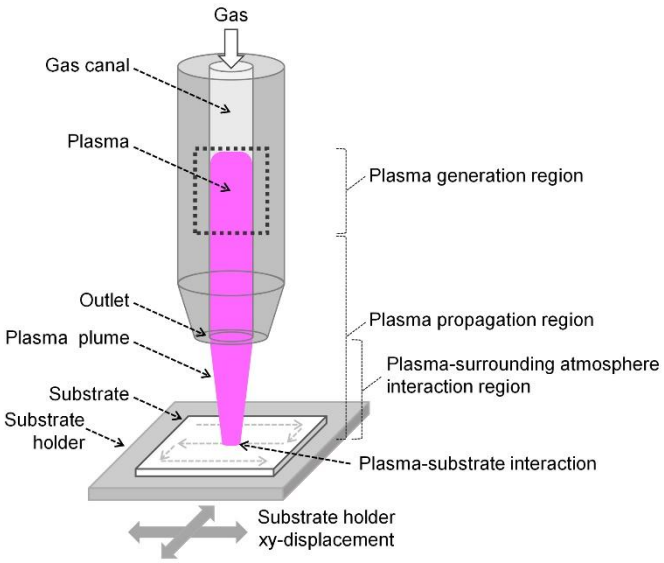

Figure 1 (color online only)

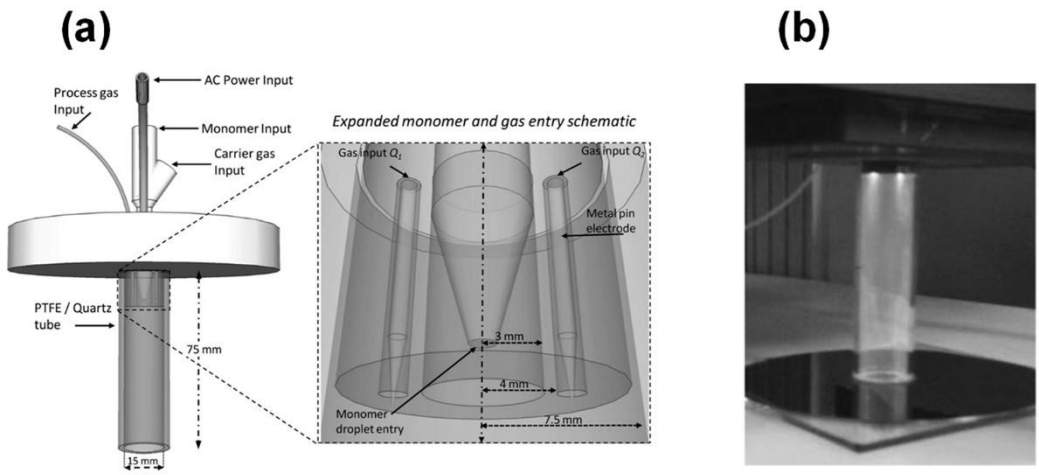
(a)
(b)
AC Power Input
Process gas Input
Monomer Input
Carrier gas Input
PTFE / Quartz tube
75 mm
15 mm
Expanded monomer and gas entry schematic
Gas input Q_1
Gas input Q_2
Metal pin electrode
3 mm
4 mm
7.5 mm
Monomer droplet entry

Figure 2

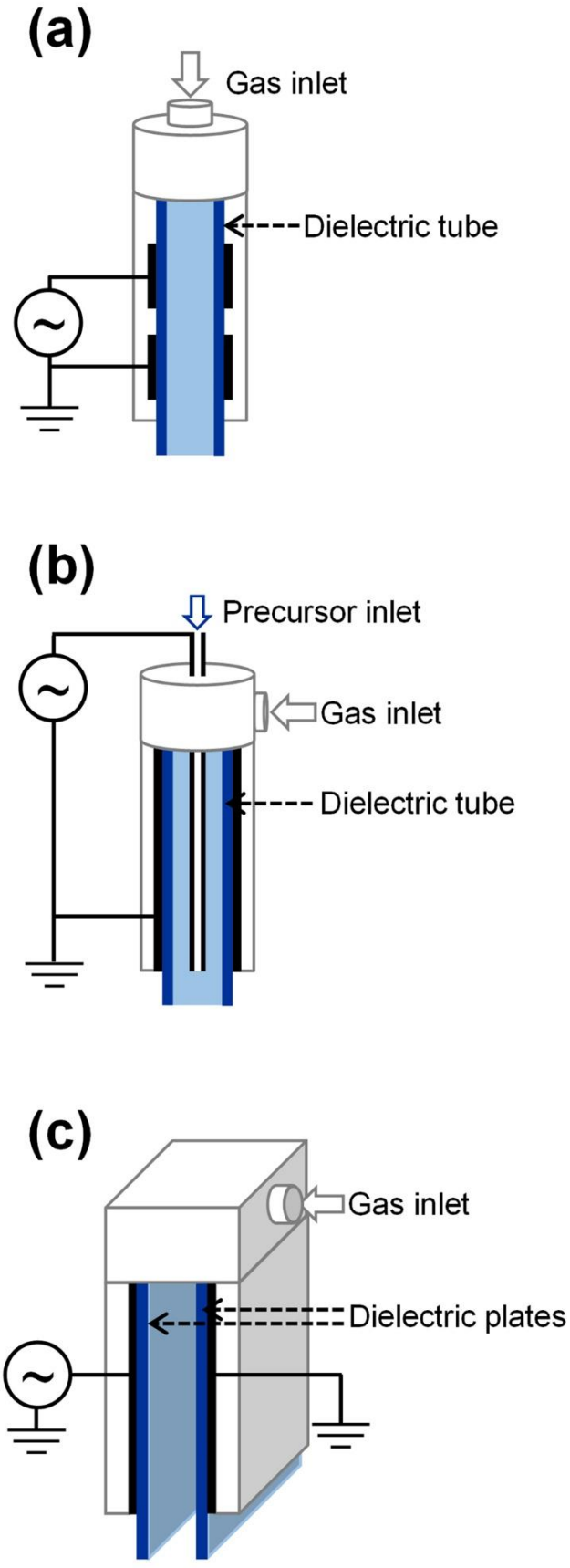

Figure 3 (color online only)

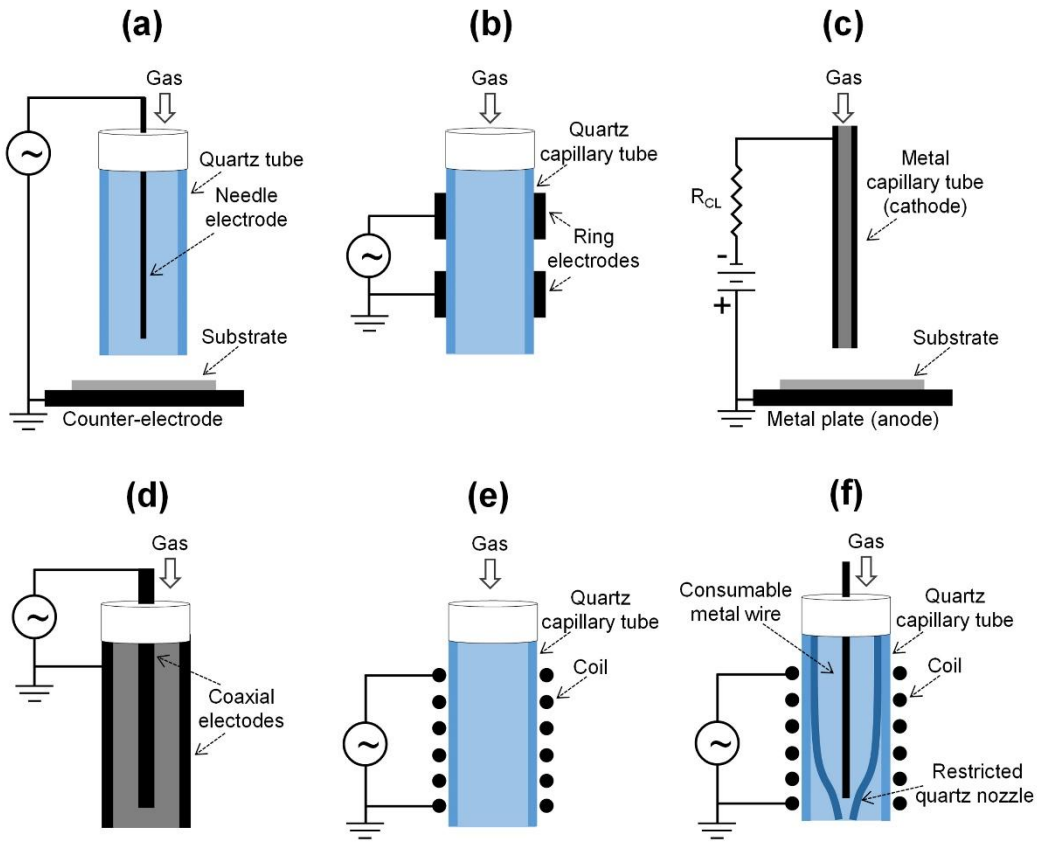

Figure 4 (color online only)

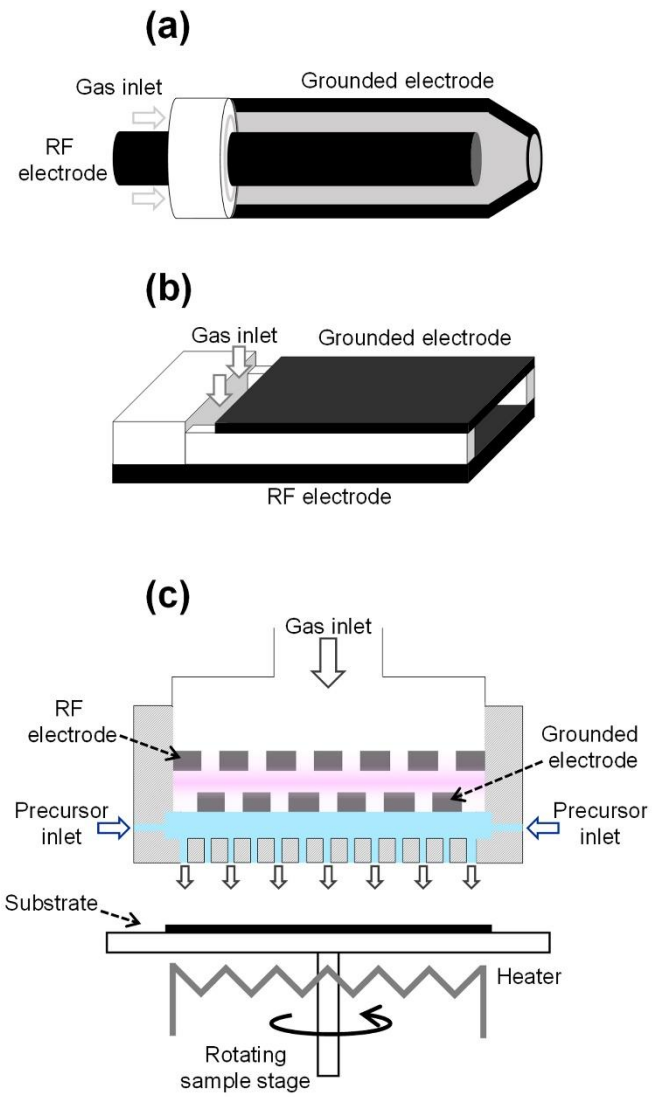

Figure 5 (color online only)

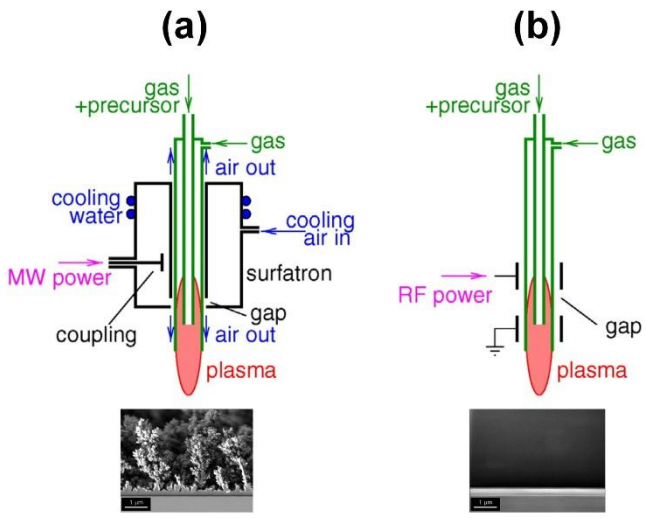

Figure 6 (color online only)

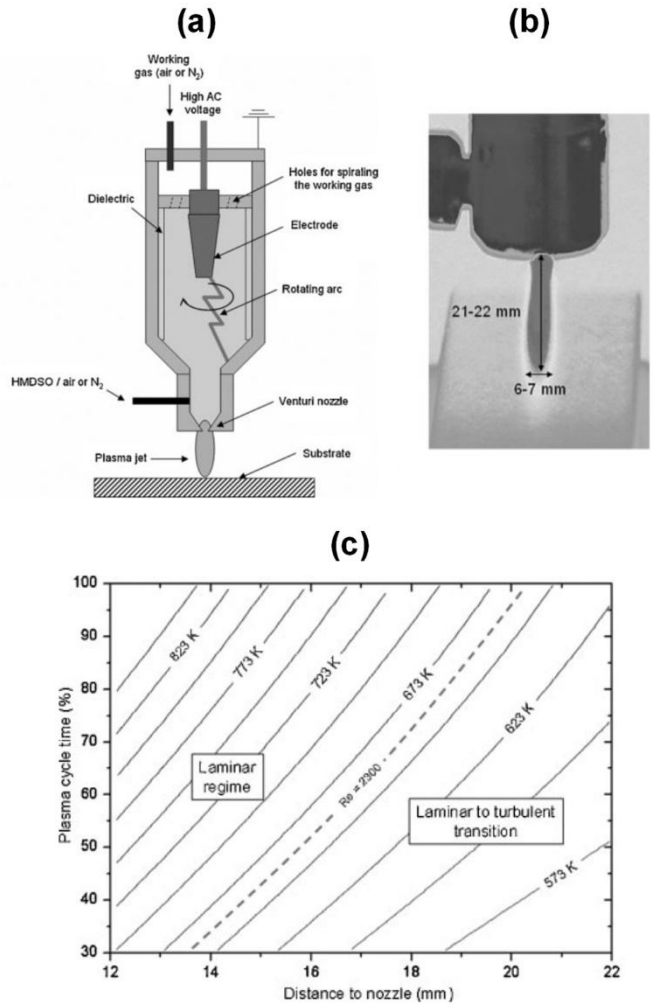
(a)
(b)
Working gas (air or N_2)
High AC voltage
Holes for spiraling the working gas
Dielectric
Electrode
Rotating arc
HMDSO / air or N_2
Venturi nozzle
Plasma jet
Substrate
21-22 mm
6-7 mm
(c)
Plasma cycle time (%)
Distance to nozzle (mm)
823 K
773 K
723 K
673 K
623 K
573 K
Laminar regime
Laminar to turbulent transition
Re = 2300

Figure 7

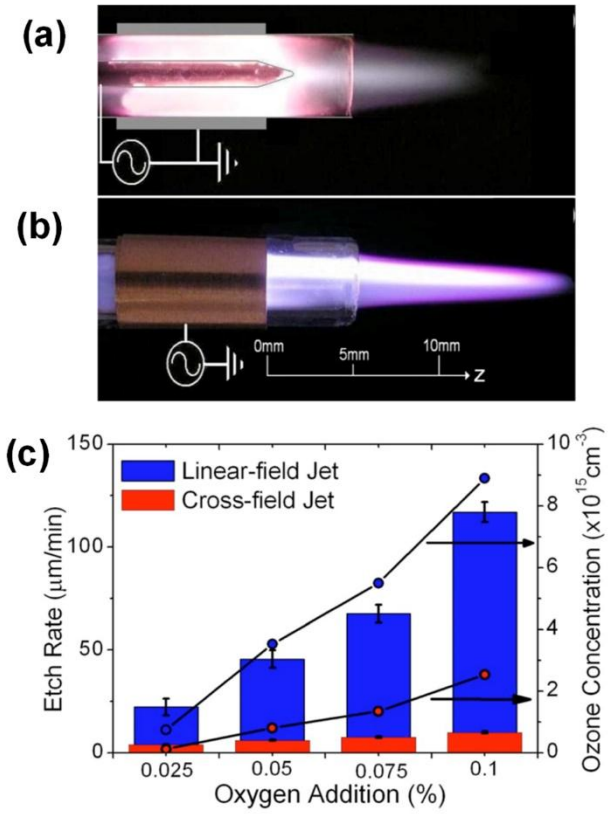

Figure 8 (color online only)

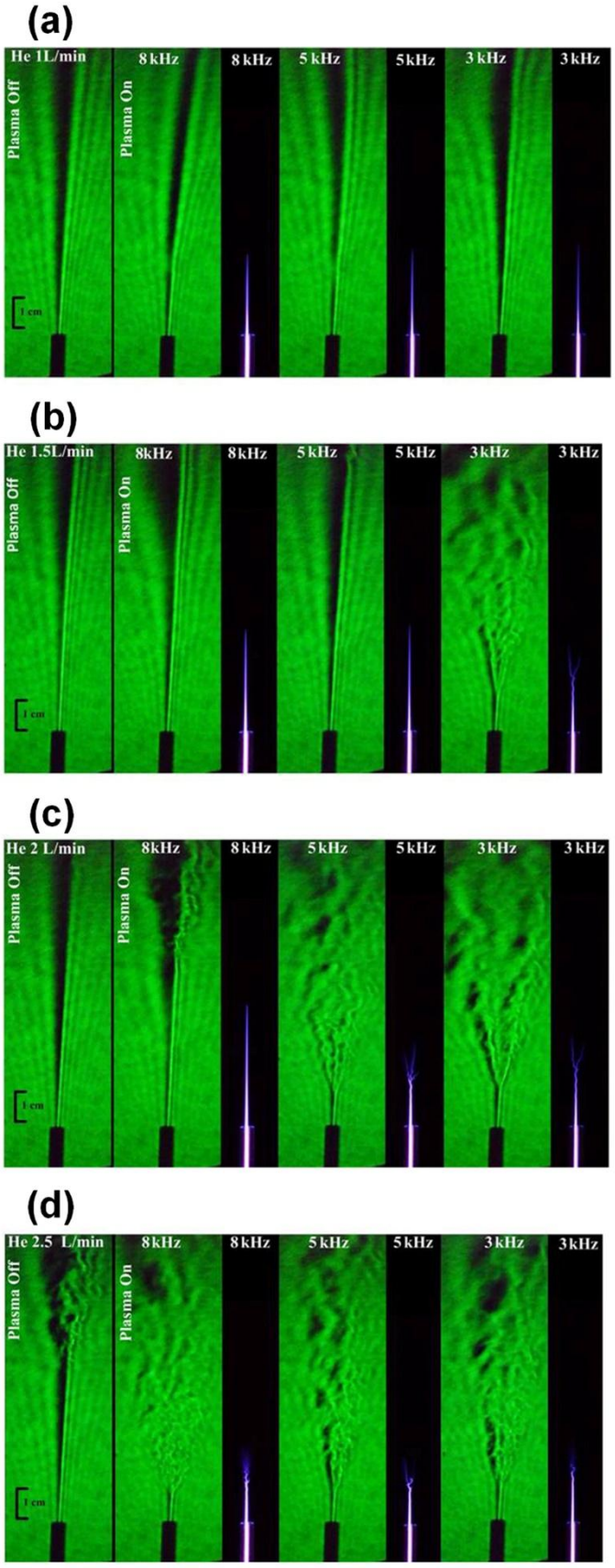

Figure 9 (color online only)

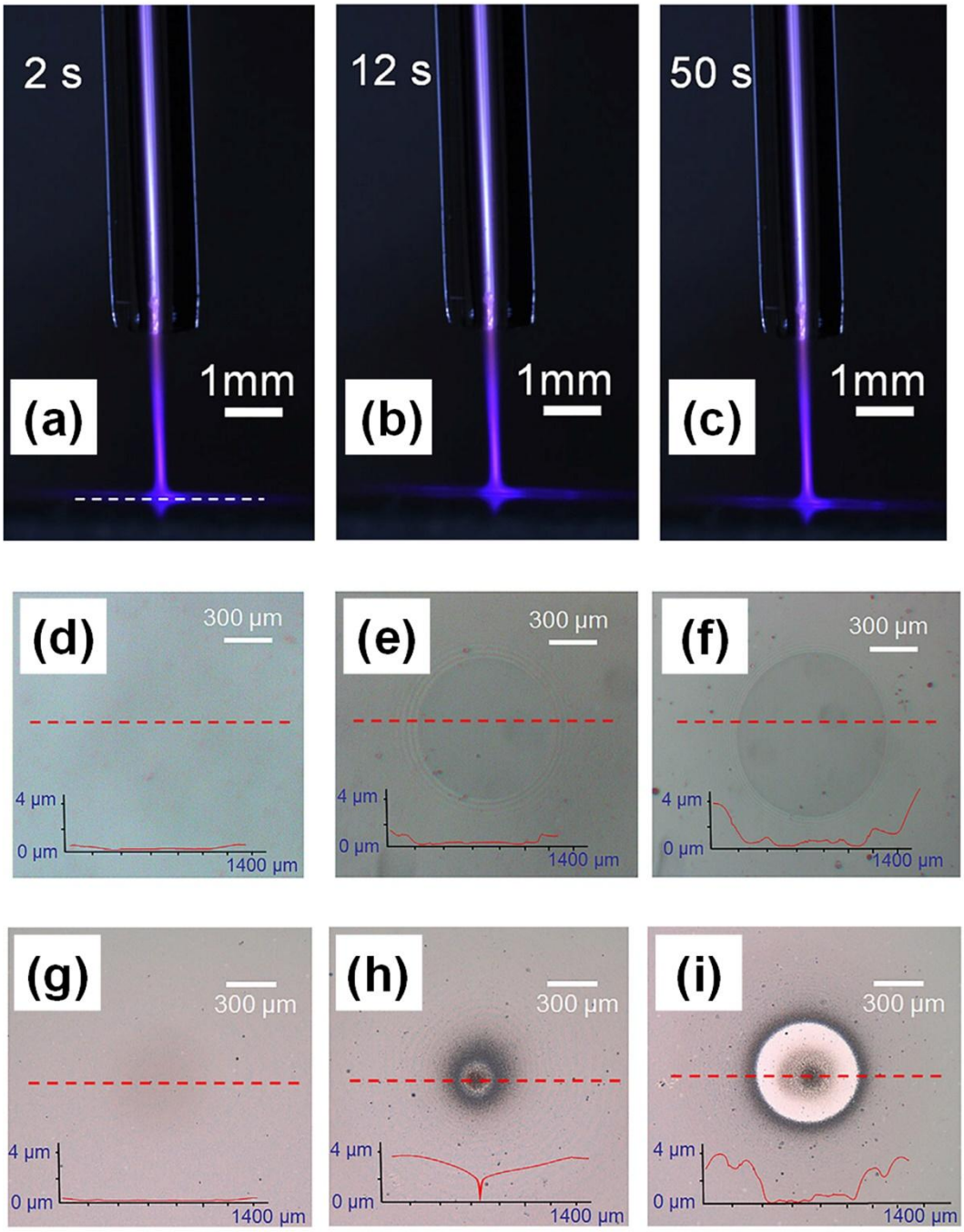

Figure 10 (color online only)

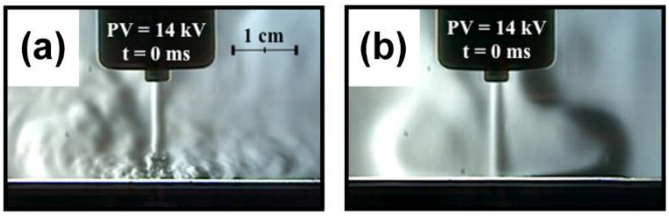

Figure 11 (color online only)

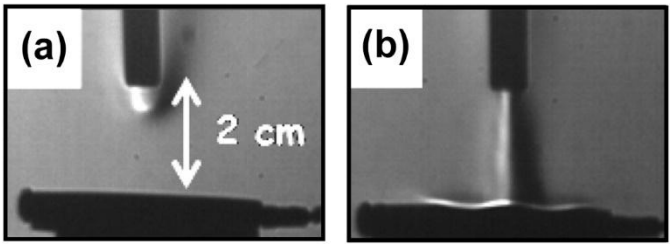

Figure 12 (color online only)

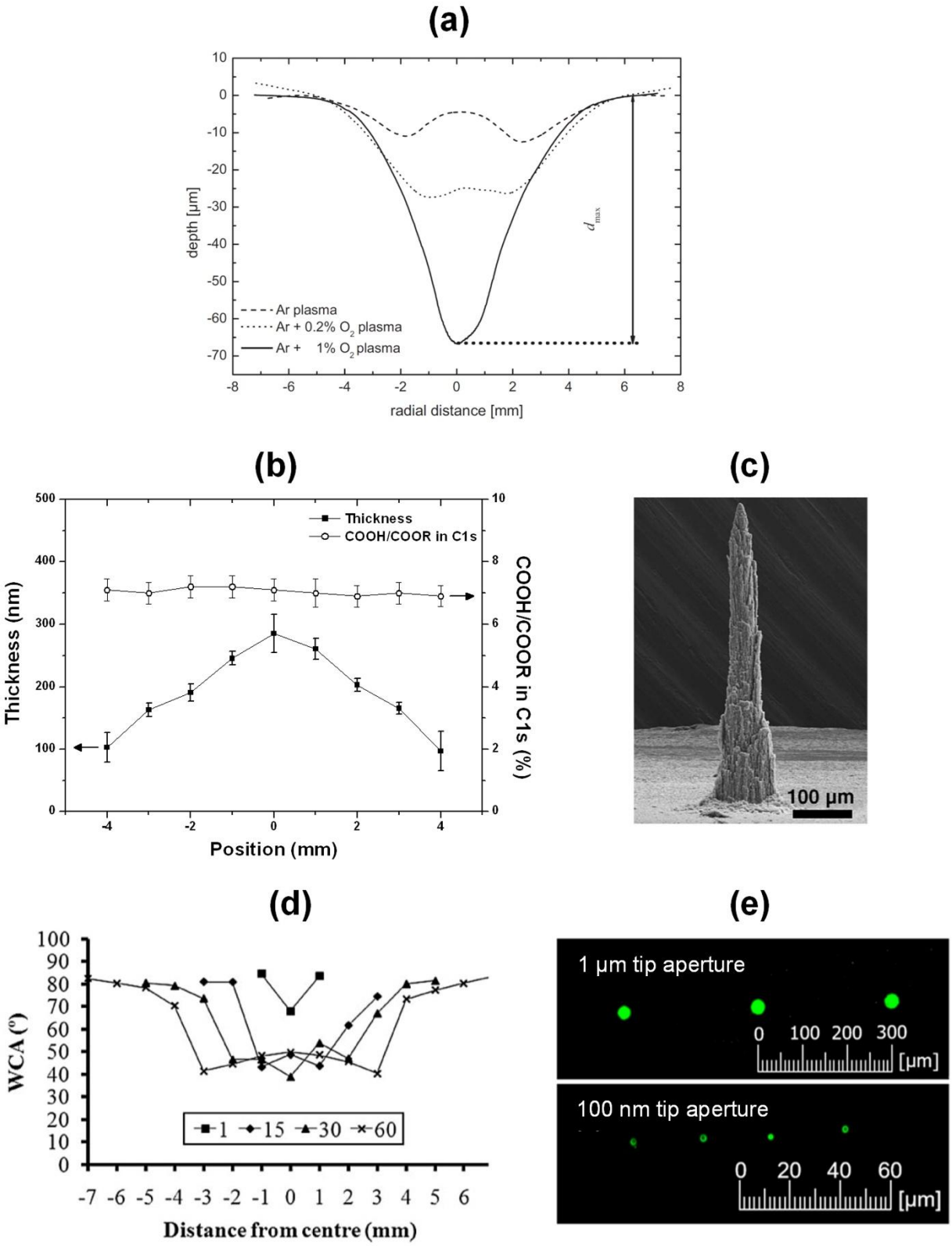

Figure 13 (color online only)

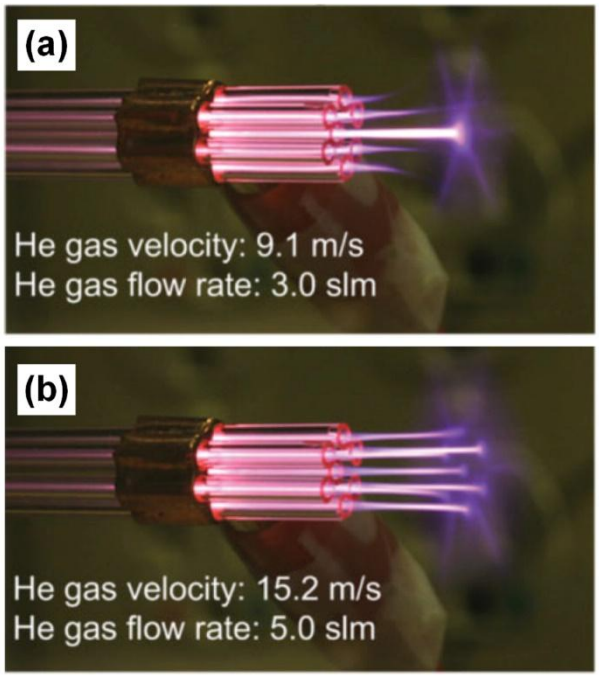

Figure 14 (color online only)